Non-equilibrium statistical mechanics: From a paradigmatic model to biological transport

T. Chou[1], K. Mallick[2], and R. K. P. Zia[3]

[1]Depts. of Biomathematics and Mathematics, UCLA, Los Angeles, CA 90095-1766, USA

[2]Institut de Physique Théorique, C. E. A. Saclay, 91191 Gif-sur-Yvette Cedex, France

[3]Department of Physics, Virginia Tech, Blacksburg, VA 24061, USA

Abstract. Unlike equilibrium statistical mechanics, with its well-established foundations, a similar widely-accepted framework for non-equilibrium statistical mechanics (NESM) remains elusive. Here, we review some of the many recent activities on NESM, focusing on some of the fundamental issues and general aspects. Using the language of stochastic Markov processes, we emphasize general properties of the evolution of configurational probabilities, as described by master equations. Of particular interest are systems in which the dynamics violate detailed balance, since such systems serve to model a wide variety of phenomena in nature. We next review two distinct approaches for investigating such problems. One approach focuses on models sufficiently simple to allow us to find exact, analytic, non-trivial results. We provide detailed mathematical analyses of a one-dimensional continuous-time lattice gas, the totally asymmetric exclusion process (TASEP). It is regarded as a paradigmatic model for NESM, much like the role the Ising model played for equilibrium statistical mechanics. It is also the starting point for the second approach, which attempts to include more realistic ingredients in order to be more applicable to systems in nature. Restricting ourselves to the area of biophysics and cellular biology, we review a number of models that are relevant for transport phenomena. Successes and limitations of these simple models are also highlighted.

1. Introduction

What can we expect of a system which consists of a large number of simple constituents and evolves according to relatively simple rules? To answer this question and bridge the micro-macro connection is the central goal of statistical mechanics. About a century ago, Boltzmann made considerable progress by proposing a bold hypothesis: When an *isolated* system eventually settles into a state of equilibrium, all its microstates are equally likely to occur over long periods of time. Known as the microcanonical ensemble, it provides the basis for computing averages of macroscopic observables: (a) by assuming (time independent) ensemble averages can replace time averages in such an equilibrium state, (b) by labeling each microstate $\mathcal{C}$, (a configuration of the constituents which can be reached via the rules of evolution) as a member of this ensemble, and (c) by assigning the same weight to every member $(P^*(\mathcal{C}) \propto 1)$. This simple postulate forms the foundation for equilibrium statistical mechanics (EQSM), leads to other ensembles for systems in thermal equilibrium, and frames the treatment of thermodynamics in essentially all textbooks. The problem of

answering the question posed above shifts, for systems in equilibrium, to computing averages with Boltzmann weights.

By contrast, there is no similar stepping stone for non-equilibrium statistical systems (NESM), especially ones far from equilibrium. Of course, given a set of rules of stochastic evolution, it is possible to write down equations which govern the time dependent weights, $P(\mathcal{C}, t)$. But that is just the starting point of NESM, as little is known, in general, about the solutions of such equations. Even if we have a solution, there is an added complication: the obvious inequivalence of time- and ensemble-averages à la Boltzmann. Instead, since our interest is the full dynamic behavior of such a statistical system, we must imagine (a) performing the same experiment many times, (b) collecting the data to form an ensemble of trajectories through configuration space, and (c) computing *time dependent* averages of macroscopic observables from this ensemble. The results can then be compared to averages obtained from $P(\mathcal{C}, t)$. Despite these daunting tasks, there are many studies [1, 2, 3] with the goal of understanding such far-from-equilibrium phenomena.

Here, we focus on another aspect of NESM, namely, systems which evolve according rules that violate detailed balance. In general, much less is known about their behavior, though they are used to model a much wider range of natural phenomena. Examples include the topic in this review – transport in biological systems, as well as epidemic spreading, pedestrian/vehicular traffic, stock markets, and social networks. A major difficulty with such systems is that, even if such a system is known (or assumed) to settle eventually in a time-independent state, the appropriate stationary weights are not generally known. In other words, there is no overarching principle, in the spirit of Boltzmann's fundamental hypothesis, which provides the weights for such *non-equilibrium* steady states (NESS). We should emphasize that, if the dynamics is Markovian, then these weights can be constructed formally from the rules of evolution [4]. However, this formal solution is typically far too intractable to be of practical use. As a result, such NESS distributions are explicitly known only for a handful of model systems. Indeed, developing a fundamental and comprehensive understanding of physics far from equilibrium is recognized to be one of the 'grand challenges' of our time, by both the US National Academy of Sciences [5] and the US Department of Energy [6]. Furthermore, these studies point out the importance of non-equilibrium systems and their impact far beyond physics, including areas such as computer science, biology, public health, civil infrastructure, sociology, and finance.

One of the aims of this review is to provide a framework in which issues of NESM are well-posed, so that readers can appreciate why NESM is so challenging. Another goal is to show that initial steps in this long journey have been taken in the form of a few mathematically tractable models. A good example is the totally asymmetric simple exclusion process (TASEP). Like the Ising model, TASEP also consists of binary constituents, but evolves with even simpler rules. Unlike the scorn Ising's model faced in the 1920's, the TASEP already enjoys the status of a paradigmatic model. Fortunately, it is now recognized that seemingly simplistic models can play key roles in the understanding fundamental statistical mechanics and in formulating applied models of real physical systems. In this spirit, our final aim is to provide potential applications of the TASEP, and its many relatives, to a small class of problems in biology, namely, transport at molecular and cellular levels.

This article is organized along the lines of these three goals. The phrase 'non-equilibrium statistical mechanics' has been used in many contexts, referring to very different issues, in a wide range of settings. The first part of the next section will help

readers discern the many facets of NESM. A more specific objective of section 2 is to review a proposal for characterizing all stationary states by a *pair* of time independent distributions, $\{P^*(\mathcal{C}), K^*(\mathcal{C} \to \mathcal{C}')\}$, where K^* is the probability current 'flowing' from $\mathcal{C}$ to $\mathcal{C}'$ [7]. In this scheme, ordinary equilibrium stationary states (EQSS) appear as the restricted set $\{P^*, 0\}$, whereas states with $K^* \neq 0$ are identified as NESS. Making an analogy with electromagnetism, this distinction is comparable to that of electrostatics *vs.* magnetostatics, as the hallmark of the latter is the presence of steady and persistent currents. Others (e.g., [8]) have also called attention to the importance of such current loops for NESS and the key role they play in the understanding of fluctuations and dissipation. Two examples of NESS phenomena, which appear contrary to the conventional wisdom developed from EQSM, will be provided here.

Section 3 will be devoted to some details on how to 'solve' the TASEP, for readers who are interested in getting involved in this type of study. In particular, we will present two complementary techniques, with one of them exploiting the relationship between two-dimensional systems in equilibrium and one-dimensional systems in NESM. While TASEP was introduced in 1970 [9] for studying interacting Markov processes, it gained wide attention two decades later in the statistical physics community [10, 11, 12]. In a twist of history, two years before its formal introduction, Gibbs and his collaborators introduced [13, 14] a more complex version of TASEP to model mRNA translation in protein synthesis. As the need for modeling molecular transport in a biological setting provided the first incentives for considering such NESM systems, it is fitting that we devote the next part, section 4, to potential applications for biological transport. In contrast to the late 60's, much more about molecular biology is known today, so that there is a large number of topics, even within this restricted class of biological systems. Though each of which deserves a full review, we will limit ourselves to a few paragraphs for each topic. The reader should regard our effort here as a bird's eye view 'tour guide', pointing to more detailed, in-depth coverages of specific avenues within this rich field. Finally, we should mention that TASEP naturally lends itself to applications in many other areas, e.g., traffic flow [15] and surface growth [16, 17], etc. All are very interesting, but clearly beyond the scope of this review, as each deserves a review of its own. In the last section, 5, we conclude with a brief summary and outlook.

2. General aspects of non-equilibrium statistical mechanics

In any quantitative description of a system in nature, the first step is to specify the degrees of freedom to focus our attention, while ignoring all others. For example, in Galileo's study of the motion of balls dropped from a tower, the degrees of freedom associated with the planets is ignored. Similarly, the motion of the atoms within the balls plays no role. The importance of this simple observation is to recognize that all investigations are necessarily limited in scope and all quantitative predictions are approximations to some degree. Only by narrowing our focus to a limited window of length- and/or time-scales can we make reasonable progress towards quantitative understanding of natural phenomena. Thus, we must start by specifying a set of configurations, $\{\mathcal{C}\}$, which accounts for all the relevant degrees of freedom of the system. For example, for the traditional kinetic theory of gases (in d spatial dimensions), $\mathcal{C}$ is a point in a $2dN$ dimensional phase space: $\{\vec{x}_i, \vec{p}_i\}$, $i = 1, ..., N$. For an Ising model with spins $s = \pm 1$, the set $\{\mathcal{C}\}$ is the 2^N vertices of an N dimensional

cube: $\{s_i\}$, $i = 1, ..., N$. In the first example, which should be suitable for describing Argon at standard temperature and pressure, the window of length scales certainly excludes Angströms or less, since the electronic and hadronic degrees of freedom within an atom are ignored. Similarly, the window in the second example also excludes many details of solid state physics. Yet, the Ising model is remarkably successful at predicting the magnetic properties of several physical systems [18, 19, 20].

Now, as we shift our focus from microscopic to macroscopic lengths, both $\{C\}$ and the description also change. Keeping detailed accounts of such changes is the key idea behind renormalization, the application of which led to the extremely successful prediction of non-analytic thermodynamic properties near second order phase transitions [21]. While certain aspects of these different levels of description change, other aspects – e.g., fundamental symmetries of the system – remain. One particular aspect of interest here is time reversal. Although physical laws at the atomic level respect this symmetry‡, 'effective Hamiltonians' and phenomenological descriptions at more macroscopic levels often do not. One hallmark of EQSM is that the dynamics, effective for whatever level of interest, retain this symmetry. Here, the concept and term 'detailed balance' is often used as well as 'time reversal.' By contrast, NESM provides a natural setting for us to appreciate the significance of this micro-macro connection and the appearance of time-irreversible dynamics. We may start with a system with many degrees of freedom evolving with dynamics obeying detailed balance. Yet, when we focus on a *subsystem* with far fewer degrees of freedom, it is often reasonable to consider a dynamics that violates detailed balance. Examples of irreversible dynamics include simple friction in solid mechanics, resistance in electrical systems, and viscosity in fluid flows.

Before presenting the framework we will use for discussing fundamental issues of NESM, let us briefly alert readers to the many settings where this term is used. Starting a statistical system in some initial configuration, C_0, and letting it evolve according to rules which respect detailed balance, it will eventually wind up in an EQSS (precise definitions and conditions to be given at the beginning of section 2 below). To be explicit, let us denote the probability to find the system in configuration C at time t by $P(C, t)$ and start with $P(C, 0) = \delta(C - C_0)$. Then, $P(C, t \to \infty)$ will approach a stationary distribution, $P^*(C)$, which is recognized as a Boltzmann distribution in equilibrium physics. Before this 'eventuality', many scenarios are possible and all of them rightly deserve the term NESM. There are three important examples from the literature. Physical systems in which certain variables change so slowly that reaching P^* may take many times the age of the universe. For time scales relevant to us, these systems are always 'far from equilibrium'. To study the statistics associated with fast variables, these slow ones might as well be considered frozen, leading to the concept of 'quenched disorder'. The techniques used to attack this class of problems are considerably more sophisticated than computing Boltzmann weights [1, 2], and are often termed NESM. At the other extreme, there is much interest in behavior of systems near equilibrium, for which perturbation theory around the EQSS is quite adequate. Linear response is the first step in such approaches [23, 24, 25, 26], with a large body of well established results and many textbooks devoted to them. Between these extremes are system which evolve very slowly, yet tractably. Frequently, these studies come under the umbrella of NESM and are found with the term 'aging'

---

‡ Strictly speaking, if we accept CPT as an exact symmetry, then time reversal is violated at the subatomic level, since CP violation has been observed. So far, there is no direct observation of T violation. For a recent overview, see, e.g., reference [22].

in their titles [3].

Another frequently encountered situation is the presence of time-dependent rates. Such a problem corresponds to many experimental realizations in which control parameters, e.g., pressure or temperature, are varied according to some time-dependent protocol. In the context of theoretical investigations, such changes play central roles in the study of work theorems [27, 28, 29, 30, 31, 32, 33, 34, 35]. In general these problems are much less tractable and will not be considered here.

By contrast, we will focus on systems which evolve according to dynamics that *violate* detailed balance. The simplest context for such a system is the coupling to two or more reservoirs (of the same resource, e.g., energy) in such a way that, when the system reaches a stationary state, there is a steady flux *through* it. A daily example is stove-top cooking, in which water in a pot gains energy from the burner and loses it to the room. At a steady simmer, the input balances the heat loss and our system reaches a non-equilibrium steady state (NESS). That these states differ significantly from ordinary EQSS's has been demonstrated in a variety of studies of simple model systems coupled to thermal reservoirs at two different temperatures. Another example, at the global scale, is life on earth, the existence of which depends on a steady influx of energy from the sun and re-radiation to outer space. Indeed, all living organisms survive (in relatively steady states) by balancing input with output – of energy and matter of some form. Labeling these reservoirs as 'the medium' in which our system finds itself, we see the following scenario emerging. Though the medium+system combination is clearly evolving in time, the system may be small enough that it has arrived at a time-independent NESS. While the much larger, combined system may well be evolving according to a time-reversal symmetric dynamics, it is quite reasonable to assume that this symmetry is violated by the effective dynamics appropriate for our smaller system with its shorter associated time scales. In other words, when we sum over the degrees of freedom associated with the medium, the dynamics describing the remaining configurations $\mathcal{C}$'s of our system should in general violate detailed balance.

In general, it is impossible to derive such effective dynamics for systems at the mesoscopic or macroscopic scales from well-known interactions at the microscopic, atomic level. There are proposals to derive them from variational principles, based on postulating some quantity to be extremized during the evolution, in the spirit of least action in classical mechanics. The most widely known is probably 'maximum entropy production'. The major challenge is to identify the constraints appropriate for each NESM system at hand. None of these approaches has achieved the same level of acceptance as the maximum entropy principle in EQSM (where the constraints are well established, e.g., total energy, volume, particle number, etc.). In particular, the NESS in the uniformly driven lattice gas is known to differ from the state predicted by this principle [36]. Readers interested in these approaches may study a variety of books and reviews which appeared over the years [37, 38, 39, 40, 41, 42, 43, 44]. How an effective dynamics (i.e., a set of rules of evolution) arise is not the purpose of our review. Instead, our goal is to explore the nature of stationary states, starting from a *given* dynamics that violates detailed balance. Specifically, in modeling biological transport, the main theme of the applications section, it is reasonable to postulate a set of transition rates for the system of interest.

2.1. Master equation and other approaches to statistical mechanics

Since probabilities are central to statistical mechanics, our starting point for discussing NESM is $P(\mathcal{C}, t)$ and its evolution. Since much of our review will be devoted to models well-suited for computer simulations, let us restrict ourselves to discrete steps ($\tau = 0, 1, ...$ of time δt) as well as a discrete, finite set of $\mathcal{C}$'s ($\mathcal{C}_1$, $\mathcal{C}_2$, .., $\mathcal{C}_{\mathcal{N}}$). Also, since we will be concerned with time reversal, we will assume, for simplicity, that all variables are even under this operation (i.e., no momenta-like variables which change sign under time reversal). To simplify notation further, let us write $P_i(\tau)$, interchangeably with $P(\mathcal{C}_i, \tau \delta t)$. Being conserved ($\sum_i P_i(\tau) = 1$ for all τ), P must obey a continuity equation, i.e., the vanishing of the time rate of change of a conserved density plus the divergence of the associated current density. Clearly, the associated currents here are *probability currents*. Since we restrict our attention to a discrete configuration space, each of these currents can be written as the flow from $\mathcal{C}_j$ to $\mathcal{C}_i$, i.e., $K_i^j(\tau)$ or $K(\mathcal{C}_j \to \mathcal{C}_i, \tau \delta t)$. As a net current, $K_j^i(\tau)$ is by definition $-K_i^j(\tau)$, while its 'divergence' associated with any $\mathcal{C}_i$ is just $\sum_j K_i^j(\tau)$. In general, K is a new variable and how it evolves must be specified. For example, in quantum mechanics, P is encoded in the amplitude of the wavefunction ψ only, while K contains information of the phase in ψ as well (e.g., $K \propto \psi^* \overset{\leftrightarrow}{\nabla} \psi$ for a single non-relativistic particle). In this review, as well as the models used in essentially all simulation studies, we follow a much simpler route: the master equation or the Markov chain. Here, K is assumed to be proportional to P, so that $P_i(\tau+1)$ depends only on linear combinations of the probabilities of the previous step, $P_j(\tau)$. In a further simplification, we focus on time-homogeneous Markov chains, in which the matrix relating K to P is constant in time. Thus, we write $P_i(\tau+1) = \sum_j w_i^j P_i(\tau)$, where w_i^j are known as the transition rates (from $\mathcal{C}_j$ to $\mathcal{C}_i$).

As emphasized above, we will assume that these rates are *given* quantities, as in a mathematical model system like TASEP or in phenomenologically-motivated models for biological systems. Probability conservation imposes the constraint $\sum_i w_i^j = 1$ for all j, of course. A convenient way to incorporate this constraint is to write the master equation in terms of the changes

$$\begin{aligned} \Delta P_i(\tau) &\equiv P_i(\tau+1) - P_i(\tau) \\ &= \sum_{j \neq i} \left[w_i^j P_j(\tau) - w_j^i P_i(\tau) \right] \end{aligned} \tag{1}$$

This equation can be written as

$$\Delta P_i(\tau) = \sum_j L_i^j P_j(\tau) \tag{2}$$

where

$$L_i^j = \begin{cases} w_i^j & \\ -\sum_{k \neq j} w_k^j & \end{cases} \quad \text{if} \quad \begin{matrix} i \neq j \\ i = j \end{matrix} \tag{3}$$

is a matrix (denoted by $\mathbb{L}$; sometimes referred to as the Liouvillian) that plays much the same role as the Hamiltonian in quantum mechanics. Since all transition rates are non-negative, w_i^j is a stochastic matrix and many properties of the evolution of our system follow from the Perron-Frobenius theorem [45]. In particular, $\sum_i L_i^j = 0$ for all j (probability conservation), so that at least one of the eigenvalues must vanish. Indeed,

we recognize the stationary distribution, P^*, as the associated right eigenvector, since $\mathbb{L}P^* = 0$ implies $P_i^*(\tau + 1) = P_i^*(\tau)$. Also, this P^* is unique, provided the dynamics is ergodic, i.e., every $\mathcal{C}_i$ can be reached from any $\mathcal{C}_j$ via the w's. Further, the real parts of all other eigenvalues must be negative, so that the system must decay into P^* eventually.

Since the right-hand side of equation (1) is already cast in the form of the divergence of a current, we identify

$$K_i^j(\tau) \equiv w_i^j P_j(\tau) - w_j^i P_i(\tau) \qquad (4)$$

as the (net) probability current from $\mathcal{C}_j$ to $\mathcal{C}_i$. Note that the antisymmetry $K_i^j = -K_j^i$ is manifest here. When a system settles into a stationary state, these time-independent currents are given simply by

$$K_i^{*j} \equiv w_i^j P_j^* - w_j^i P_i^* \qquad (5)$$

As we will present in the next subsection, a reasonable way to distinguish EQSS from NESS is whether the K^* vanish or not. Before embarking on that topic, let us briefly remark on two other common approaches to time dependent statistical mechanics. More detailed presentations of these and related topics are beyond the scope of this review, but can be found in many books [46, 47, 48, 49].

Arguably the most intuitive approach to a stochastic process is the Langevin equation. Originating with the explanation of Brownian motion [50] by Einstein and Smoluchowski [51, 52], this equation consists of adding a random drive to an otherwise deterministic evolution. The deterministic evolution describes a single trajectory through configuration space: $\mathcal{C}(\tau)$ (starting with $\mathcal{C}(0) = \mathcal{C}_0$), governed by say, an equation of the form $\Delta\mathcal{C}(\tau) = \mathcal{F}[\mathcal{C}(\tau)]$. In a Langevin approach, $\mathcal{F}$ will contain both a deterministic part and a noisy component. Of course, a trajectory (or history, or realization) will depend on the specific noise force appearing in that run. Many trajectories are therefore generated, each depending on a particular realization of the noise and the associated probability. Although each trajectory can be easily understood, the fact that many of them are possible means the system at time τ can be found at a collection of $\mathcal{C}$'s. In this sense, the evolution is best described by a probability distribution, $P(\mathcal{C}, \tau)$, which is controlled by both the deterministic and the noisy components in $\mathcal{F}$. Historically, such considerations were first provided for a classical point particle, where $\Delta\mathcal{C} = \mathcal{F}$ would be Newton's equation, $\partial_t^2 \vec{x}(t) = \vec{F}/m$, with continuous time and configuration variables. How the deterministic and noisy parts of $\vec{F}$ are connected to each other for the Brownian particle is the celebrated Einstein-Smoluchowski relation. Of course, $P(\mathcal{C}, \tau)$ becomes $P(\vec{x}, t)$ in this context, while the Langevin approach can be reformulated as a PDE for $P(\vec{x}, t)$

$$\partial_t P(\vec{x}, t) = \frac{\partial^2}{\partial x_\alpha \partial x_\beta} D_{\alpha\beta}(\vec{x}) P(\vec{x}, t) - \frac{\partial}{\partial x_\alpha} V_\alpha(\vec{x}) P(\vec{x}, t) \qquad (6)$$

Here, $D_{\alpha\beta}$ and V_α are the diffusion tensor and the drift vector, respectively, and are related to the noisy and deterministic components of the drive**S**. This PDE is referred to as the Fokker-Planck equation, although it was first introduced for the velocity distribution of a particle [48].

S Note that $D_{\alpha\beta}(\vec{x})$ here derives from the rate of change of the variance of the distribution and is different from the diffusion coefficient used to define Fick's law. Here, both spatial derivatives operate on $D_{\alpha\beta}(\vec{x})$.

An experienced reader will notice that the master equation (1) for $P(\mathcal{C}, \tau)$ and the Fokker-Planck equation (6) for $P(\vec{x}, t)$ are both linear in P and first order in time, but that the right-hand sides are quite different. Let us comment briefly on their similarities and differences. Despite the simpler appearance, equation (1) is the more general case, apart from the complications associated with discrete *vs.* continuous variables. Thus, let us facilitate the comparison by considering a discrete version of equation (6), i.e., $t \to \tau \delta t$ and $\vec{x} \to \vec{\zeta} \delta x$, so that $P(\vec{x}, t) \to P(\vec{\zeta}, \tau)$. In this light, it is clear that the derivatives on the right correspond to various linear combinations of $P(\zeta_\alpha \pm 1, \zeta_\beta \pm 1; \tau)$. In other words, only a handful of the 'nearest configurations' are involved in the evolution of $P(\vec{\zeta}, \tau)$. By contrast, the range of w_i^j, as written in equation (1), is not restricted.

Let us illustrate by a specific example. Consider a system with N Ising spins (with any interactions between them) evolving according to random sequential Glauber spin-flip dynamics [53]. In a time step, a random spin is chosen and flipped with some probability. Now, as noted earlier, the configuration space is the set of vertices of an N dimensional cube. Therefore, the only transitions allowed are moves along an edge of the cube, so that the range of w_i^j is 'short'. In this sense, field theoretic formulations of the Ising system evolving with Glauber dynamics are possible, taking advantage of Fokker-Planck like equations, cast in terms of path integrals. On the other hand, consider updating according to a cluster algorithm, e.g., Swendsen-Wang [54], in which a large cluster of spins (say, M) are flipped in a single step. Such a move clearly corresponds to crossing the body diagonal of an M dimensional cube. Since M is conceivably as large as N, there is no limit to the range of this set of w's. It is hardly surprising that field theoretic approach for such systems are yet to be formulated, as they would be considerably more complex.

2.2. Non-equilibrium vs. equilibrium stationary states, persistent probability currents

Following the footsteps of Boltzmann and Gibbs, we study statistical mechanics of systems in thermal equilibrium by focusing on time independent distributions such as $P^*(\mathcal{C}) \propto 1$ or $\exp[-\beta \mathcal{H}(\mathcal{C})]$ (where $\mathcal{H}$ is the total energy associated with $\mathcal{C}$ and β is the inverse temperature). Apart from a few model systems, it is not possible to compute, analytically and in general, averages of observable quantities, i.e.,

$$\langle \mathcal{O} \rangle \equiv \sum_j \mathcal{O}(\mathcal{C}_j) P^*(\mathcal{C}_j). \tag{7}$$

Instead, remarkable progress over the last fifty years was achieved through computer simulations, in which a small subset of $\{\mathcal{C}\}$ is generated – with the appropriate (relative) weights – and used for computing the desired averages. This approach is an advanced art [55], far beyond the scope (or purpose) of this review. Here, only some key points will be mentioned and exploited – for highlighting the contrast between the stationary distributions of Boltzmann-Gibbs and those in NESS.

In a classic paper [56], Metropolis, *et.al.* introduced an algorithm to generate a set of configurations with relative Boltzmann weights. This process also simulates a dynamical evolution of the system, in precisely the sense of the master equation. Starting from some initial $\mathcal{C}(0) = \mathcal{C}_0$, a new one, $\mathcal{C}_k$, is generated (by some well defined procedure) and accepted with probability w_k^0. Thus, $\mathcal{C}(1)$ is $\mathcal{C}_k$ or $\mathcal{C}_0$. with relative probability $w_k^0 / (1 - w_k^0)$. After some transient period, the system is expected to settle into a stationary state, i.e., the frequencies of $\mathcal{C}_i$ occurring in the run are proportional

to a time independent $P^*(\mathcal{C}_i)$. To implement this Monte-Carlo method, a set of transition rates, w_j^i, must be fixed. Further, if the desired outcome is $P^* \propto e^{-\beta\mathcal{H}}$, then w_j^i cannot be arbitrary. A sufficient (but not necessary) condition is referred to, especially in the simulations community [55], as 'detailed balance':

$$w_k^i P^*(\mathcal{C}_i) = w_i^k P^*(\mathcal{C}_k). \tag{8}$$

In other words, it suffices to constrain the ratio w_k^i/w_i^k to be $\exp[-\beta\Delta\mathcal{H}]$, where $\Delta\,\mathcal{H} \equiv \mathcal{H}(\mathcal{C}_k) - \mathcal{H}(\mathcal{C}_i)$ is just the difference between the configurational energies. A common and simple choice is $w_k^i = \min\{1, e^{-\beta\Delta\mathcal{H}}\}$.

Of course, constraining the ratios still leaves us with many possibilities. To narrow the choices, it is reasonable to regard a particular set of w's as the simulation of a physical dynamics‖. In that case, other considerations will guide our choices. For example, the Lenz-Ising system is used to model spins in ferromagnetism [57] as well as occupations in binary alloys [58, 59]. In the former, individual spins can be flipped and it is quite appropriate to exploit Glauber [53] dynamics, in which the w's connect $\mathcal{C}$'s that differ by only one spin. In the latter however, a Zn atom, say, cannot be changed into a Cu atom, so that exchanging a neighboring pair of different 'spins' – Kawasaki [60, 61] dynamics – is more appropriate. In terms of the N dimensional cube representation of $\{\mathcal{C}\}$, these w's connect two vertices along an edge (Glabuer) or across the diagonal of a square face or plaquette (Kawasaki). Both dynamics involve w's that only connect $\mathcal{C}$'s with one or two different spins. The idea is that, in a short δt, exchanging energy with the thermal reservoir can randomly affect only one or two spins. Also, in this sense, we can regard the w's as how the system is coupled to the surrounding medium. Clearly, $\Delta\mathcal{H}$ measures the energy exchanged between the two. Another important quantity is entropy production, whether associated with the system or the medium, in which the w's will play a crucial role.

It is significant that regardless of the details of the associated dynamics, a set of w's that obey detailed balance (8) necessarily leads the system to a state in which *all* stationary currents vanish. This follows trivially from the definition (5). By contrast, transition rates that violate detailed balance necessarily lead to some *non-vanishing* stationary currents. To appreciate this statement, let us provide a better criterion, due to Kolmogorov [62], for rates that respect/violate detailed balance. In particular, while equation (8) gives the wrong impression that detailed balance is defined with respect to a given $\mathcal{H}$, the Kolmogorov criterion for detailed balance is applicable to all Markov processes, whether an underlying Hamiltonian exists or not.

Consider a closed loop in configuration space, e.g., $\mathcal{L} \equiv \mathcal{C}_i \rightarrow \mathcal{C}_j \rightarrow \mathcal{C}_k \rightarrow ... \rightarrow \mathcal{C}_n \rightarrow \mathcal{C}_i$. Define the product of the associated rates in the 'forward' direction by $\Pi[\mathcal{L}] \equiv w_j^i w_k^j ... w_i^n$ and also for the 'reverse' direction: $\Pi[\mathcal{L}_{rev}] \equiv w_i^j w_j^k ... w_n^i$. The set of rates are said to satisfy detailed balance if and only if

$$\Pi[\mathcal{L}] = \Pi[\mathcal{L}_{rev}] \tag{9}$$

for *all loops.* If this criterion is satisfied, then we can show that a (single valued) functional in configuration space can be constructed simply from the set of ratios w_k^i/w_i^k, and that it is proportional to $P^*(\mathcal{C})$. If this criterion is violated for certain loops, these will be referred to here as 'irreversible rate loops' (IRLs). Despite the lack

---

‖ In this light, the sequence of configurations generated $(\mathcal{C}_{j_1}, \mathcal{C}_{j_2}, \ldots, \mathcal{C}_{j_\tau})$ can be regarded as a history, or trajectory, of the system. By collecting many (M) such sequences, $\left\{\mathcal{C}_j^\alpha\right\}, \alpha = 1, ..., M$, time dependent averages $\langle\mathcal{O}\rangle_\tau \equiv \sum_j \mathcal{O}(\mathcal{C}_j) P_j(\tau)$ are simulated by $M^{-1}\sum_\alpha \mathcal{O}\left(\mathcal{C}_{j_\tau}^\alpha\right)$.

of detailed balance, $P^*(\mathcal{C})$ exists and can still be constructed from the w's, though much more effort is required. Established some time ago [4, 63, 64], this approach to P^* is similar to Kirchhoff's for electric networks [65]. More importantly, this construction provides the framework for showing that, in the stationary state, some K^*'s must be non-trivial [66, 7]. Since the divergence of these currents must vanish, they must form current loops. As time-independent current loops, they remind us of magnetostatics. The distinction between this scenario and the case with detailed balance w's is clear: The latter resembles electrostatics. In this light, it is reasonable to label a stationary state as an equilibrium one if and only if *all* its (probability) currents vanish, associated with a set of w's with no IRLs. Similarly, a non-equilibrium steady state – NESS – would be associated with non-trivial current loops, generated by detailed balance-violating rates with IRLs [66, 7]. Our proposal is that all stationary states should be characterized by the pair $\{P^*, K^*\}$. In this scheme, 'equilibrium states' correspond to the subset $\{P^*, 0\}$, associated with a dynamics that respect detailed balance and time reversal.

The presence of current loops and IRLs raises a natural and intriguing question: Is there a intuitively accessible and simple relationship between them? Unfortunately, the answer remains elusive so far. Venturing further, it is tempting to speculate on the existence of a gauge theory, along the lines of that in electromagnetism, for NESM. If such a theory can be formulated, its consequences may be far-reaching.

Time-independent probability current loops also carry physical information about a NESS. Referring readers to a recent article [7] for the details, we provide brief summaries here for a few key points.

(i) In particular, it is shown how the K's can be used to compute currents associated with physical quantities, such as energy or matter. In addition, we have emphasized that a signature of NESS is the existence of a steady flux (of, e.g., energy) *through* the system. All aspects of such through-flux, such as averages and correlation, can also be computed with the K's.

(ii) Following Schnakenberg [63], we may define the *total* entropy production Σ_{tot} as a quantity associated with the rates $\{w_j^i\}$. This Σ_{tot} can be written as the sum of two terms, $\Sigma_{\text{sys}} + \Sigma_{\text{med}}$. The first is associated with entropy production within our system (recognizable as the derivative of the Gibbs' entropy, $-\sum_i P_i \ln P_i$, in the continuous time limit):

$$\Sigma_{\text{sys}}(\tau) \equiv \frac{1}{2} \sum_{i,j} K_i^j(\tau) \ln \frac{P_j(\tau)}{P_i(\tau)} . \tag{10}$$

It is straightforward to show that for a NESS with $K^* \neq 0$, Σ_{sys} vanishes as expected. However, a second contribution to entropy production is associated with the medium:

$$\Sigma_{\text{med}}(\tau) \equiv \frac{1}{2} \sum_{i,j} K_i^j(\tau) \ln \frac{w_i^j}{w_j^i}, \tag{11}$$

where the positivity of $\sum K_i^{*j} \ln(w_i^j / w_j^i)$ has been demonstrated. This result is entirely consistent with our description of a NESS, namely, a system coupled to surroundings which continue to evolve and generate entropy.

(iii) The following inverse question for NESS is also interesting. As we noted, given a Boltzmann distribution, a well known route to generate it is to use a dynamics which

obey detailed balance (8). If we accept that a NESS is characterised not only by the stationary distribution, but by the pair $\{P^*, K^*\}$, then the generalized condition is $w_k^i P_i^* = w_i^k P_k^* + K_k^{*i}$, or more explicitly,

$$w_k^i P^* \left(\mathcal{C}_i \right) = w_i^k P^* \left(\mathcal{C}_k \right) + K^* \left(\mathcal{C}_i \to \mathcal{C}_k \right). \tag{12}$$

It is possible to phrase this condition more elegantly (perhaps offering a little insight) by performing a well-known similarity transform on w_k^i: Define the matrix $\mathbb{U}$, the elements of which are

$$U_k^i \equiv (P_k^*)^{-1/2} \, w_k^i \, (P_i^*)^{1/2} .$$

The advantage of this form of 'coding' the dynamics is that $\mathbb{U}$ is symmetric if rates obey detailed balance. Meanwhile, since K^* is a current, we can exploit the analog $J = \rho v$ to define the 'velocity matrix' $\mathbb{V}$, the elements of which are

$$V_k^i \equiv (P_k^*)^{-1/2} \, K_k^{*i} \, (P_i^*)^{-1/2} ,$$

associated with the flow from $\mathcal{C}_i$ to $\mathcal{C}_k$. Our generalized condition (12) now reads simply: The antisymmetric part of $\mathbb{U}$ is $\mathbb{V}/2$. Similar ideas have also been pursued recently [67].

   To summarize, if a dynamics is to lead a system to a desired $\{P^*, K^*\}$, then the associated antisymmetric part of $\mathbb{R}$ is completely fixed by K^*. By contrast, its symmetric part is still unconstrained, corresponding to dynamics that takes us to the same $\{P^*, K^*\}$.

(iv) As long as $K^* \neq 0$ for a transition, we can focus on the direction with positive current (say, $K_k^{*i} > 0$) and choose the maximally asymmetric dynamics, namely, $w_i^k \equiv 0$ and $w_k^i = K_k^{*i}/P_i^*$. (Understandably, such choices are impossible for systems in thermal equilibrium, except for $T = 0$ cases.) Whether systems with such apparently unique dynamics carry additional significance remains to be explored. Certainly, TASEP – the paradigmatic model of NESS, to be presented next – belongs in this class. Before embarking on the next section, let us briefly comment on some typical features of NESS which are counter-intuitive, based on our notions of EQSM.

2.3. Beyond expectations of equilibrium statistical mechanics

Equilibrium statistical mechanics has allowed us to develop physical intuition that can be valuable guides when we are faced with new problems in unfamiliar settings. A good example is energy-entropy competition, which tends to serve us well when we encounter novel phase transitions: The former/latter 'wins' for systems at low/high temperatures, so that it displays order/disorder phenomena. Another example is 'positive response': To ensure thermodynamic stability, we expect the system to respond in a certain manner (positively) when its control parameters are changed. Thus, it is reasonable to expect, e.g., positive specific heat and compressibility for systems in thermal equilibrium. A final example is long-range correlations, which are generically absent in equilibrium systems with short-range interactions and dynamics. There are exceptions, of course, such as in critical phenomena associated with second order phase transitions. When we encounter systems in NESS however, we should be aware that such physical intuition often leads us astray. At present, we are not aware of another set of overarching principles which are generally applicable for NESS. Instead, in the following, we will provide two specific circumstances in which our expectations fail.

Negative response. In order for a system to be in thermal equilibrium, it must be stable against small perturbations. Otherwise, fluctuations will drive it into another state. Such consistent behaviors of a system may be labeled as 'positive response'. Related to the positivity of certain second derivatives of the free energy, elementary examples include positive specific heat and compressibility. By contrast, a surprisingly common hallmark of NESS is 'negative response.' For example, imagine a room in which the internal energy decreases when the thermostat is turned up! One of the first systems in NESS where this type of surprising behavior surfaced is the driven Ising lattice gas [36]. Referring the reader to, for example, reference [68] for details, the key ingredients are the following. An ordinary Ising system (with nearest neighbor ferromagnetic interactions on a square lattice) is subjected to an external drive, and observed to undergo the phase transition at a temperature *higher* than that expected from Onsager's solution. Since the external drive tends to break bonds, its effect is similar to coupling the system to another energy reservoir with a *higher* temperature. Nevertheless, this NESS system displays more order than its equilibrium counterpart. In other words, despite the fact that more energy appears to be 'pumped into' the system, the internal energy decreases. A more direct manifestation of this form of 'negative response' has been observed in the two-temperature Ising lattice gas, in which particle hops in the x or y direction are updated by Metropolis rates appropriate to exchanging energy with a thermal reservoir set at temperature T_x or T_y. Changing T_x, with T_y held fixed, the average internal energy, U (i.e., $\langle \mathcal{H} \rangle$), is found to vary with $\partial U / \partial T_y < 0$ [69]! Such surprising negative response is so generic that it can be found in exceedingly simple, exactly solvable cases [70].

Of course, we should caution the reader that 'negative response' may be simply a misnomer, poor semantics, or careless interpretation of an observed phenomenon. After all, fluctuations of observables in a stationary state must be positive and if the appropriate conjugate variable is used, then the response to that variable will again be positive. In particular, for any observable $\mathcal{O}$, we can always define the cumulant generating function $\Xi(\omega) \equiv \ln \langle e^{\omega \mathcal{O}} \rangle$ and its derivative $X(\omega) \equiv \Xi'(\omega)$. Of course, the average $\langle \mathcal{O} \rangle$ is $\Xi'(0)$, while $X(\omega)$ is, in general, the average of $\mathcal{O}$ in the *modified distribution* $\tilde{P}^*(\mathcal{C}) \propto e^{\omega \mathcal{O}(\mathcal{C})} P^*(\mathcal{C})$. Then, we are guaranteed 'positive response:' $\partial X / \partial \omega > 0$. However, unlike internal energy and temperature for systems in thermal equilibrium, simple physical interpretations of these mathematical manipulations for NESS's are yet to be established. Clearly, this issue is related to the fluctuation-dissipation theorem in EQSM. General results valid for NESM have been derived during the last two decades; we refer the reader to the seminal articles [71, 72, 73, 27, 28]. The generalization of the fluctuation-dissipation theorem to NESM is a major topic [74, 34] and lies outside our scope. Here, let us remark that the foundations of this theorem lies in the time reversal properties of the underlying dynamics [75, 76], which control the nature of the fluctuations of the random variables. To characterize these fluctuations quantitatively, large-deviation functions (LDF) have been introduced. They play a crucial role in NESM, akin to that of thermodynamic potentials in EQSM [77, 78]. Valid for systems far from equilibrium, the fluctuation theorem can be stated as a symmetry property of the LDF (see the next section for a explicit example in the case of TASEP). Near an equilibrium state this theorem implies the fluctuation-dissipation relation, previously derived from linear response theory [79, 80]. A related set of significant results is the non-equilibrium work relations [27, 32, 29, 28, 30, 35, 33, 34, 31], also a topic worthy of its own review (see, e.g., [81, 82] and references therein). Here, in the context of the exact solution of TASEP (section

3), another result along this theme – the macroscopic fluctuation theory developed by Jona-Lasinio *et al.* [83] – plays an important role.

Generic long-range correlations. For systems with short-range interactions in thermal equilibrium, the static (i.e., equal time) correlations of the fluctuations are generically short-ranged. This is true even if the dynamics were to contain long ranged components (e.g., the 'artificial' Swendsen-Wang [54] dynamics): As long as it obeys detailed balance, we are assured of $P^* \propto e^{-\beta\mathcal{H}}$. Of course, time-dependent correlations are *not* similarly constrained. An excellent example is diffusive dynamics obeying certain conservation laws (e.g., hydrodynamics or Kawasaki [60, 61] dynamics modeling Cu-Zn exchange), where long time tails (power law decays) are well known phenomena: The autocorrelation function, $G(r = 0, t)$, decays as $t^{-d/2}$ in d dimensions, even for a single particle. As pointed out by Grinstein [84], a simple scaling argument, along with $r \sim t^{1/z}$, would lead to *generic* long-range correlations, $G(r, t = 0) \to Ar^{-zd/2}$ (i.e., r^{-d} in the case of random walkers subjected to short-range interactions, where $z = 2$). Yet, $G(r, t = 0)$ generally decays as an exponential in equilibrium systems! These seemingly contradictory statements can be reconciled when the amplitude A is examined. In the equilibrium case, detailed balance (or the fluctuation-dissipation theorem) constrains A to vanish. For NESS, there is no such constraint, leaving us with long-range correlations generically. For further details of these considerations, the reader may consult references [68, 85].

To end the discussion on such correlations, we should caution the readers on a subtle point. Although we emphasized how long-range correlations can emerge from a short-range dynamics that violates detailed balance, the latter is not *necessary*. An excellent example is a driven diffusive system with three species – the ABC model [86, 87] – in one dimension. The system evolves with a short-range dynamics which generally violate detailed balance, and displays long-range *order* (as well as correlations). Remarkably, for a special set of parameters, detailed balance is restored and so, an exact P^* was easily found. When interpreted as a Boltzmann factor (i.e., $P^* \propto e^{-\beta\mathcal{H}}$), the Hamiltonian contains inter-particle interactions which range over the entire lattice! Despite having an $\mathcal{H}$ with long-range interactions, it is possible to construct a short-range dynamics (e.g., w's that involve only nearest neighbor particle exchanges) that will lead the system to an EQSS: $\{P^* \propto e^{-\beta\mathcal{H}}, K^* \equiv 0\}$. To appreciate such a counter-intuitive situation, consider $\Delta\mathcal{H} = \mathcal{H}(\mathcal{C}_i) - \mathcal{H}(\mathcal{C}_j)$ for a pair of configurations that differ in some local variables. The presence of long-range terms in $\mathcal{H}$ typically induce similar terms in $\Delta\mathcal{H}$, leading to a long-range dynamics. If such terms conspire to cancel, then $\Delta\mathcal{H}$ becomes short-ranged and it is simple to choose w's with no long range components. We believe it is important to investigate whether such examples belong to a class of mathematical curiosities or form the basis for a wide variety of physical/biological systems. With these two examples, we hope to have conveyed an important lesson we learned from our limited explorations of NESS: Expect the unexpected, when confronted with a novel system evolving according to detailed balance violating dynamics.

In this section, we attempted to provide a bird's eye view of the many facets of non-equilibrium statistical mechanics, and then to focus on a particular aspect: stationary states associated with dynamics that violate detailed balance. We emphasized the importance of this class of problems and pointed out significant features of NESS that run counter to the physical intuition learned from equilibrium statistical mechanics. In the next two sections, we will turn our attention to specific systems. As common in all theoretical studies, there are two typically diverging goals

associated with the models we pursue. One goal is to account for as many features found in nature as realistically possible. The other is to consider models with just one or two features so that they are simple enough to be solved analytically and exactly. These goals obviously diverge since more realistic models are typically mathematically intractable while exactly solvable models generally lack essential aspects of physical systems (or those in chemistry, biology, finance, sociology, etc.). Nevertheless, we believe is it worthwhile to devote our attention to both of them, albeit separately. In this spirit, we will next present a simple model: the exclusion process, with the TASEP being an extreme limit. Arguably the simplest possible model with a nontrivial NESS, the TASEP is not only amenable to exact and approximate solution strategies, but it also has shed considerable light on problems in the real world. In section (4), we turn to a number of generalizations of this model, each taking into account new physical features required for modeling various aspects of transport in biological systems.

3. A paradigmatic model: The asymmetric simple exclusion process (ASEP)

Building a simple representation for complex phenomena is a common procedure in physics, leading to the emergence of paradigmatic models: the harmonic oscillator, the random walker, the Ising magnet. All these beautiful models often display wonderful mathematical structures [88, 89]. In the field of NESM, and for investigating the role of detailed balance violating dynamics in particular, the asymmetric simple exclusion process (ASEP) is reaching the status of such a paradigm. A model with possibly the simplest of rules, it nevertheless displays a rich variety of NESS's. Further, it is sufficiently simple to allow us to exploit rigorous mathematical methods and, over the last two decades, to arrive at a number of exact results. In this way, valuable insights into the intricacies of NESM have been garnered. In this section, we delve into some details of two such methods, in the hope that readers unfamiliar with these techniques can join in these efforts. Of course, as we consider models which are more suited for physical/biological systems, we will encounter more complex ingredients than in ASEPs. As a result, these models are not exactly solvable at present. In these cases, approximations are necessary for further progress. One successful scheme is the mean field approximation, leading to hydrodynamics equations (PDE's) for density fields. Since this strategy is the only one to offer some quantitative understanding of the more realistic/complex models, we will devote the last subsection 3.11 here to this approach.

   In the previous section, we presented the master equation (1) in discrete time, which is clearly the most appropriate description for computer simulations. On the other hand, for analytic studies, it is often far easier to use continuous variables (or infinite systems, in a similar vein). Thus, all the discussions in this section will be based on continuous time, t. As discussed in the context of the Fokker-Planck equation (6), we introduced this connection: $t = \tau \delta t$. Here, let us be explicit and write the continuous version of equation (2) as

$$\partial_t P_i(t) = \sum_j M_i^j P_j(t) \tag{13}$$

where the matrix on the right, $\mathbb{M}$, is just $\mathbb{L}/\delta t$. Taking the limit $\delta t \to 0$ in the formal solution, $P(\tau) = [\mathbb{I} + \mathbb{L}]^\tau P(0)$ ($\mathbb{I}$ being the identity), leads then to $P(t) = \exp[\mathbb{M}t] P(0)$.

3.1. Motivation and definition of ASEP and TASEP

The ASEP is a many-body dynamical system, consisting of particles located on a discrete lattice that evolves in continuous time. The particles hop randomly from a site on a lattice to one of its immediate neighbors, provided the target site is empty. Physically, this constraint mimics short-range interactions amongst particles. In order to drive this lattice gas out of equilibrium, non-vanishing currents must be established in the system. This can be achieved by various means: by starting from non-uniform initial conditions, by coupling the system to external reservoirs that drive currents [90] through the system (transport of particles, energy, heat), or by introducing some intrinsic bias in the dynamics that favors motion in a privileged direction. Then, each particle is an asymmetric random walker that drifts steadily along the direction of an external driving force. Due to its simplicity, this model has appeared in different contexts. As noted in the Introduction, it was first proposed by Gibbs, *et al.* in 1968 [13, 14] as a prototype to describe the dynamics of ribosomes translating along an mRNA. In the mathematical literature, Brownian processes with hard-core interactions were defined in 1970 by Spitzer [9] who coined the term 'exclusion process' (see also [91, 92, 11, 10]). In addition to motivation from issues in molecular biology – the main focus of section 4, the ASEP has also been used to describe transport in low-dimensional systems with strong geometrical constraints [93] such as macromolecules transiting through anisotropic conductors, or quantum dots, where electrons hop to vacant locations and repel each other via Coulomb interaction [94], while many of its variants are ubiquitous in modeling traffic flow [95, 15]. More generally, the ASEP belongs to the class of driven diffusive systems defined by Katz, Lebowitz and Spohn in 1984 [36, 68, 12, 96, 93]. We emphasize that the ASEP is defined through dynamical rules, while no energy is associated with a microscopic configuration. More generally, the kinetic point of view seems to be a promising and fruitful approach to non-equilibrium systems (see e.g., [97]).

To summarize, the ASEP is a minimal model to study non-equilibrium behavior. It is simple enough to allow analytical studies, however it contains the necessary ingredients for the emergence of a non-trivial phenomenology:

- *Asymmetric*: The external driving breaks detailed balance and creates a stationary current. The system settles into a NESS.
- *Exclusion*: The hard-core interaction implies that there is at most one particle per site. The ASEP is a genuine many-body problem, with arguably the simplest of all interactions.
- *Process*: With no underlying Hamiltonian, the dynamics is stochastic and Markovian.

Having a general picture of an ASEP, let us turn to a complete definition of the model. Focusing on only exactly solvable cases, we restrict ourselves here to a one dimensional lattice, with sites labeled by $i = 1, ..., L$ (here, we will use i to label a site rather than a configuration). The stochastic evolution rules are the following: A particle located at site i in the bulk of the system jumps, in the interval $[t, t + \mathrm{d}t]$, with probability $p\mathrm{d}t$ to site $i + 1$ and with probability $q\mathrm{d}t$ to site $i - 1$, provided the target site is empty (*exclusion rule*). The rates p and q are the parameters of our system. By rescaling time, p is often set to unity, while q is left as a genuine control parameter. In the totally asymmetric exclusion process (TASEP), the jumps are totally biased in one direction (e.g., $q = 0$). On the other hand, the *symmetric* exclusion process (SEP)

647 corresponds to the choice $p = q$. The physics and the phenomenology of the ASEP is
648 extremely sensitive to the boundary conditions. We will mainly discuss three types of
649 boundary conditions:

650 *Periodic boundary conditions:*

651   The exclusion process is defined on a ring, so that sites i and $L + i$ are identical.
652 The system is filled with $N \leq L$ particles (figure 1(a)). Of course, the dynamics
653 conserves N.

654 *Infinite lattice:*

655   Here, the boundaries are sent to $\pm\infty$. Boundary conditions are here of a different
656 kind. This system always remains sensitive to the initial conditions. Therefore, an
657 initial configuration, or a statistical set of configurations, must be carefully specified.
658 Figure 1(b) is an illustration of this system.

659 *Open boundaries:*

660   Here, the boundary sites $i = 1, L$ play a special role, as they are coupled to
661 particles in reservoirs just outside the system. Thus, if site 1 is empty, a particle can
662 enter (from the 'left reservoir') with rate α. If it is occupied, the particle can exit
663 (into this reservoir) with rate γ. Similarly, the interactions with the 'right reservoir'
664 are: If site L is empty/occupied, a particle can enter/exit the system with rate δ/β
665 respectively. These rates can be regarded as the coupling of our finite system with
666 infinite reservoirs set at different 'potentials'. Figure 1(c) illustrates this system. A
667 much simpler limiting case is the TASEP, with $q = \gamma = \delta = 0$, in which particles
668 injected from the left, hopping along the lattice only to the right, and finally exiting
669 to the right.
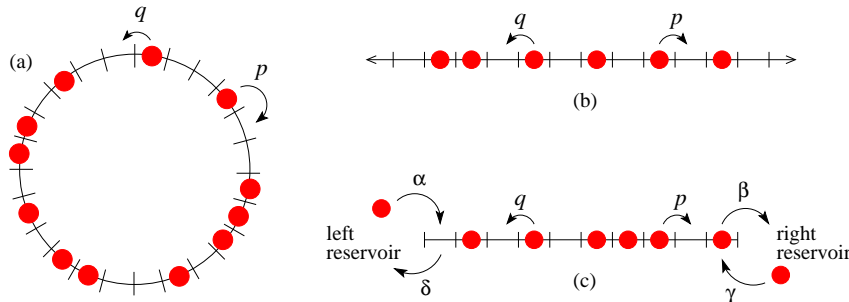
Figure 1. (a) The asymmetric simple exclusion process on a ring of L sites filled
with N particles ($L = 24$, $N = 12$ here). The total number of configurations is
just $\Omega = \binom{L}{N}$. (b) ASEP on an infinite lattice. The particles perform asymmetric
random walks ($p \neq q$) and interact through the exclusion constraint. (c) A
schematic of a ASEP with open boundaries on a finite lattice with $L = 10$ sites.

670   We emphasize that there are very many variants of the ASEP. The dynamical
671 rules can be modified, especially in computer simulation studies using discrete-time
672 updates (e.g., random sequential, parallel, or shuffle updates). The hopping rates
673 can be modified to be either site- or particle-dependent, with motivations for such
674 additions from biology provided below. In modeling vehicular traffic, the former is
675 suitable, e.g., for including road work or traffic lights. The latter can account for the
676 range of preferred driving velocities, while a system can also be regarded as one with

many 'species' of particles. In addition, these disorders can be dynamic or quenched [98, 99, 100, 101, 102, 103, 104, 105]. Further, the exclusion constraint can be relaxed, so that fast cars are allowed to overtake slower ones, which are known as 'second class' or 'third class' particles [106, 107, 108, 109, 110, 111, 112]. Finally, the lattice geometry itself can be generalized to multi-lanes, higher dimensions, or complex networks. All these modifications drastically alter the collective behavior displayed in the system, as hundreds of researchers discovered during the last two decades. Though more relevant for applications, more realistic models cannot, in general, be solved exactly. As the primary focus of this section is exact solutions, we will focus only on the homogeneous systems presented above. These problems are amenable to sophisticated mathematical analysis thanks to a large variety of techniques: Bethe Ansatz, quadratic algebras, Young tableaux, combinatorics, orthogonal polynomials, random matrices, stochastic differential equations, determinantal representations, hydrodynamic limits etc. Each of these approaches is becoming a specific subfield that has its own links with other branches of theoretical physics and mathematics. Next, we will present some of these methods that have been developed for these three ideal cases.

3.2. Mathematical setup and fundamental issues

The evolution of the system is given by equation (13) and controlled by the Markov operator $\mathbb{M}$ as follows. In order distinguish the two uses of i – label for configurations and for sites on our lattices, let us revert to using $\mathcal{C}$ for configurations. Then, this master equation reads

$$\frac{dP(\mathcal{C}, t)}{dt} = \sum_{\mathcal{C}'} M(\mathcal{C}, \mathcal{C}')P(\mathcal{C}', t). \tag{14}$$

As a reminder, the off-diagonal matrix elements of $\mathbb{M}$ represent the transition rates, which the diagonal part $M(\mathcal{C}, \mathcal{C}) = -\sum_{\mathcal{C}' \neq \mathcal{C}} M(\mathcal{C}', \mathcal{C}')$ accounts for the exit rate from $\mathcal{C}$. Thus, the sum of the elements in any given column vanishes, ensuring probability conservation. For a finite ASEP, $\{\mathcal{C}\}$ is finite and the Markov operator $\mathbb{M}$ is a matrix. For the infinite system, $\mathbb{M}$ is an operator and its precise definition needs more sophisticated mathematical tools than linear algebra, namely, functional analysis [92, 10]. Unless stated otherwise, we will focus here on the technically simpler case of finite L and deduce results for the infinite system by taking $L \to \infty$ limit formally. An important feature of the finite ASEP is ergodicity: Any configuration can evolve to any other one in a finite number of steps. This property ensures that the Perron-Frobenius theorem applies (see, e.g., [45, 113]). Thus, $E = 0$ is a non-degenerate eigenvalue of $\mathbb{M}$, while all other eigenvalues have a strictly negative real part, $\text{Re}(E) < 0$. The physical interpretation of the spectrum of $\mathbb{M}$ is clear: The right eigenvector associated with the eigenvalue $E = 0$ corresponds to the stationary state of the dynamics. Because all non-zero eigenvalues have strictly negative real parts, these eigenvectors correspond to relaxation modes, with $-1/\text{Re}(E)$ being the relaxation time and $\text{Im}(E)$ controlling the oscillations.

We emphasize that the operator $\mathbb{M}$ encodes all statistical information of our system, so that any physical quantity can be traced ultimately to some property of $\mathbb{M}$. We will list below generic mathematical and physical properties of our system that motivate the appropriate calculation strategies:

(i) Once the dynamics is properly defined, the basic question is to determine the steady-state, P^*, of the system, i.e., the right eigenvector of $\mathbb{M}$ with eigenvalue

0. Given a configuration $\mathcal{C}$, the value of the component $P^*(\mathcal{C})$ is known as the measure (or stationary weight) of $\mathcal{C}$ in the steady-state, i.e., it represents the frequency of occurrence of $\mathcal{C}$ in the stationary state.

(ii) The vector P^* plays the role of the Boltzmann factor in EQSM, so that all steady-state properties (e.g., all equal-time correlations) can be computed from it. Some important questions are: what is the mean occupation ρ_i of a given site i? What does the most likely density profile, given by the function $i \to \rho_i$, look like? Can one calculate density-density correlation functions between different sites? What is the probability of occurrence of a density profile that differs significantly from the most likely one? The last quantity is known as the large deviation of the density profile.

(iii) The stationary state is a dynamical state in which the system constantly evolves from one micro-state to another. This microscopic evolution induces macroscopic fluctuations (the equivalent of the Gaussian Brownian fluctuations at equilibrium). How can one characterize such fluctuations? Are they necessarily Gaussian? How are they related to the linear response of the system to small perturbations in the vicinity of the steady-state? These issues can be tackled by considering tagged-particle dynamics, anomalous diffusion, time-dependent perturbations of the dynamical rules [114].

(iv) As expected, the ASEP carries a finite, non-zero, steady-state particle current, J, which is clearly an important physical observable. The dependence of J on the external parameters of the system allows us to define different phases of the system.

(v) The existence of a non-zero J in the stationary state implies the physical transport of an extensive number of particles, Q, through the lattice. The total number of particles Q_t, transported up to time t is a random quantity. In the steady-state, the mean value of Q_t is just Jt, while in the long time limit, the distribution of the random variable $Q_t/t - J$ represents exceptional fluctuations (i.e., large deviations) of the mean-current. This LDF is an important observable that provides detailed properties of the transport through the system. While particle current is the most obvious quantity to study in an ASEP, similar questions can be asked of other currents and the transport of their associated quantities, such as mass, charge, energy, etc., in more realistic NESM models.

(vi) The way a system relaxes to its stationary state is also an important characteristic. The typical relaxation time of the ASEP scales with the system size as L^z, where z is the dynamical exponent. The value of z is related to the spectral gap of the Markov matrix $\mathbb{M}$, i.e., to the largest $-\mathrm{Re}(E)$. For a diffusive system, $z = 2$. For the ASEP with periodic boundary condition, an exact calculation leads to $z = 3/2$. More generally, the transitory state of the model can be probed using correlation functions at different times.

(vii) The matrix $\mathbb{M}$ is generally a non-symmetric matrix and, therefore, its right eigenvectors differ from its left eigenvectors. For instance, a right eigenvector ψ_E corresponding to the eigenvalue E is defined as

$$\mathbb{M}\psi = E\psi. \tag{15}$$

Because $\mathbb{M}$ is real, its eigenvalues (and eigenvectors) are either real numbers or complex conjugate pairs. However, M is generally asymmetric, so that its

768 left eigenvectors are different from its right eigenvectors. Powerful analytical
769 techniques, such as the Bethe Ansatz, can be exploited to diagonalize $\mathbb{M}$ in some
770 specific cases, providing us with crucial information on its spectrum.

771 (viii) Solving the master equation (14) analytically would allow us to calculate exactly
772 the evolution of the system. A challenging goal is to determine the finite-time
773 Green function (or transition probability) $P(\mathcal{C}, t|\mathcal{C}_0, 0)$, the probability for the
774 system to be in configuration $\mathcal{C}$ at time t, given that the initial configuration at
775 time $t = 0$ was $\mathcal{C}_0$. Formally, it is just the $\mathcal{C}, \mathcal{C}_0$ element of the matrix $\exp[\mathbb{M}t]$
776 here. In principle, it allows us to calculate all the correlation functions of the
777 system. However, explicit results for certain quantities will require not only the
778 knowledge of the spectrum and eigenvectors of $\mathbb{M}$, but also explicit evaluations of
779 matrix elements associated with the observable of interest.

780 The following sections are devoted to a short exposition of several analytical
781 techniques that have been developed to answer some of these issues for the ASEP.

782 *3.3. Steady state properties of the ASEP*

783 Given a stochastic dynamical system, the first question naturally concerns the
784 stationary measure. We will briefly discuss the ASEP with periodic boundary
785 conditions and the infinite line case. More details will be provided for the highly
786 non-trivial case of the open ASEP.

787

788 *Periodic boundary conditions:*
789 This is the simplest case, with the stationary measure being flat [96]. That the
790 uniform measure is also stationary can be understood as follows. A given configuration
791 consists of k clusters of particles separated by holes. A particle that leads a cluster can
792 hop in the forward direction with rate p whereas a particle that ends a cluster can hop
793 backwards with rate q; thus the total rate of leaving a configuration consisting of k
794 clusters is $k(p+q)$. Similarly, the total number of *ancestors* of this configuration (i.e.,
795 of configurations that can evolve into it) is also given by $k(p+q)$. The fact that these
796 two quantities are identical suffices to show that the uniform probability is stationary.
797 To obtain the precise value of P^*, $1/\Omega$, is also elementary. Since N is a constant, we
798 only need the total number of configurations for N particles on a ring with L sites,
799 which is just $\Omega = L!/[N!(L-N)!]$.

800

801 *Infinite lattice:*
802 For the exclusion process on an infinite line, the stationary measures are studied
803 and classified in [92, 11]. There are two one-parameter families of invariant measures.
804 One family, denoted by ν_ρ, is a product of local Bernoulli measures of constant density
805 ρ: this means that each site is occupied with probability ρ. The other family is
806 discrete and is concentrated on a countable subset of configurations. For the TASEP,
807 this second family corresponds to *blocking measures*, which are point-mass measures
808 concentrated on step-like configurations (i.e., configurations where all sites to the
809 left/right of a given site are empty/occupied).

810

811 *Open boundaries:*
812 Turning to the case of the ASEP on a finite lattice with open boundaries, we
813 note that the only knowledge we have, without detailed analysis, is the existence of a

unique stationary measure (thanks to the Perron-Frobenius theorem), i.e., the vector P^* with 2^L components. We emphasize again that finding P^* is a non-trivial task because we have no *a priori* guiding principle at our disposal. With no underlying Hamiltonian and no temperature, no fundamental principles of EQSM are relevant here. The system is far from equilibrium with a non-trivial steady-state current that does not vanish for even large L.

To simplify the discussion, we focus on the TASEP where particles enter from the left reservoir with rate α, hop only to the right and leave the system from the site L with rate β. A configuration $\mathcal{C}$ can be represented by the binary string, $(\sigma_1, \ldots, \sigma_L)$, of occupation variables: $\sigma_i = 1$ if the site i is occupied and $\sigma_i = 0$ otherwise. Our goal is to determine $P^*(\mathcal{C})$, with which the steady-state current J can be expressed simply and *exactly*:

$$J = \alpha\left(1 - \langle\sigma_1\rangle\right) = \langle\sigma_1(1 - \sigma_2)\rangle = \ldots = \langle\sigma_i(1 - \sigma_{i+1})\rangle = \beta\langle\sigma_L\rangle. \quad (16)$$

Here, the brackets $\langle\ \rangle$ denote expectation values as defined in equation (7). Even if J were known somehow, this set of equations is not sufficient for fixing the (unknown) density profile $\rho_i = \langle\sigma_i\rangle$ and the nearest neighbor (NN) correlations $\langle\sigma_i\sigma_{i+1}\rangle$. Typical in a truly many-body problem, there is a hierarchy [115, 116, 117, 47] of equations that couple k-site and $(k+1)$-site correlations. A very important approximation, which often provides valuable insights, is the *mean-field assumption* in which the hierarchy is simply truncated at a given level. If the correlations beyond this level are small, this approximation can be quite good. Applying this technique here consists of replacing two-sites correlations by products of single-site averages:

$$\langle\sigma_i\sigma_j\rangle \to \langle\sigma_i\rangle\langle\sigma_j\rangle = \rho_i\rho_j. \quad (17)$$

Thus, equation (16) becomes

$$J \simeq \alpha\left(1 - \rho_1\right) = \rho_1(1 - \rho_2) = \ldots = \rho_i(1 - \rho_{i+1}) = \beta\rho_L. \quad (18)$$

and we arrive at a closed recursion relation between ρ_{i+1} and ρ_i, namely $\rho_{i+1} = 1 - J/\rho_i$. Of course, J is an unknown, to be fixed as follows. Starting with $\rho_1 = 1 - J/\alpha$, the recursion eventually leads us to ρ_L as a rational function of J (and α). Setting this to J/β gives a polynomial equation for J. Solving for J, we obtain the desired dependence of the steady-state current on the control parameters: $J(\alpha, \beta, L)$. This approach to an approximate solution was known to Gibbs, *et al.* [13, 14] (within the context of a more general version of TASEP) and explored further in [118] recently.

Analyzing $J(\alpha, \beta, L)$ gives rise to the phase diagram of the TASEP (see figure 2). For studying these aspects of the TASEP, the mean-field method provides us with a reasonably good approximation. Indeed, the correct phase diagram of the model was obtained in [90] ¶ through physical reasoning by using such mean-field arguments along with the hydrodynamic limit. Since this strategy is quite effective and more widely applicable, we will briefly discuss how it is applied to ASEP in section 3.11 below. Despite many effective MFT-based strategies, exact solutions to ASEP are desirable, especially for an in-depth analysis. In particular, MFT cannot account for correlations, fluctuations, or rare events. In fact, the mean-field density profile (from solving the recursion relation (18) numerically) does not agree with the exact profile (from evaluating the expression (23) below). Of course, it is rare that we are able to calculate the stationary measure for a non-equilibrium interacting model. Not surprisingly, the exact steady-state solution of the TASEP [118, 120, 121] was considered a major breakthrough.

¶ See also [10] and [119] for a pedagogical example.

860 *3.4. The matrix representation method for the open TASEP*

861 The exact calculation of the stationary measure for the TASEP with open boundaries
862 and the derivation of its phase diagram triggered an explosion of research on exactly
863 solvable models in NESM. The fundamental observation [118] is the existence of
864 recursion relations for the stationary probabilities between systems of different sizes.
865 These recursions are particularly striking when $\alpha = \beta = 1$ [118]; they can be
866 generalized to arbitrary values of α and β [121, 120] and also to the more general
867 case in which backward jumps are allowed (also known as a partially asymmetric
868 exclusion process, or PASEP). The most elegant and efficient way to encode these
869 recursions is to use the matrix Ansatz [120]. We caution readers that the matrices
870 to be presented in this subsection have nothing to do with the transition matrices $\mathbb{M}$
871 discussed above. They do not represent the intrinsic physics of TASEP, but instead,
872 provide a convenient framework for representing the algebra that arises from the
873 recursion relations. In particular, we need only two matrices ($\mathbf{D}$ and $\mathbf{E}$) and two
874 'eigenvectors' (a bra $\langle W|$ and a ket $|V\rangle$, normalized by $\langle W|V\rangle = 1$) here. The algebra
875 we need is

$$
\begin{aligned}
\mathbf{DE} &= \mathbf{D} + \mathbf{E} \\
\mathbf{D}\,|V\rangle &= \frac{1}{\beta}|V\rangle \\
\langle W|\,\mathbf{E} &= \frac{1}{\alpha}\langle W|\ .
\end{aligned}
\tag{19}
$$

876 We emphasize that in general the operators $\mathbf{D}$ and $\mathbf{E}$ do not commute with each other,
877 so that an explicit representation would be typically infinite dimensional.

878 Remarkably, it was shown that the stationary $P^*(\mathcal{C})$ for TASEP can be written
879 as the scalar

$$
P^*(\sigma_1,\ldots,\sigma_L) = \frac{1}{Z_L}\langle W|\prod_{i=1}^{L}(\sigma_i\mathbf{D} + (1-\sigma_i)\mathbf{E})\,|V\rangle\,.
\tag{20}
$$

881 where

$$
Z_L = \langle W|\,(\mathbf{D} + \mathbf{E})^L\,|V\rangle
\tag{21}
$$

883 is a normalization constant. Each operation of the matrices $\mathbf{D}$ or $\mathbf{E}$ is associated with
884 a filled or empty site on the lattice. For example, the weight of the configuration shown
885 in figure 1(c) is $\langle W|\mathbf{EDDEDEDEDE}|V\rangle/Z^{10}$. To obtain explicit values for (20), one
886 method is to find an explicit representation of this algebra. Another possibility is
887 to use systematically the algebraic rules (19) without referring to any representation.
888 Indeed, a product of $\mathbf{D}$'s and $\mathbf{E}$'s in an arbitrary order can be decomposed as a linear
889 combination of monomials of the type $\mathbf{E}^n\mathbf{D}^m$ by using repeatedly the rule $\mathbf{DE} = \mathbf{D}+\mathbf{E}$.
890 Then, using $\langle W|\mathbf{E}^n\mathbf{D}^m\,|V\rangle = \alpha^{-n}\beta^{-m}$, we find that any matrix element of the type
891 (20) is a polynomial in $1/\alpha$ and $1/\beta$. In particular, we find the following general
892 formula [120] for Z_L:

$$
\begin{aligned}
Z_L &= \langle W|\,(\mathbf{D} + \mathbf{E})^L\,|V\rangle \\[2mm]
&= \sum_{p=1}^{L} \frac{p\,(2L-1-p)!}{L!\,(L-p)!}\frac{\beta^{-p-1} - \alpha^{-p-1}}{\beta^{-1} - \alpha^{-1}}.
\end{aligned}
\tag{22}
$$

When $\alpha = \beta = 1$, Z_L is a Catalan number [120]. Another special case is $\alpha = 1 - \beta$, for which the scalar representation, $\mathbf{D} = 1/\beta, \mathbf{E} = 1/\alpha$, suffices and P^* simplifies greatly. In all cases, quantities of physical interest (current, profile, correlations) can be explicitly computed using the algebra (19). In this sense, the TASEP is 'solved:' All equal time correlations in the stationary state are known.

The matrix method may look puzzling at first sight. One informal way to motivate it is the following: the steady state weight of a configuration cannot be expressed in general as a product of single site occupancy or vacancy probabilities because in the presence of interactions there are non-zero correlations (i.e., mean-field theory is not exact). However, by writing the stationary measure as a product of matrices, a sort of factorization still holds and at the same time correlations are taken into account by the fact that the matrices do not commute.

3.5. Phase diagram of the open TASEP

Thanks to the matrix representation method, exact expressions for the phase diagram of the TASEP, as well as stationary equal-time correlations and density profiles, can be readily obtained. For example, the mean occupation of a site i (with $1 \leq i \leq L$) is given by

$$\langle \sigma_i \rangle = \frac{1}{Z_L} \langle W | (\mathbf{D} + \mathbf{E})^{i-1} \mathbf{D} (\mathbf{D} + \mathbf{E})^{L-i} | V \rangle. \tag{23}$$

This expression is obtained by summing over all configurations in which site i is occupied.

Similarly, the average value of the steady state current J through the "bond" connecting site i and $i+1$ can be calculated as

$$
\begin{aligned}
J(\alpha, \beta, L) &= \langle \sigma_i (1 - \sigma_{i+1}) \rangle \\[2mm]
&= \frac{1}{Z_L} \langle W | (\mathbf{D} + \mathbf{E})^{i-1} \mathbf{D}\mathbf{E} (\mathbf{D} + \mathbf{E})^{L-i-1} | V \rangle \\[2mm]
&= \frac{Z_{L-1}}{Z_L},
\end{aligned}
\tag{24}
$$

where we have used the algebra (19). We note that this value does not depend on the specific bond considered. This was expected because particles are neither created nor destroyed in the system.

In the limit of large system sizes, the phase diagram (figure 2) consists of three main regions

- In the *Low-Density Phase*, when $\alpha < \min\{\beta, 1/2\}$, the bulk-density is $\rho = \alpha$ and the average current $J = \alpha(1 - \alpha)$ is a function only of the rate-limiting injection process.

- In the *High Density phase*, when $\beta < \min\{\alpha, 1/2\}$, the typical density is characterized by $\rho = 1 - \beta$ and the steady-state current, $J = \beta(1 - \beta)$, is a function only of the rate-limiting extraction step.

- In the *Maximal Current Phase*, when $\alpha > 1/2$ and $\beta > 1/2$, the bulk behavior is independent of the boundary conditions and one finds $\rho = 1/2$ and $J = 1/4$. In this phase, particle-particle correlations decay only algebraically away from the

boundaries, in contrast to exponentially decaying correlations in both the low and high density phases.

- The low and high density phases are separated by the 'shock-line', $\alpha = \beta \leq 1/2$, across which the bulk-density is discontinuous. In fact, the profile on this line is a mixed-state of shock-profiles interpolating between the lower density $\rho = \alpha$ and the higher density $\rho = 1 - \beta$.

Detailed properties of the phase diagram are reviewed in [96, 122, 123].
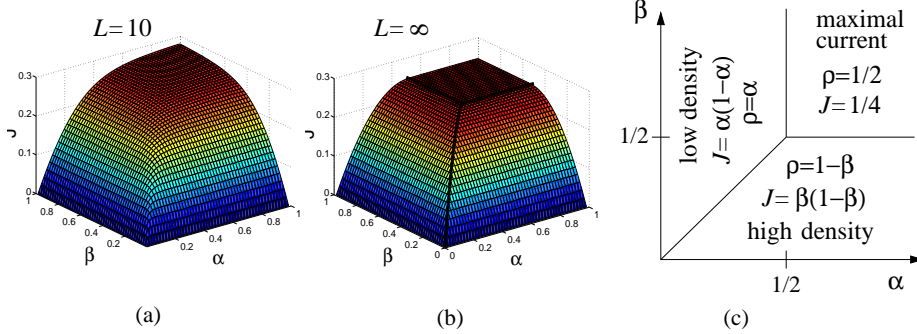
Figure 2. (a) Exact solution (derived from eqs. (24) and (22) for the steady-state current J of a TASEP with $L = 10$ sites. (b) The steady-state current J plotted in the $L \to \infty$ limit. (c) The phase diagram for the current of an infinite lattice ($L = \infty$) TASEP as a function of the injection and extraction rates.

The particle density profiles in the large L limit, described in each phase above, are only approximately uniform in that they are asymptotically accurate only in the bulk, but must vary near the boundaries in order to satisfy conditions determined by the steady-state particle injection and extraction [124]. It turns out that the MFT approaches, recursion and hydrodynamic equations, reproduce the exact $L \to \infty$ phase diagram; however, the matrix product approach finds the correct density profile which is not obtained by mean-field approximations.

3.6. Some extensions of the matrix Ansatz

Extension to the general ASEP model:

If we allow jumps in both directions and entrance/exit at both ends of the system, the matrix technique can still be applied. The algebra (19) must be replaced by the more general rules

$$
\begin{aligned}
p\,\mathbf{D}\,\mathbf{E} - q\,\mathbf{E}\,\mathbf{D} &= \mathbf{D} + \mathbf{E} \\
(\beta\mathbf{D} - \delta\mathbf{E})\,|V\rangle &= |V\rangle \\
\langle W|\,(\alpha\,\mathbf{E} - \gamma\,\mathbf{D}) &= \langle W|\,.
\end{aligned}
\tag{25}
$$

This new algebra allows one to calculate the general phase diagram of the open ASEP using orthogonal polynomials [125, 123, 126, 127]. The phase diagram of the ASEP turns out to be identical to that of the TASEP in a two-dimensional slice across effective parameters that are functions of the intrinsic rates $\alpha, \beta, \gamma, \delta, p, q$.

Multispecies exclusion processes:

The matrix method can be used to represent the stationary measure of periodic systems with defects or with different classes of particles [106, 107, 108, 109, 110, 111, 112]. In particular, this allows us to investigate shock profiles that appear in the ASEP and to prove that these shocks, predicted by Burgers' equation, do exist at the microscopic level and are not artifacts of the hydrodynamic limit [106, 128, 129, 130].

Macroscopic density profiles:

Knowing exactly the microscopic invariant measure allows us to rigorously coarse-grain the problem and to determine the probability of occurrence of a density profile that differs from the average profile. The calculation of such 'free energy functionals' is an important step in understanding how non-equilibrium macroscopic behavior emerges from the microscopic model. For a review of these very important issues and for relevant references, we refer the reader to [77, 131].

Other models:

We emphasize that the matrix product representation method has proved to be very fruitful for solving many one-dimensional systems; a very thorough review of this method can be found in [123].

3.7. Time-dependent properties: the Bethe Ansatz

In order to investigate the behavior of the system away from stationarity, the spectrum of the Markov matrix is needed. For an arbitrary stochastic system, the evolution operator cannot be diagonalized analytically for any system sizes. However, the ASEP belongs to a very special class of models: it is *integrable* and it can be solved using the Bethe Ansatz as first noticed by D. Dhar in 1987 [132]. Indeed, the Markov matrix that encodes the stochastic dynamics of the ASEP can be rewritten in terms of Pauli matrices; in the absence of a driving field, the *symmetric* exclusion process can be mapped exactly into the Heisenberg spin chain. The asymmetry due to a non-zero external driving field breaks the left/right symmetry and the ASEP becomes equivalent to a non-Hermitian spin chain of the XXZ type with boundary terms that preserve the integrable character of the model. The ASEP can also be mapped into a six vertex model [88, 133, 134]. These mappings suggest the use of the Bethe Ansatz to derive spectral information about the evolution operator, such as the spectral gap [132, 135, 136, 137, 138, 139] and large deviation functions [140, 141].

Here, we will apply the Bethe Ansatz to the ASEP on a ring. A configuration can also be characterized by the positions of the N particles on the ring, $(x_1, x_2, \ldots, x_N)$ with $1 \le x_1 < x_2 < \ldots < x_N \le L$. With this representation, the eigenvalue equation (15) becomes

$$E\psi(x_1, \ldots, x_N) =$$

$$\sum_i p\left[\psi(x_1, \ldots, x_{i-1},\ x_i - 1,\ x_{i+1}, \ldots, x_N) - \psi(x_1, \ldots, x_n)\right] + \tag{26}$$

$$\sum_j q\left[\psi(x_1, \ldots, x_{j-1},\ x_j + 1,\ x_{j+1}, \ldots, x_N) - \psi(x_1, \ldots, x_N)\right],$$

where the sum runs over the indices i such that $x_{i-1} < x_i - 1$ and over the indices j such that $x_j + 1 < x_{j+1}$; these conditions ensure that the corresponding jumps are allowed.

We observe that equation (26) is akin to a discrete Laplacian on a N-dimensional lattice: the major difference is that the terms corresponding to forbidden jumps are absent. Nevertheless, this suggests that a trial solution, or *Ansatz*, in the form of plane waves may be useful. This is precisely the idea underlying the Bethe Ansatz, originally developed to study the Heisenberg spin chain model of quantum magnetism [142]. Following Bethe's method, we will also refer to ψ as a 'wavefunction,' but the reader should not confuse our problem with one in quantum mechanics. In our opinion, the ASEP is the one of the simplest system with which one can learn the Bethe Ansatz. The next subsection is devoted to such a tutorial.

3.8. Bethe Ansatz for ASEP: a crash-course

Our aim is to solve the linear eigenvalue problem (26) which corresponds to the relaxation modes of the ASEP with N particles on a ring of L sites. We will study some special cases with small N to illustrate the general structure of the solution.

The single particle case: For $N = 1$, equation (26) reads

$$E\psi(x) = p\psi(x - 1) + q\psi(x + 1) - (p + q)\psi(x), \tag{27}$$

with $1 \leq x \leq L$ and where periodicity is assumed

$$\psi(x + L) = \psi(x). \tag{28}$$

Equation (27) is simply a linear recursion of order 2 that is solved as

$$\psi(x) = A z_+^x + B z_-^x, \tag{29}$$

where $r = z_\pm$ are the two roots of the characteristic equation

$$qr^2 - (E + p + q)r + p = 0. \tag{30}$$

The periodicity condition imposes that at least one of the two characteristic values is a L-th root of unity (Note that because $z_+ z_- = p/q$, only one of them can be a root of unity when $p \neq q$). The general solution is given by

$$\psi(x) = A z^x \qquad \text{with} \quad z^L = 1, \tag{31}$$

i.e., simple *plane waves* with 'momenta' being integer multiples of $2\pi/L$ and associated with eigenvalue

$$E = \frac{p}{z} + qz - (p + q). \tag{32}$$

The two-particle case: The case $N = 2$ where two particles are present is more interesting because when the particles are located on adjacent sites the exclusion effect plays a role. Indeed, the general eigenvalue equation (26) can be split into two different cases:

- In the generic case, x_1 and x_2 are separated by at least one empty site:

$$E\psi(x_1, x_2) = p\left[\psi(x_1 - 1, x_2) + \psi(x_1, x_2 - 1)\right]$$
$$+q\left[\psi(x_1 + 1, x_2) + \psi(x_1, x_2 + 1)\right] - 2(p + q)\psi(x_1, x_2). \tag{33}$$

- In the (special) adjacency case, $x_2 = x_1 + 1$, some jumps are forbidden and the eigenvalue equation reduces to:

$$E\psi(x_1, x_1 + 1) = p\psi(x_1 - 1, x_1 + 1) + q\psi(x_1, x_1 + 2) - (p + q)\psi(x_1, x_1 + 1). \quad (34)$$

This equation differs from the generic equation (33) in which we substitute $x_2 = x_1 + 1$. An equivalent way to take into account the adjacency case is to impose that the generic equation (33) is valid *for all values* of x_1 and x_2 and add to it the following *cancellation boundary condition:*

$$p\psi(x_1, x_1) + q\psi(x_1 + 1, x_1 + 1) - (p + q)\psi(x_1, x_1 + 1) = 0. \quad (35)$$

We now examine how these equations can be solved. In the generic case particles behave totally independently (i.e., they do not interact). The solution of the generic equation (33) can therefore be written as a product of plane waves $\psi(x_1, x_2) = A z_1^{x_1} z_2^{x_2}$, with the eigenvalue

$$E = p\left(\frac{1}{z_1} + \frac{1}{z_2}\right) + q(z_1 + z_2) - 2(p + q). \quad (36)$$

However, the simple product solution cannot be the full answer: the cancellation condition for the adjacency case (35) also has to be satisfied. The first crucial observation, following H. Bethe [142], is that the eigenvalue E, given in (36) is invariant by the permutation $z_1 \leftrightarrow z_2$. In other words, there are two plane waves $A z_1^{x_1} z_2^{x_2}$ and $B z_2^{x_1} z_1^{x_2}$ with the same eigenvalue E which has a two-fold degeneracy. The full eigenfunction corresponding to E can thus be written as

$$\psi(x_1, x_2) = A_{12} z_1^{x_1} z_2^{x_2} + A_{21} z_2^{x_1} z_1^{x_2}, \quad (37)$$

where the amplitudes A_{12} and A_{21} are yet arbitrary. The second key step is to understand that these amplitudes can now be chosen to fulfill the adjacency cancellation condition: substitution of (37) into equation (35), we obtain

$$\frac{A_{21}}{A_{12}} = -\frac{q z_1 z_2 - (p + q) z_2 + p}{q z_1 z_2 - (p + q) z_1 + p}. \quad (38)$$

The eigenfunction (37) is therefore determined, but for an overall multiplicative constant. We now implement the periodicity condition that takes into account the fact that the system is defined on a ring. This constraint can be written as follows for $1 \le x_1 < x_2 \le L$

$$\psi(x_1, x_2) = \psi(x_2, x_1 + L). \quad (39)$$

This relation plays the role of a quantification condition for the scalars z_1 and z_2, which we will call *Bethe roots*. If we now impose the condition that the expression (37) satisfies equation (39) for all generic values of the positions x_1 and x_2, new relations between the amplitudes arise:

$$\frac{A_{21}}{A_{12}} = z_2^L = \frac{1}{z_1^L}. \quad (40)$$

Comparing equations (38) and (40) leads to a set of algebraic equations obeyed by the Bethe roots z_1 and z_2:

$$z_1^L = -\frac{q z_1 z_2 - (p + q) z_1 + p}{q z_1 z_2 - (p + q) z_2 + p} \quad (41)$$

$$z_2^L = -\frac{q z_1 z_2 - (p + q) z_2 + p}{q z_1 z_2 - (p + q) z_1 + p} \quad (42)$$

These equations are known as the *Bethe Ansatz Equations*. Finding the spectrum of the matrix $\mathbb{M}$ for two particles on a ring of size L is reduced to solving these two coupled polynomial equations of degree of order L with unknowns z_1 and z_2. Surely, this still remains a very challenging task but the Bethe equations are explicit and very symmetric. Besides, we emphasize that the size of the matrix $\mathbb{M}$ (and the degree of its characteristic polynomial) is of order L^2.

The three-particle case: We are now ready to consider the case $N = 3$. For a system containing three particles, located at $x_1 \leq x_2 \leq x_3$, the generic equation, valid when the particles are well separated, can readily be written using equation (26). But now, the special adjacency cases are more complicated:

(i) Two particles are next to each other and the third one is far apart; such a setting is called a 2-body collision and the boundary condition that results is identical to the one obtained for the case $N = 2$. There are now two equations that correspond to the cases $x_1 = x \leq x_2 = x + 1 \ll x_3$ and $x_1 \ll x_2 = x \leq x_3 = x + 1$:

$$p\psi(x, x, x_3) + q\psi(x + 1, x + 1, x_3) - (p + q)\psi(x, x + 1, x_3) = 0 \tag{43}$$

$$p\psi(x_1, x, x) + q\psi(x_1, x + 1, x + 1) - (p + q)\psi(x_1, x, x + 1) = 0. \tag{44}$$

We emphasize again that these equations are identical to equation (35) because the third particle, located far apart, is simply a *spectator* (x_3 is a spectator in the first equation; x_1 in the second one).

(ii) There can be 3-body collisions, in which the three particles are adjacent, with $x_1 = x, x_2 = x + 1, x_3 = x + 2$. The resulting boundary condition is then given by

$$p\left[\psi(x, x, x + 2) + \psi(x, x + 1, x + 1)\right] + q\left[\psi(x + 1, x + 1, x + 2) + \psi(x, x + 2, x + 2)\right]$$
$$-2(p + q)\psi(x, x + 1, x + 2) = 0. \tag{45}$$

The fundamental remark is that *3-body collisions do not lead to an independent constraint*. Indeed, equation (45) is simply a linear combination of the constraints (43) and (44) imposed by the 2-body collisions. To be precise: equation (45) is the sum of equation (43), with the substitutions $x \to x$ and $x_3 \to x + 2$, and of equation (44) with $x_1 \to x$ and $x \to x + 1$. Therefore, *it is sufficient to fulfill the 2-body constraints because then the 3-body conditions are automatically satisfied.* The fact that 3-body collisions decompose or 'factorise' into 2-body collisions is the *crucial property* that lies at the very heart of the Bethe Ansatz. If it were not true, the ASEP would not be exactly solvable or 'integrable'.

For $N = 3$, the plane wave $\psi(x_1, x_2, x_3) = A z_1^{x_1} z_2^{x_2} z_3^{x_3}$ is a solution of the generic equation with the eigenvalue

$$E = p\left(\frac{1}{z_1} + \frac{1}{z_2 + z_3^{-1}}\right) + q\left(z_1 + z_2 + z_3\right) - 3(p + q). \tag{46}$$

However, such a single plane wave does not satisfy the boundary conditions (43) and (44). Again, we note that the eigenvalue E is invariant under the permutations of z_1, z_2 and z_3. There are 6 such permutations, that belong to S_3, the permutation group of 3 objects. The Bethe wave-function is therefore written as a sum of the 6 plane waves, corresponding to the same eigenvalue E, with unknown amplitudes:

$$\psi(x_1, x_2, x_3) = A_{123}\, z_1^{x_1} z_2^{x_2} z_3^{x_3} + A_{132}\, z_1^{x_1} z_3^{x_2} z_2^{x_3} + A_{213}\, z_2^{x_1} z_1^{x_2} z_3^{x_3}$$
$$+ A_{231}\, z_2^{x_1} z_3^{x_2} z_1^{x_3} + A_{312}\, z_3^{x_1} z_1^{x_2} z_2^{x_3} + A_{321}\, z_3^{x_1} z_2^{x_2} z_1^{x_3}$$

$$= \sum_{s \in S_3} A_s z_{s(1)}^{x_1} z_{s(2)}^{x_2} z_{s(3)}^{x_3}. \tag{47}$$

The 6 amplitudes A_s are uniquely and unambiguously determined (up to an overall multiplicative constant) by the 2-body collision constraints. It is therefore absolutely crucial that 3-body collisions do not bring additional independent constraints that the Bethe wave function could not satisfy. We encourage the reader to perform the calculations (which are very similar to the $N = 2$ case) of the amplitude ratios.

Finally, the Bethe roots z_1, z_2 and z_3 are quantized through the periodicity condition

$$\psi(x_1, x_2, x_3) = \psi(x_2, x_3, x_1 + L), \tag{48}$$

for $1 \le x_1 < x_2 < x_3 \le L$. This condition leads to the Bethe Ansatz equations (the equations for general N are given below).

The general case: Finally, we briefly discuss the general case $N > 3$. Here one can have k-body collisions with $k = 2, 3, \ldots N$. However, all multi-body collisions 'factorize' into 2-body collisions and ASEP can be diagonalized using the Bethe Wave Function

$$\psi(x_1, x_2, \ldots, x_N) = \sum_{s \in S_N} A_s\, z_{s(1)}^{x_1} z_{s(2)}^{x_2} \cdots z_{s(N)}^{x_N}, \tag{49}$$

where S_N is the permutation group of N objects. The $N!$ amplitudes A_s are fixed (up to an overall multiplicative constant) by the 2-body collisions constraints. The corresponding eigenvalue is given by

$$E = p \sum_{i=1}^{N} \frac{1}{z_i} + q \sum_{i=1}^{N} z_i - N(p + q). \tag{50}$$

The periodicity condition

$$\psi(x_1, x_2, \ldots, x_N) = \psi(x_2, x_3, \ldots, x_N, x_1 + L), \tag{51}$$

where $1 \le x_1 < x_2 < \ldots < x_N \le L$, leads to a set of algebraic equations satisfied by the Bethe roots $z_1, z_2, \ldots, z_N$. The Bethe Ansatz equations are given by

$$z_i^L = (-1)^{N-1} \prod_{j \neq i} \frac{q z_i z_j - (p + q) z_i + p}{q z_i z_j - (p + q) z_j + p}, \tag{52}$$

for $i = 1, \ldots N$. The Bethe Ansatz thus provides us with a set of N coupled algebraic equations of degree of order L (Recall that the size of the matrix $\mathbb{M}$ is of order 2^L, when $N \simeq L/2$). Although the degree of the polynomials involved are extremely high, a large variety of methods have been developed to analyze them [88, 143, 144].

We remark that for $p = q = 1$ the Bethe equations are the same as the ones derived by H. Bethe in 1931. Indeed, the symmetric exclusion process is mathematically equivalent to the isotropic Heisenberg spin chain (although the two systems describe totally different physical settings).

3.9. Some applications of the Bethe Ansatz

1135 The Bethe Ansatz allows us to derive information about the spectrum of the Markov
1136 matrix that governs the evolution of ASEP. Below, we review some applications and
1137 refer to the original works.

1138 *Structure of the Bethe wave function:*
1139 In the totally asymmetric case (TASEP), the Bethe equations simplify and it is
1140 possible to perform analytical calculations even for finite values of L and N. Besides,
1141 the TASEP Bethe wave function takes the form of a determinant:

$$\psi(\xi_1, \ldots, \xi_N) = \det(\mathbb{R}), \tag{53}$$

1143 where $\mathbb{R}$ is a $N \times N$ matrix with elements

$$R_{ij} = \frac{z_i^{\xi_j}}{(1 - z_i)^j} \quad \text{for } 1 \le i, j \le N, \tag{54}$$

1145 $(z_1, \ldots, z_N)$ being the Bethe roots. By expanding the determinant, one recovers the
1146 generic form (49) for the Bethe wave function. The formulas (53) and (54) can be
1147 verified directly by proving that the eigenvalue equation (26) and all the boundary
1148 conditions are satisfied [112, 145]. As we will see in the next subsection, determinantal
1149 representations of the eigenvectors and of the exact probability distribution at finite
1150 time play a very important role in the study of the TASEP [146, 147, 148, 149].

1151 *Spectral gap and dynamical exponent:*
1152 The Bethe Ansatz allows us to determine the spectral gap which amounts to
1153 calculating the eigenvalue E_1 with the largest real part. For a density $\rho = N/L$, one
1154 obtains for the TASEP

$$E_1 = \underbrace{-2\sqrt{\rho(1-\rho)}\frac{6.509189337\ldots}{L^{3/2}}}_{\text{relaxation}} \pm \underbrace{\frac{2i\pi(2\rho-1)}{L}}_{\text{oscillations}}. \tag{55}$$

1156 The first excited state consists of a pair of conjugate complex numbers when ρ is
1157 different from $1/2$. The real part of E_1 describes the relaxation towards the stationary
1158 state: we find that the largest relaxation time scales as $T \sim L^z$ with the dynamical
1159 exponent $z = 3/2$ [150, 132, 135, 136, 138]. This value agrees with the dynamical
1160 exponent of the one-dimensional Kardar-Parisi-Zhang equation that belongs to the
1161 same universality class as ASEP (see the review of Halpin-Healy and Zhang 1995
1162 [151]). The imaginary part of E_1 represents the relaxation oscillations and scales as
1163 L^{-1}; these oscillations correspond to a kinematic wave that propagates with the group
1164 velocity $2\rho-1$; such traveling waves can be probed by dynamical correlations [152, 99].
1165 The same procedure also allows us to classify the higher excitations in the spectrum
1166 [153]. For the partially asymmetric case ($p, q > 0, p \ne q$), the Bethe equations do not
1167 decouple and analytical results are much harder to obtain. A systematic procedure
1168 for calculating the finite size corrections of the upper region of the ASEP spectrum
1169 was developed by Doochul Kim [136, 137].

1170 *Large deviations of the current:*
1171 The exclusion constraint modifies the transport properties through the ASEP
1172 system. For instance, if one considers the ASEP on a ring and tags an individual
1173 particle (without changing its dynamics), the particle displays diffusive behavior in
1174 the long time limit, but with a tracer diffusion coefficient $\mathcal{D}$ that depends on the

size of the system. It is different from the free, non-interacting particle diffusion constant: $\mathcal{D}_{\text{ASEP}} \neq \mathcal{D}_{\text{free}}$. In a ring of size L, $\mathcal{D}_{\text{ASEP}}$ scales as $L^{-1/2}$ in presence of an asymmetric driving. In the case of symmetric exclusion, one has $\mathcal{D}_{\text{SEP}} \sim L^{-1}$. These scaling behaviors indicate that in the limit of an infinite system the diffusion constant vanishes and fluctuations become anomalous [154]. In the classic result [91, 92, 97] of the SEP on an infinite line, root-mean square displacement of a tagged particle scales as $t^{1/4}$. In the ASEP, subtleties associated with the initial conditions arise. For a *fixed initial condition*, the position of the tagged particle spreads as $t^{1/3}$. However, if an average is carried out by choosing random initial conditions (with respect to the stationary measure), then a normal $t^{1/2}$ diffusion is recovered. The latter is a trivial effect due to the local density fluctuations that result from varying the initial condition; these fluctuations completely overwhelm and mask the intrinsic dynamical fluctuations. Another feature that one expects is a non-Gaussian behavior, i.e., cumulants beyond the second are present.

An alternative observable that carries equivalent information (and is amenable to analytical studies) is the total current transported through the system. Consider the statistics of Y_t, the total distance covered by all the particles between the time 0 and t. It can be shown (see e.g., [112] and references therein) that in the long time limit the cumulant generating function of the random variable Y_t behaves as

$$\left\langle e^{\mu Y_t} \right\rangle \simeq e^{E(\mu)t} \,. \tag{56}$$

This equation implies that all the cumulants of Y_t grow linearly with time and can be determined by taking successive derivatives of the function $E(\mu)$ at $\mu = 0$. Another way to characterize the statistics of Y_t is to consider the *large-deviation function* of the current, defined as follows

$$\text{Prob}\left(\frac{Y_t}{t} = j\right) \sim e^{-tG(j)} \,. \tag{57}$$

From equations (56,57), we see that $G(j)$ and $E(\mu)$ are the *Legendre transforms* of each other. Large deviation functions play an increasingly important role in non-equilibrium statistical physics [78], especially through application of the Fluctuation Theorem [76]. Thus, determining exact expressions for these large deviation functions for interacting particle processes, either analytically or numerically, is a major challenge in the field [77]. Moreover, higher cumulants of the current and large deviations are also of experimental interest in relation to counting statistics in quantum systems [158].

The crucial step in the calculation of the cumulants is to identify the generating function $E(\mu)$ as the dominant eigenvalue of a matrix $\mathbb{M}(\mu)$, obtained by the following deformation of the original Markov matrix $\mathbb{M}$:

$$\mathbb{M}(\mu) = \mathbb{M}_0 + e^{\mu}\mathbb{M}_1 + e^{-\mu}\mathbb{M}_{-1}, \tag{58}$$

where $\mathbb{M}_0$ is the matrix of the diagonal of $\mathbb{M}$, and $\mathbb{M}_1$ ($\mathbb{M}_{-1}$) is a matrix containing the transitions rates of particle hopping in the positive (negative) direction. Hence, the statistics of the transported mass has been transformed into an eigenvalue problem. The deformed matrix $\mathbb{M}(\mu)$ can be diagonalized by the Bethe Ansatz by solving the following Bethe Ansatz equations

$$z_i^L = (-1)^{N-1} \prod_{j=1}^{N} \frac{q e^{-\mu} z_i z_j - (p+q) z_i + p e^{\mu}}{q e^{-\mu} z_i z_j - (p+q) z_j + p e^{\mu}} \,. \tag{59}$$

The corresponding eigenvalues are given by

$$E(\mu; z_1, z_2 \ldots z_N) = pe^{\mu} \sum_{i=1}^{N} \frac{1}{z_i} + qe^{-\mu} \sum_{i=1}^{N} z_i - N(p+q). \tag{60}$$

For $\mu = 0$ we know that the largest eigenvalue is 0. For $\mu \neq 0$ the cumulant generating function corresponds to the continuation of this largest eigenvalue (the existence of this continuation, at least for small values of μ is guaranteed by the Perron-Frobenius theorem).

We remark that equations (59) and (60) are invariant under the transformation

$$z \to \frac{1}{z}$$
$$\mu \to \mu_0 - \mu \quad \text{with} \quad \mu_0 = \log \frac{q}{p}. \tag{61}$$

This symmetry implies that the spectra of $\mathbb{M}(\mu)$ and of $\mathbb{M}(\mu_0 - \mu)$ are identical. This functional identity is in particular satisfied by the largest eigenvalue of $\mathbb{M}$ and we have

$$E(\mu) = E(\mu_0 - \mu). \tag{62}$$

Using the fact that the LDF $G(j)$ is the Legendre transform of $E(\mu)$, we obtain the canonical form of the *Fluctuation Theorem* (or Gallavotti-Cohen relation)

$$G(j) = G(-j) - \mu_0 j. \tag{63}$$

We observe that in the present context this relation manifests itself as a symmetry of the Bethe equations. However, it is satisfied by a large class of systems far from equilibrium [71, 72, 73]. The validity of the Fluctuation Theorem does not rely on the integrability of the system and it can be proved for Markovian or Langevin dynamical systems using time-reversal symmetry [75, 76] as well as measure-theoretic considerations [159, 160].

The complete calculation of the current statistics in the ASEP is a difficult problem that required more than a decade of effort. The breakthrough was the solution of the TASEP, by B. Derrida and J. L. Lebowitz in 1998 [140]. These authors obtained the following parametric representation of the function $E(\mu)$ in terms of an auxiliary parameter B:

$$E(\mu) = -N \sum_{k=1}^{\infty} \left(\begin{array}{c} kL - 1 \\ kN \end{array} \right) \frac{B^k}{kL - 1}, \tag{64}$$

where $B(\mu)$ is implicitly defined through

$$\mu = -\sum_{k=1}^{\infty} \left(\begin{array}{c} kL \\ kN \end{array} \right) \frac{B^k}{kL}. \tag{65}$$

These expressions allow us to calculate the cumulants of Y_t, for example the mean-current J and a 'diffusion constant' D:

$$J = \lim_{t \to \infty} \frac{\langle Y_t \rangle}{t} = \frac{dE(\mu)}{d\mu} \bigg|_{\mu=0} = \frac{N(L-N)}{L-1},$$

$$D = \lim_{t \to \infty} \frac{\langle Y_t^2 \rangle - \langle Y_t \rangle^2}{t} = \frac{d^2 E(\mu)}{d\mu^2} \bigg|_{\mu=0} = \frac{N^2 \, (2L-3)! \, (N-1)!^2 \, (L-N)!^2}{(L-1)!^2 \, (2N-1)! \, (2L-2N-1)!}. \tag{66}$$

When $L \to \infty$, $\rho = L/N$, and $|j - L\rho(1-\rho)| \ll L$, the large deviation function $G(j)$ can be written in the following scaling form:

$$G(j) = \sqrt{\frac{\rho(1-\rho)}{\pi N^3}} H\left(\frac{j - L\rho(1-\rho)}{\rho(1-\rho)}\right) \tag{67}$$

with

$$H(y) \simeq -\frac{2\sqrt{3}}{5\sqrt{\pi}} y^{5/2} \quad \text{for} \quad y \to +\infty\,, \tag{68}$$

$$H(y) \simeq -\frac{4\sqrt{\pi}}{3} |y|^{3/2} \quad \text{for} \quad y \to -\infty\,. \tag{69}$$

The shape of the large deviation function is skewed: it decays with a $5/2$ power as $y \to +\infty$ and with a $3/2$ power as $y \to -\infty$. For the general case $q \neq 0$ on a ring, the solution was found by rewriting the Bethe Ansatz as a functional equation and restating it as a purely algebraic problem [161, 162]. For example, this method allows us to calculate the first two cumulants, J and D:

$$J = \frac{(p-q)}{p} \frac{N(L-N)}{L-1} \sim \frac{(p-q)}{p} L\rho(1-\rho) \text{ for } L \to \infty\,,$$

$$D = \frac{(p-q)}{p} \frac{2L}{L-1} \sum_{k>0} k^2 \frac{C_L^{N+k}}{C_L^N} \frac{C_L^{N-k}}{C_L^N} \left(\frac{p^k + q^k}{p^k - q^k}\right)\,, \tag{70}$$

where C_L^N are the binomial coefficients. Note that the formula for D was previously derived using the matrix product representation discussed above [163]. Higher cumulants can also be found and their scaling behavior investigated. For ASEP on a ring, the problem was completely solved recently by S. Prolhac [164], who found a parametric representation analogous to equations (64) but in which the binomial coefficients are replaced by combinatorial expressions enumerating some tree structures. A particularly interesting case [165] is a weakly driven limit defined by $q/p = 1 - \frac{\nu}{L}$, $L \to \infty$. In this case, we need to rescale the fugacity parameter as μ/L and the following asymptotic formula for the cumulant generating function can be derived

$$E\left(\frac{\mu}{L}, 1 - \frac{\nu}{L}\right) \simeq \frac{\rho(1-\rho)(\mu^2 + \mu\nu)}{L} - \frac{\rho(1-\rho)\mu^2\nu}{2L^2} + \frac{1}{L^2}\phi[\rho(1-\rho)(\mu^2 + \mu\nu)]\,, \tag{71}$$

$$\text{with} \qquad \phi(z) = \sum_{k=1}^{\infty} \frac{B_{2k-2}}{k!(k-1)!} z^k\,, \tag{72}$$

and where B_j's are Bernoulli Numbers. We observe that the leading order (in $1/L$) is quadratic in μ and describes Gaussian fluctuations. It is only in the subleading correction (in $1/L^2$) that the non-Gaussian character arises. This formula was also obtained for the symmetric exclusion case $\nu = 0$ in [166]. We observe that the series that defines the function $\phi(z)$ has a finite radius of convergence and that $\phi(z)$ has a singularity for $z = -\pi^2$. Thus, non-analyticities appear in $E(\mu, \nu)$ as soon as

$$\nu \geq \nu_c = \frac{2\pi}{\sqrt{\rho(1-\rho)}}\,.$$

By Legendre transform, non-analyticities also occur in the large deviation function $G(j)$ defined in (57). At half-filling, the singularity appears at $\nu_c = 4\pi$ as can be seen

1270 in figure 3. For $\nu < \nu_c$ the leading behavior of $G(j)$ is quadratic (corresponding to
1271 Gaussian fluctuations) and is given by

$$G(j) = \frac{(j - \nu\rho(1-\rho))^2}{4L\rho(1-\rho)} \,. \tag{73}$$

1273 For $\nu > \nu_c$, the series expansions (71,72) break down and the LDF $G(j)$ becomes
1274 non-quadratic even at leading order. This phase transition was predicted by T.
1275 Bodineau and B. Derrida using macroscopic fluctuation theory [167, 168, 169]. These
1276 authors studied the optimal density profile that corresponds to the total current j
1277 over a large time t. They found that this optimal profile is flat for $j < j_c$ but it
1278 becomes linearly unstable for $j > j_c$. In fact, when $j > j_c$ the optimal profile is
1279 time-dependent. The critical value of the total current for which this phase-transition
1280 occurs is $j_c = \rho(1-\rho)\sqrt{\nu^2 - \nu_c^2}$ and therefore one must have $\nu \geq \nu_c$ for this transition
1281 to occur. One can observe in figure 3 that for $\nu \geq \nu_c$, the large deviation function
1282 $G(j)$ becomes non-quadratic and develops a kink at a special value of the total current
1283 j.
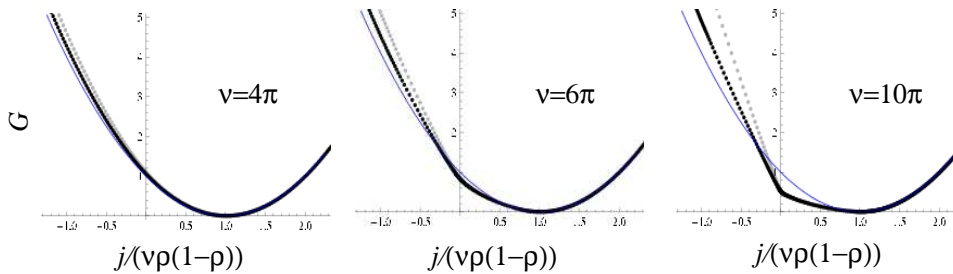
Figure 3. Behaviour of the large deviation function G as a function of the current $j/(\nu\rho(1-\rho))$ for different values of ν. The gray dots correspond to $L = 50, N = 25$ and the black dots correspond to $L = 100, N = 50$. The curves are formally obtained by numerically solving the Bethe Ansatz equations (59), and Legendre transforming $E(\mu)$. The thin blue curve represents the leading Gaussian behavior indicated by equation (73).

1284 *Bethe Ansatz for other systems out of equilibrium:*

1285   We have discussed in this review the Bethe Ansatz for a system on a periodic ring
1286 where the total number of particles is a conserved quantity. It is possible to extend
1287 the Bethe Ansatz for the finite ASEP with open boundaries in which the total number
1288 of particles is not constant. The resulting Bethe equations have a more complicated
1289 structure; they have been thoroughly analyzed in a series of papers by J. de Gier and
1290 F. Essler [170, 153, 171] who calculated the spectral gaps in the different phases of
1291 the open ASEP. In particular, they discovered sub-phases in the phase diagram that
1292 could not be predicted from the steady state measure alone. We note that the Bethe
1293 Ansatz can be applied to variants of the ASEP, such as models with impurities [141],
1294 multispecies exclusion processes [172, 173, 174] as the zero-range process [175], the
1295 raise and peel model [125], vicious walkers [176], or the Bernoulli matching model of
1296 sequence alignment [177, 178].

3.10. ASEP on an infinite lattice: Bethe Ansatz and random matrices

In this last subsection, we briefly review some important analytical results that have been obtained for exclusion processes on an infinite line, especially in connection with the Bethe Ansatz method discussed above. this approach will allow us to derive some insight into the dyanmics of the systems. More detailed results and historical discussions can be found in the literature cited in the text.

We first consider the case of the ASEP on the infinite lattice $\mathbb{Z}$ but with only a *finite* number N of particles. Because the particles cannot overtake one another, the ordering of the particles is conserved by the dynamics, and we can label the particles from right to left. Suppose that at $t = 0$, the particles are located at positions $y_1 > \ldots > y_N$ and at some later time t, they are located at $x_1 > \ldots > x_N$.

The transition probability, $P(x_1, \ldots, x_N, t | y_1, \ldots, y_N, 0)$, for reaching the final configuration $x_1, \ldots, x_N$ at t starting from $y_1, \ldots, y_N$ at $t = 0$ has the following exact expression:

$$P(x_1, \ldots, x_N, t | y_1, \ldots, y_N, 0) = \sum_{s \in S_N} \prod_{k=1}^{N} \oint_{C_R} \frac{dz_k}{2\pi i z_k} A_s(\{z\}) e^{(\frac{p}{z_k} + q z_k - 1)t} z_{s(k)}^{x_k - y_{s(k)}}. \quad (74)$$

The crucial observation is that there exists a closed formula for the amplitude A_s, given by

$$A_s(\{z\}) = \text{sgn}(s) \frac{\prod_{i<j} \left(p + q z_{s(i)} z_{s(j)} - z_{s(i)} \right)}{\prod_{i<j} \left(p + q z_i z_j - z_i \right)}, \quad (75)$$

where we use the convention $p + q = 1$. The expressions (74) and (75) are reminiscent of the formulae given by the Bethe Ansatz. These results were initially derived for the TASEP on $\mathbb{Z}$ by G. Schütz in 1997, who constructed them from the Bethe Ansatz [147] and then proved rigorously that equation (74) solves exactly the time-dependent Markov equation with the correct initial condition (generalized to the periodic case by V. Priezzhev in [148, 149]). The general result for the ASEP was found by Tracy and Widom in 2008 [179] and has motivated many studies in the last few years. Equation (74) is a seminal result: it is an exact expression for the Green function of the ASEP from which, in principle, individual particle distributions and correlations functions can be extracted (this can be an extremely difficult task in practice). Finally, we emphasize that the 'Bethe roots' z_i are not quantified in the infinite system: each of them takes a continuous set of values along the circular contour C_R of radius R, so small that the poles of $A_s(\{z\})$ lie outside C_R.

To give one specific example, consider the *totally* asymmetric exclusion with unit hopping rate $p = 1$ (and $q = 0$) and with a *step initial condition*, where all sites right of the origin ($i > 0$) are empty and all to the left ($i \leq 0$) are occupied. If we are interested in the behaviour of *only* the right most N particles after time t, then we can replace the semi-infinite string by a finite segment of N particles. The point is, in a TASEP, none of the particles hops to the left and so, particles to the left of our N-particle string cannot affect their behaviour. Thus, it is sufficient to consider $P(x_1, \ldots, x_N, t | y_1 = 0, \ldots, y_N = 1 - N, 0)$. Now, suppose we ask a more restricted question: What is $\tilde{P}(M, N, t)$, the probability that the N-th particle (initially located

at $i = 1 - N$, has performed at least M hops by time t? In terms of P, we write

$$\tilde{P}(M, N, t) = \sum_{x_1 > \ldots > x_N > M-N} P(x_1, \ldots, x_N, t | y_1 = 0, \ldots, y_n = 1 - N, 0) \tag{76}$$

We next exploit a determinantal representation, analogous to (53) and (54) for ψ, and express P as:

$$P(x_1, \ldots, x_N, t | y_1, \ldots, y_N, 0) = \det(\mathbb{B}), \tag{77}$$

where $\mathbb{B}$ is a $N \times N$ matrix with elements

$$B_{ij} = \oint_{C_R} \frac{dz}{2\pi i z} z^{x_i - y_j} (1 - z)^{j-i} e^{(\frac{1}{z} - 1)t} \quad \text{for} \quad 1 \le i, j \le N, \tag{78}$$

After some calculation [180], these equations allow us to express $\tilde{P}(M, N, t)$ compactly:

$$\tilde{P}(M, N, t) = \frac{1}{Z_{M,N}} \int_{[0,t]^N} d^N x \prod_{1 \le i < j \le N} (x_i - x_j)^2 \prod_{j=1}^N x_j^{M-N} e^{-x_j}. \tag{79}$$

where $Z_{M,N}$ is a normalization factor. The integral on the right hand side has a direct interpretation in random matrix theory: it is the probability that the largest eigenvalue of the random matrix $\mathbb{A}\mathbb{A}^\dagger$ is less than or equal to t, with $\mathbb{A}$ being a $N \times M$ matrix of complex random variables with zero mean and variance $1/2$ (unitary Laguerre random matrix ensemble).

Finally, we note that $\tilde{P}(N, N, t)$ can also be interpreted as the probability that the integrated current Q_t through the bond (0,1) is at least equal to N (Q_t is the number of particles that have crossed the bond (0,1) between time 0 and t). From the classical Tracy-Widom laws for the distribution of the largest eigenvalue of a random matrix [181], one can write

$$Q_t = \frac{t}{4} + \frac{t^{1/3}}{2^{4/3}} \chi. \tag{80}$$

where the distribution of the random variable χ is given by

$$\text{Prob}\left(\chi \le s\right) = 1 - F_2(-s). \tag{81}$$

The Tracy-Widom function $F_2(s)$ is the cumulative distribution of the maximum eigenvalue λ_{max} in the Gaussian Unitary Ensemble (self-adjoint Hermitian matrices) *i.e.*

$$\text{Prob}\left(\frac{\lambda_{\max} - \sqrt{2N}}{(8N)^{-1/6}} \le s\right) = F_2(s), \tag{82}$$

where $N \gg 1$ represents here the size of the random matrix. Exact expressions for $F_2(s)$ can be found, for example, in [182]. This crucial relation between random matrix theory and the asymmetric exclusion process, first established by K. Johansson in 2000 [183], has stimulated many works in statistical mechanics and probability theory (see e.g., [184, 185, 186]). The mathematical study of the infinite system has grown into a subfield *per se* that displays fascinating connections with random matrix theory, combinatorics and representation theory. We note that K. Johansson did not use the Bethe Ansatz in his original work. He studied a discrete-time version of the TASEP in which the trajectories of the particles were encoded in a waiting-time

matrix, which specifies how long a given particle stays at each given site. This integer-valued matrix can be mapped via the Robinson-Schensted-Knuth correspondence into a Young Tableau. The value of the total current through the bond (0,1) is linearly related to the length of the longest line of this Young Tableau. The statistics of the length of the longest line can be found by using asymptotic analysis techniques *à la* Tracy-Widom. In fact, a closely related question, the classical Ulam problem of the longest increasing subsequence in a random permutation, was solved a few years earlier by J. Baik, K. Deift and K. Johansson, using related methods [187].

Very recently, in a series of articles [179, 188, 189, 190, 191], C. A. Tracy and H. Widom have generalized Johansson's results to the partially asymmetric exclusion process by deriving some integral formulas for the probability distribution of an individual particle starting from the step initial condition. These expressions can be rewritten as a single integral involving a Fredholm determinant that is amenable to asymptotic analysis. In particular, a limit theorem is proved for the total current distribution. Going from TASEP to ASEP is a crucial progress because the weakly asymmetric process leads to a well-defined continuous limit: the Kardar-Parisi-Zhang (KPZ) equation, a universal model for surface growth. Indeed, a very important outgrowth of these studies is the exact solution of the KPZ equation in one dimension. The distribution of the height of the surface at any finite time is now known exactly (starting from some special initial conditions), solving a problem that remained open for 25 years: a description of the historical development of these results and the contributions of the various groups can be found in [192, 186, 193, 194, 195, 196, 197, 198, 199]. One important feature to keep in mind is that the results (and therefore the universality class) depend strongly on the chosen initial conditions. Lately, n-point correlation functions of the height in KPZ have also been exactly derived by H. Spohn and S. Prolhac [200, 201]. For an overview of these fascinating problems, we recommend the article by T. Kriecherbauer and J. Krug [182], and the reviews by D. Aldous and P. Diaconis [202] and I. Corwin [203].

3.11. Hydrodynamic mean field approach

Though elegant and rigorous, the methods presented above cannot be applied to systems much more complex than the TASEP. Typically, further progress relies on a very successful approach, based on the mean field approximation and a continuum limit, leading to PDE's for various densities in the system. Known as the hydrodynamic limit, such equations can be 'derived' from the master equation (14). The strategy starts with the exact evolution equation for $\rho_i(t) \equiv \langle \sigma_i \rangle_t = \sum_{\mathcal{C}} \sigma_i P(\mathcal{C}, t)$. Differentiating this $\rho_i(t)$ with respect to t and using equation (14), we see that new operators appear:

$$\mathcal{O}(\mathcal{C}') = \sum_{\mathcal{C}} \sigma_i(\mathcal{C}) M(\mathcal{C}, \mathcal{C}'). \tag{83}$$

In the case of ASEP, $M(\mathcal{C}, \mathcal{C}')$ is sufficiently simple that the sum over $\mathcal{C}$ can be easily performed, leaving us with products of σ's (associated with configurations $\mathcal{C}'$). Applying the mean field approximation (equation (17)), the right-hand side now consists of products of $\rho_i(t)$ and $\rho_{i\pm1}(t)$.

Taking the thermodynamic and continuum limit, we let $i, L \to \infty$ with finite $x = i/L$ and write $\rho_i(t) \simeq \rho(x,t)$. Next, we expand $\rho_{i\pm1}(t) \simeq \rho(x,t) \pm \varepsilon \partial_x \rho + (\varepsilon^2/2)\partial_x^2 \rho + \ldots,$

where $\varepsilon \equiv 1/L \to 0$. The result is a hydrodynamic PDE for the particle density [124]:

$$\frac{\partial \rho(x,t)}{\partial t} = \varepsilon \frac{\partial}{\partial x}\left[(q-p)\rho(1-\rho)\right] + \frac{\varepsilon^2}{2}\frac{\partial}{\partial x}\left[(1-\rho)\frac{\partial}{\partial x}\left[(p+q)\rho\right] + (p+q)\rho\frac{\partial \rho}{\partial x}\right]. \quad (84)$$

where $\varepsilon \equiv 1/L \to 0$. Note that even slow variations in the hopping rates ($p_i \to p(x)$ and $q_i \to q(x)$) can be straightforwardly incorporated [204]. Analogous hydrodynamic equations have also been derived for ASEPs with particles that occupy more than one lattice site [205, 206, 207]. In addition to spatially slowly varying hopping rates, this approach is useful for exploring more complex models, e.g., a TASEP with particles that can desorb and/or attach to every site (Section 4.2). Of course, such equations are also the starting point for very successful field theoretic approaches to dynamic critical phenomena near-equilibrium [208, 209, 210, 211] as well as ASEPs (even with interacting particles) in higher dimensions [212, 213, 214, 215, 216, 217]. Supplemented with noise terms, these become Langevin equations for the density or mangetisation fields. Then, fluctuations and correlations can be computed within, typically, a perturbative framework.

Returning to equation (84), it is especially easy to analyse in the steady-state limit where the resulting equation is an ODE in x. But, the highest power of ε multiplies the largest derivative, so that we are dealing with 'singularly perturbed' differential equations [124, 218, 219]. The solutions for the steady-state mean field density $\rho(x)$ consist of 'outer solutions' that hold in the bulk, matched to 'inner solutions' corresponding to boundary layers of thickness ε at the open ends. For the ASEP, this approach correctly determines the phase boundaries and the self-consistently determined steady-state current J (which arise both in the integration constant of equation (84) and in the boundary conditions). However, as anticipated, the density profiles are not exactly determined, even when $L \to \infty$. Nevertheless, for more realistic physical models such as the ones to be discussed in the next section, such a mean-field approach (or some of its variants) is often the only available analytical method at our disposal.

4. Biological and related applications of exclusion processes

In this section, we review a number of applications of stochastic exclusion models to problems of transport in materials science, cell biology, and biophysics. While quantitative models of these real-world applications often require consideration of many microscopic details (and their corresponding parameters), simple one-dimensional lattice models nonetheless can be used to capture the dominant mechanisms at play, providing a succint representation of the system. Moreover, these types of models can be extended in a number of ways, and are amenable to concise analytic solutions. As we will see, application of lattice models to complex biophysical systems is aided by a few main extensions and modifications to the TASEP presented above. These modified dynamics are illustrated respectively, by figures 4-9.

(i) **Longer-ranged interactions:** Objects represented by particles in an exclusion process may have molecular structure that carry longer-ranged particle-particle interactions. For example, to model ribosomes on an mRNA or cargo-carrying molecular motors, we should use large particles taking small discrete steps and introduce a rule beyond on-site exclusion. We may regard these as 'extended particles' that occlude $\ell > 1$ lattice sites (figure 4).
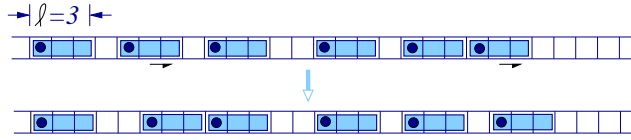
Figure 4. An interior section of an asymmetric exclusion process with extended particles of size $\ell = 3$. The individual particles occlude three of the lattice sites on which the hops occur.

(ii) **Particle detachment and attachment:** Particles such as molecular motors have finite processivity. That is, they can spontaneously detach from their lattices before reaching their destination. Conversely, particles in a bulk reservoir can also attach at random positions on the lattice. The coupling of the particle number to a bulk reservoir is analogous to the problem of Langmuir kinetics [219, 220] on a one-dimensional lattice, except that the particles are directionally driven on the substrate (figure 5).
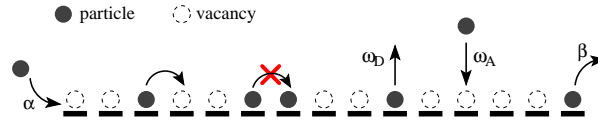
Figure 5. A TASEP with Langmuir kinetics where particles can spontaneously detach and attach at every site with rates ω_D and ω_A, respectively. Adapted from [221].

(iii) **Multiple species:** Usually, biological transport involves multiple interacting species in confined geometries, often one-dimensional in nature. For example, these secondary species may represent particles that are co-transported or counter-transported with the primary particles, or, they may represent species that bind to pores and regulate primary particle transport [222](figure 6).
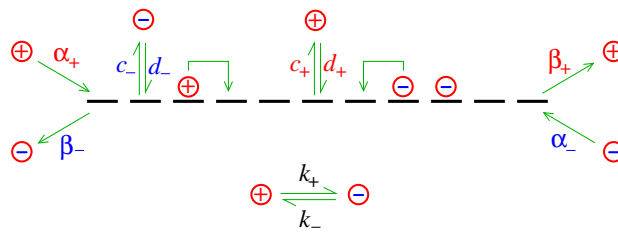
Figure 6. A two-species exclusion model, adapted from [223], where $+$ and $-$ particles move in opposite directions but can interconvert with rate $k_{\pm}$. Attachment and detachment are also allowed with rates $c_{\pm}$ and $d_{\pm}$, respectively.

(iv) **Partial exclusion & coupled chains:** Often, the strict one-dimensional nature of the exclusion dynamics can be relaxed to account for particles that, while strongly repelling each other, can on occasion pass over each other. This scenario might arise when pores are wide enough to allow particle passing.

Related extensions of single-chain exclusion processes are exclusion processes across multiple interacting chains (figure 7).
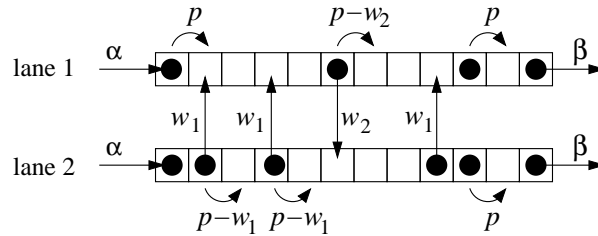
Figure 7. Two coupled TASEP lattices with interchain hopping rates w_1 and w_2. Adapted from [224].

(v) **Internal states and nonexponentially distributed dwell times:** The physical mechanisms of how excluding particles are inserted, extracted, and hop in the interior of the lattice are often complex, involving many intermediate chemical steps [225, 226]. Therefore, the distribution of times between successive hops, even when unimpeded by exclusion interactions, is often non-exponential. Specific hopping time distributions can be incorporated into lattice particle models by explicitly evolving internal particle states (figure 8).
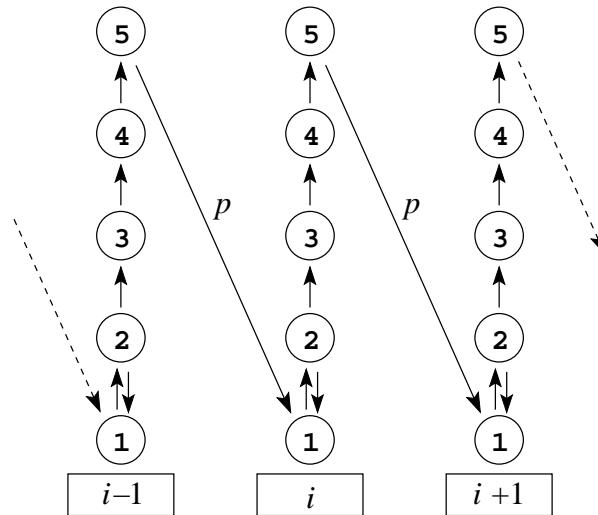
Figure 8. Internal states (1-5) that determine the timing between particle hops (adapted from [226]). Here, a linear sequence of Poisson processes generates a Gamma-distributed [227] interhopping time distribution (dwell time). This model for the internal dynamics has been used to model mRNA translation by ribosome enzymes.

(vi) **Variable lattice lengths:** The lattices on which the exclusion processes occur may not be fixed in some settings. A dynamically varying length can arise in systems where growth of the lattice is coupled to the transport of particles to the dynamically-varying end of the lattice [228, 229, 230, 231]. While no exact

solutions have been found, mean-field and hydrodynamic approaches have been successfully applied [232]. In the continuum limit, this problem is analogous to the classic Stefan problem [232, 233], except with nonlinear particle density dynamics (figure 9).
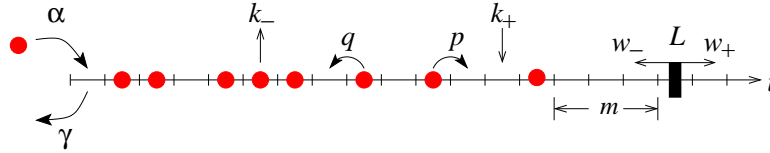
Figure 9. Schematic of an ASEP (adapted from [232]) with detachment and attachment rates k_- and k_+, respectively, and a 'confining' wall at site L. The wall has intrinsic dynamics described by hopping rates $w_\pm$.

Not surprisingly, the techniques presented in the previous section are typically not powerful enough for obtaining exact results for these variants of the basic exclusion processes. Of course, for sufficiently small systems (e.g., $L \lesssim 10$), high performance computers can be used to diagonalize $\mathbb{M}$, but that method is not viable for many physical or biological systems. There are also some cases, including special cases of two-species exclusion and ASEP with extended particles on a ring (to be discussed below, within their own contexts), where exact solutions can be found for all L. Despite the lack of progress in finding analytic results, there are two other approaches which provide valuable insights into these more complex yet more realistic systems. One is computer simulations, exploiting Monte Carlo techniques on our lattice models. Once the stochastic rules of a model are specified, then, this technique corresponds to implementing equation (1). In addition, molecular dynamics simulations with off-lattice systems also proved to be very successful. The other approach is based on designing good approximation schemes for attacking exact equations (or expressions for specific quantities). Mean field theory (MFT), or mean field *approximation*, is most often used. An example is equation (17) for the TASEP. However, systematically improving these approximations it is not generally straightforward. Thus, we will see that, for TASEP with extended objects, the substitution (17) is very poor (when compared to simulation results). Instead, a more sophisticated scheme, implemented by Gibbs, *et.al.* [13, 14], is much more successful at predicting, say, the average current. In turn, when this scheme fails to predict other quantities, another level of approximation [103] (in the spirit of the Bethe-Williams approximation for the Ising model) is designed. Nevertheless, if the predictions are in good agreement with simulations, the MFT provides some confidence that we are 'on the right track' towards our goal: understanding these generalized ASEPs which have found wide applicability in modeling complex biological processes.

4.1. Pore Transport

Transport of atoms and small molecules arises in both man-made structures and cell biological systems. Materials such as zeolites form networks of one-dimensional channels within which molecules, such as light hydrocarbons, can pass through and/or react. A number of authors have used exclusion processes as simple descriptions of single-file or near single-file transport. It has long been known that tracer diffusion in

single-file channels follows subdiffusive dynamics [234, 235, 236, 237, 97]. A mean-square displacement of the form $\langle x^2 \rangle \sim \sqrt{t}$ is found by considering equilibrium fluctuations of the density around the tagged particle in an infinite system. For steady-state particle transport across finite pores, the lattice exclusion process has proved a more useful starting point. Given the frequent application of exclusion processes to pore transport, two important points should be stressed.

First, the standard lattice exclusion process assumes that waiting times are exponentially distributed and, other than lattice site exclusion, are independent. This assumption can fail if, say, an attractive interaction between particles is comparable to the interaction between substrate (e.g., atoms that make up the pore walls) and the particles. Here, concerted motion can arise and has been shown to be important in particle transport. For example, Sholl and Fichthorn have shown using molecular dynamics (MD) simulations how concerted motions of clusters of water affects its overall transport in molecular sieves [238]. Similarly, Sholl and Lee also showed that concerted motions of clusters of CF_4 and Xe in $AlPO_4$-5 and $AlPO_4$-31 zeolites, respectively, contribute significantly to their overall mobilities [239]. Concerted motion has also been predicted to occur in transport across carbon nanotubes [240]. These concerted motions arise from frustration due to a mismatch between particle-particle and particle-pore interaction ranges, allowing for a lower barrier of motion for bound pair of particles that for an isolated, individual particle. Although concerted motion arises from geometrically complicated arrangements of particles that form low energy pathways in the high dimensional energy landscapes, if a small number of these pathways support most of the probability flux, simplifying assumptions can be made. For example, coarse-grained treatments of concerted motion were developed by Sholl and Lee [239]. Concerted motion has also been implemented within lattice models of exclusion processes in a more draconian manner. Gabel, Krapivsky, and Redner have formulated a 'faciliated exclusion' process on a ring whereby a particle hops forward to an empty site *only* if the site behind it is also occupied [241]. They find a maximal current of $3 - 2\sqrt{2}$ which is less than the maximal current of $1/4$ arising in the standard TASEP. A model that incorporates concerted motion might be described by a facilitated exclusion model where motion in either direction occurs faster if the particle is adjacent to another one. The hopping rate might also be increased if an isolated particle moves to a site that results in it having an additional adjacent particle. If these accelerated steps occur much faster than individual particle hops, then the dynamics will resemble motion of pairs of particles. It would be interesting to determine how this model of near-concerted hops increase the overall particle flux.

A second important point to emphasize is that different physical systems are best modeled with varying degrees of asymmetry in the exclusion processes. Two extreme limits are the totally asymmetric process, where particles only hop in one direction, and symmetric exclusion, where particle hopping between any two adjacent sites obeys detail-balance. In this case, detailed balance is violated only at the two ends of the lattice. Net particle current arises only when there exists an asymmetry in the injection and extraction rates at the two ends. This latter scenario corresponds to boundary-driven exclusion processes where differences in the chemical potential of the particles in the two reservoirs drive the flux. Osmotic and pressure-driven flows (when local equilibrium thermodynamics holds and particle inertia is negligible) are examples of processes best described using *symmetric* exclusion processes [242]. However, when particles in the lattice are charged, and an external field is applied, the internal jumps are asymmetric since there is a direct force acting on the particles, breaking detailed

balance. A heuristic delineation between asymmetric and symmetric (boundary-driven) exclusion processes can be motivated by considering the *single-particle* free energy profiles. Figure 10 depicts two hypothetical single-particle free energy profiles experienced by an isolated particle under local thermodynamic equilibrium.
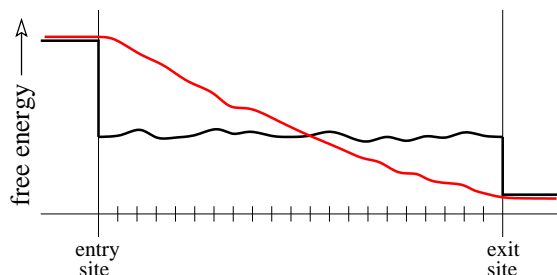

Figure 10. Representative single-particle, one-dimensional free energy landscapes over which excluding particles travel. The black curve free energy profile could represent a symmetric exclusion process, while the red landscape would describe an asymmetric exclusion processes. In the former, detailed balance is assumed to be violated at the entrance and exit sites and the particle flux is driven by differences between the chemical potentials of the two reservoirs.

In biological systems, channels that transport water and neutral (e.g., sugars) or charge-screened molecules, can be described by symmetric exclusion, while motion of charged ions in single-file channels would be best characterized by partially asymmetric exclusions. Modeling uncharged particles allows equal internal hopping rates ($p = q$) with drive originating only at the boundaries The steady-state current is easily found and is a function of the asymmetry in the boundary injection and extraction rates [242, 243]

$$J = \frac{p(\alpha\beta - \gamma\delta)}{(L-1)(\alpha + \delta)(\beta + \gamma) + p(\alpha + \beta + \gamma + \delta)}. \tag{85}$$

The boundary injection and extraction rates are those defined in figure 1(c). As expected, this expression for J is similar to that arising from simple diffusive flux in the $L \to \infty$ limit. However, as discussed, nontrivial current fluctuations, which cannot be accounted for by simple diffusion, have also been worked out [161, 162, 164, 244, 245]. When particles are 'charged', the level of asymmetry (the relative difference between an ion hopping forward and hopping backwards) is controlled by the magnitude of the externally applied 'electric field'. Besides the exact solutions for the steady-state current [125], cumulants of the current in a weakly asymmetric exclusion process have also been derived [165], the slowest dynamic relaxation mode computed [171], and the tracer diffusivity derived [163].

Specific biological realisations of driven transport include ion transport across ion channels [242], while transport across nuclear pore complexes [246, 247], and osmosis [248] are typically boundary-driven, or ratcheted (see the section on molecular motors). In 1998, the X-ray crystal structure of the K$^+$ ion channel was published [+], allowing a more detailed mechanistic understanding of the ion conduction and selectivity across a wide class of related, and biologically important, ion channels [249].

[+] This achievement was partially responsible for Peter Agre and Roderick McKinnonin being awarded the Nobel Prize in chemistry in 2003, "for discoveries concerning channels in cell membranes."

The crystal structure showed three approximately in-line vestibules that can each hold one K^+ ion. Representations of the voltage-gated Kv1.2 channel are shown in figure 11. Ion conduction can thus be modeled by a simple three-site partially asymmetric exclusion process provided the hopping rates at each occupation configuration are physically motivated [248, 250, 251]. However, note that there is evidence that ion dynamics within some ion channels are 'concerted' because the free energy barriers between ion binding sites are small and ions entering an occupied channel can knock the terminal ion out of the channel. This 'knock-on' mechanism [252] has been motivated by molecular dynamics simulations [253, 254] and studied theoretically via a reduced one-dimensional dynamical model [255].

(a) (b)
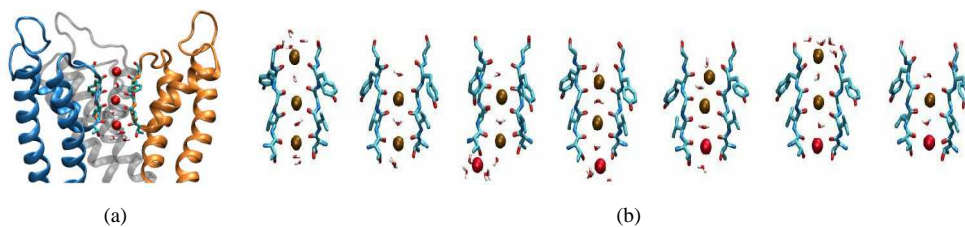
Figure 11. (a) A ribbon figure of the Kv1.2 voltage-gated potassium ion channel embedded in a model lipid membrane. The pore structure clearly shows three dominant interior binding sites. This potassium channel image was made with VMD and is owned by the Theoretical and Computational Biophysics Group, NIH Resource for Macromolecular Modeling and Bioinformatics, at the Beckman Institute, University of Illinois at Urbana-Champaign. (b) A time series of a molecular dynamics simulation suggesting a concerted 'knock-on' mechanism. Image adapted from [254] with original labels removed, and used with their permission.

The symmetric exclusion process has also been used to consider osmotic flow across membrane-spanning, single-file channels [248]. Here, the solvent flux is driven by differences in the injection rates at the two pore ends connected to two separate particle reservoirs. Simple osmosis across a strictly semipermeable membrane can be described by a single species symmetric exclusion process where the injection rate of the solvent from one of the reservoirs is reduced due to its smaller mole fraction arising from the presence of solute in that reservoir [248]. The solvent current is approximately linearly proportional to the difference in injection rates at the two ends of the lattice, inversely proportional to the length of the lattice, but with a weak suppression due to multiple pore occupancy [242].

Another transport channel in cells are nuclear pore complexes (NPC), responsible for the selective shuttling of large molecules and proteins (such as transcription factors, histones, ribosomal subunits) through the double nuclear membrane. Exclusion processes have been employed as theoretical frameworks for describing the efficiency and selectivity NPC transport [247, 256].

In all of the above applications, extensions exploiting multispecies exclusion processes are often motivated. In biological systems ion transport is typically 'gated' by cofactors that bind to the pore, either blocking ion transport, or inducing a conformational change in the pore structure thereby affecting the entrance, exit, and internal hopping rates [222]. The inclusion of additional species of particles in the exclusion process has been used to describe 'transport factor' mediated nuclear

pore transport [246, 247, 256]. For osmosis, solutes that are small enough to enter membrane pores may also interfere with the transport of solvent particles through channels. The solvent and solute species would have different entry, exit, and internal hopping rates, describing their different interactions with the pore. In [248], a simple two-species, three-site, partially asymmetric exclusion model was used to show how solutes that can enter a pore and suppress solvent flux. Moreover, it was found that a small amount of slippage (passing of the solvent and solute particles over each other) and a pore that was slightly permeable to solute can very effectively shunt osmotic flow. When both solute and solvent can pass through the channel (with equal forward and backward hopping rates in the interior), an interesting possibility arises whereby the flux of one of the species can drive the other species from its low concentration reservoir to the high concentration reservoir. Since the mechanism relies on entrainment of particles that are driven up its chemical potential, slippage between the pumping and convected particles destroys this entropic pumping mechanism. The efficiency of using a pumping particle that travels from high chemical potential reservoir to low chemical potential reservoir to pump the secondary particle was found using Monte-Carlo simulations [257].
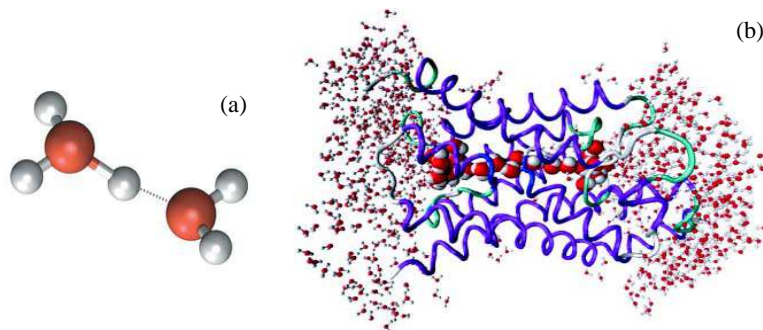
Figure 12. (a) Schematic of the Grotthuss proton transfer mechanism. (b) An MD simulation showing the persistence of a 'water wire' within a membrane-spanning Aquaporin-1 water channel protein [258]. The waters within the pore are shown magnified.

An even more interesting application of multispecies exclusion processes to biological transport arises when the transported ion is a proton. In addition to regulating ionic concentrations, pH regulation is an important aspect of cellular function. It has been known for quite some time that the diffusivity of protons is about an order of magnitude faster than that of small cations [259, 260]. The physical mechanism invoked to explain accelerated motion of protons is based on a proton transfer or shuttling mechanism, analogous to electronic conduction. For a simple ion to traverse a narrow ion channel, it must shed its hydration shell and push any possible water molecules ahead of it within the pore. An extra proton, however, can hop along an oxygen 'backbone' of a line of water molecules, transiently converting each water molecule it visits into a hydronium ion H_3O^+. The Grotthuss mechanism of proton conduction has been conjectured to occur across many narrow pores, including those in gramicidin-A channels [261, 262], proton transfer enzymes such as carbonic anhydrase [263], voltage gated proton channels such as Hv1 [264], Aquaporin water channels [265, 258, 266], and carbon nanotubes [267]. All of these structures have in

common the existence of a relatively stable water wire as shown on the right of figure 12.
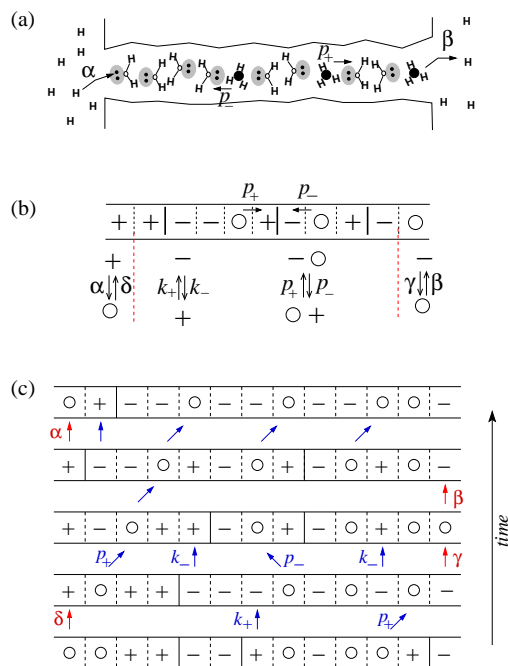
Figure 13. (a) A cartoon of water-wire proton conduction. Hydrogen atoms and lone electron pairs of the water oxygen are shown. (b) A lattice model for the Grotthuss proton conduction mechanism. The symbols $\bigcirc, +$, and $-$ correspond to hydronium ions, water with lone pair pointing to the left, and water with lone electron pair pointing to the right, respectively. Proton movement from left to right leaves the donor site in a $-$ configuration and can occur only if the receptor site is originally in the $+$ configuration. The spontaneous left-right water flipping rates are $k_\pm$ and the proton forward and backward hopping rates (assuming a compatible configuration) are $p_\pm$. (c) A time-sequence of a trajectory of configurations. Figures adapted from [268, 269].

The basic water wire mechanism can be mapped onto a three-species exclusion model as shown in figure 13.* Unlike models where only one extra proton is allowed in the channel at any given time [270], the general exclusion model allows each site to be in one of three states, protonated, water lone pair electrons pointing to the left and to the right. In this particular application, no exact results are known, but mean-field treatments have been used to extract qualitative phenomena [268, 269]. For example, in order to sustain a steady-state proton current, the lone-pair electrons of a water molecule need to flip in order to relay successive protons. Not only was proton conduction found to be mediated by water flipping, but nonlinear effects such as saturation at high voltages and even negative differential resistances were exhibited by the model [268, 269].

* We caution the reader that the usage of 'M species' in the literature is not uniform or unique. Thus, 'three-species' here refer to three types of particles on the lattice, *without* holes. Thus, in terms of states at each site, it is the same as the 'two species' model describing solvent, solute, and holes at each site.

The issue of concerted motions and precise definitions of the proton carrier species also arises in more detailed considerations of proton transport. There has been considerable effort devoted to identifying the precise molecular species that solvates and relays the protons [271]. Moreover, there is some evidence that proton dynamics in water wire conduction may be concerted [263]. Nonetheless, the three-species exclusion model and its potential extensions are fruitful ways of understanding the gross mechanisms in proton conduction.

4.2. Simple models of molecular motors

Perhaps the simplest models of active biological transport are those of isolated molecular motors that move along one-dimensional tracks such as actin, microtubules, DNA, or RNA. Motors are enzymes such as dynein, kinesin, and myosin that hydrolyze molecules such as ATP or GTP, turning the free energy released to directed motion along their one-dimensional substrate [272, 273]. Motoring is necessary for sustaining cell functions such as mediating cell swimming and motility and intracellular transport of biomolecules, particularly at length scales where diffusion is not efficient, or where spatial specificity is required. Due to the importance of molecular motors in intracellular transport and cell motility, there is an enormous literature on the detailed structure and chemo-mechanical transduction mechanisms of molecular motors.

From the theoretical physics point of view, molecular motors are useful examples of non-equilibrium systems. Indeed, such motors typically operate far from equilibrium, in a regime where the usual thermodynamic laws do not apply. A molecular motor is kept far from equilibrium by a coupling with some external 'agent' (e.g., a chemical reaction, or a load-force): under certain conditions, work can be extracted, although the motor operates in a medium with constant (body) temperature. We emphasize that there is no contradiction with thermodynamics: the system is far from equilibrium and the motor simply plays the role of a transducer between the energy put in by the agent (e.g., chemical energy) and the mechanical work extracted. Molecular motors have been described theoretically either by continuous ratchet models or by models based on master equations on a discrete space, which are similar to exclusion-type systems, to which some of the exact analytical techniques described above can be applied. Using an extension of the discrete two-state motor model, Lau *et al.* [274] investigated theoretically the violations of Einstein and Onsager relations and calculated the efficiency for a single processive motor in [274]. Furthermore, it can be shown that the fluctuation relations (such as the Gallavotti-Cohen theorem, the Jarzysnki-Crooks relations) play the role of a general organizing principle. Indeed, cellular motors are systems of molecular size which operate with a small number of molecules, and for these reasons undergo large thermal fluctuations. The fluctuation relations impose general constraints on the function of these nanomachines that go beyond classical thermodynamics. They provide a way to better understand the non-equilibrium energetics of molecular motors and to map out various operating regimes [274, 275, 276].

Significant effort in the investigation into molecular motors has focussed on identifying and understanding the molecular mechanics and the coupling of molecular motion with a chemical reaction such as ATP hydrolysis. Form these studies, complex descriptions of molecular motors have been developed, including a somewhat artificial classification of motors employing 'power stroke' or 'Brownian ratchet' mechanisms. This classification refers to how detailed balance is violated *within* the large motor

molecule or enzyme. If certain internal degrees of freedom in a molecule are made inaccessible at the right times, a net flux along these states can arise, ratcheting the motion. If a particular transition is strongly coupled to specific chemical step such as the hydrolysis of an ATP molecule bound in a pocket of the motor molecule, the motion has been described as a power stroke motor. It has been shown that this distinction is quantitative, rather than qualitative [277]. From a stochastic processes point of view, when the dynamics of the microscopic internal motor degrees of freedom are represented by, e.g., a Markov chain, power stroke and ratchet mechanisms can be distinguished by where detailed balance is violated in the cycle. For example, if the relative amount of violation occurs duriong transitions across states that are directly coupled to motion against a load, the motor will be "ratchet-like".

If the absicca in figure 10 represents sequential internal molecular states, a purely ratchet mechanism is naturally represented by a state evolving along the flat energy profile. In this case, a steady-state probability flux, or molecular motion, arises from the absorbing and emitting boundary conditions that ratchet the overall motion. In this stochastic picture, the power-stroke/Brownian ratchet distinction is mathematically recapitulated by state-space boundary conditions and by the relative amount of convection through state-space. How much a motor utilizes a power-stroke mechanisms would be described by the Peclet number within the framework of single-particle convection-diffusion or Fokker-Planck type equations. For a more detailed delineation of regimes of mechanical-chemical coupling, see the review by Astumian [278].

In many cellular contexts, molecular motors are crowded and interact with each other and exhibit collective behavior. Examples include connected myosin motors in muscle, multiple motors and motor types on cellular filaments and microtubules (often carrying large cargo such as vesicles), and motors that process DNA and RNA. To model such systems, the details of how an isolated motor generates force and moves may be best subsumed into a single parameter representing the mean time between successive motor displacements. The internal dynamics, whether power-stroke or Brownian ratchet, moves the motor one step against a load or resistance at random times. These times are drawn from a distribution of hopping times that is determined by the underlying, internal stochastic process.

One can simplify the modeling of molecular motors by assuming that the motor stepping time is exponentially distributed with an inverse mean that defines the hopping rate. Each motor hops along a one-dimensional track and can exclude other motors. Typically, concerted motions are also neglected in this application. That is, a motor is not allowed to push another one in front of it, moving both motors ahead simultaneously. In the extreme limit, multiple motors are coupled with, e.g., elastic elements and have been extensively modeled using simple Fokker-Planck equations that incorporate mechanical and thermal forces [280, 281, 282, 283, 284, 285, 286]. Weaker interactions that do not bound the distance between motors can be modeled using the excluding particle picture by assigning different rules for the hopping of two adjacent particles, analogous to the facilitated diffusion models of Gabel, Krapivsky, and Redner [241]. Given the assumptions discussed above, exclusion processes can be directly used to model collections of motors moving on one-dimensional tracks. Additional effects particular to applications in biomolecular motors include detachment and attachment kinetics and different types of motors that move in opposing directions.

Molecular motors 'walk' along filaments but have a finite 'processivity' since
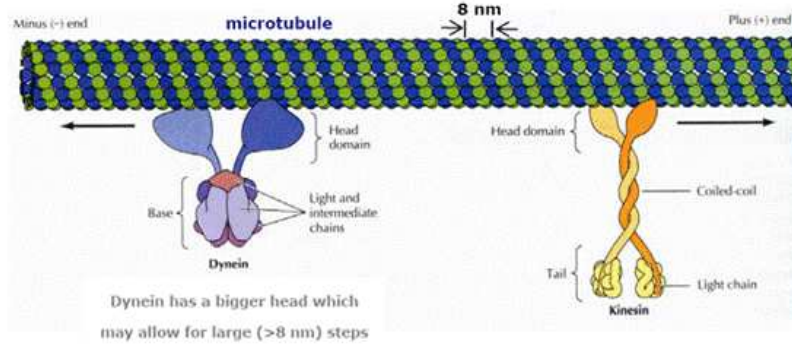
Figure 14. A schematic of two types of molecular motors moving along a cellular microtubule (adapted from [279]). In this picture, kinesin moves to the right while dynein moves to the left. Each motor can be attached to large cargoes such as vesicles or other filaments. Note that the microtubule is constructed of twisted lanes of repeated molecular subunits.

they can spontaneously detach. Thus, they have a distribution of run lengths. Conversely, motor molecules diffusing in the 'bulk' cytoplasmic space can attach to interior locations of the lattice. Detachment violates particle conservation on the lattice and has been studied using mean field models, hydrodynamic approximations [287, 288], and Monte-Carlo simulations [219, 218, 289, 290]. The detachment and possible reattachment of particles on a lattice have been extensively studied in the context of gas adsorption isotherms or 'Langmuir kinetics' (see [291] and references within). While many models of Langmuir isotherms exist, previous studies considered only passive, undriven particles. In the new work combining Langmuir kinetics with driven exclusion processes, analytic progress can be made by considering the infinite site, continuum hydrodynamic limit. If attachment and/or detachment occurs, the hopping rates must be rescaled by the number of lattice sites such that the rates $\omega_{\mathrm{A,D}}$ (cf. figure 5) at each site are inversely proportional to the number of sites L. If this is not done, particles would only occupy a small region near the injection end of a long lattice. To arrive at a nontrivial structure, the attachment and detachment rates must be decreased so that the cumulative probability of desorption is a length-independent constant.

As we mentioned in section 3, continuum hydrodynamic equations allow more complicated models to be approximately treated. This has been the case for one-dimensional exclusion processes with Langmuir kinetics. In the steady-state limit, Parmeggiani *et al.* find [219]

$$\frac{\varepsilon}{2}\frac{\partial^2 \rho(x)}{\partial x^2} + (2\rho - 1)\frac{\partial \rho(x)}{\partial x} + \Omega_{\mathrm{A}}(1 - \rho(x)) - \Omega_{\mathrm{D}}\rho(x) = 0, \qquad (86)$$

where $\Omega_{\mathrm{A,D}} = \omega_{\mathrm{A,D}}L \equiv \omega_{\mathrm{A,D}}/\varepsilon$ represents appropriately rescaled detachment and attachment rates that in this simple model are *independent* of L. A detailed asymptotic analysis of equation (86) was performed and a phase diagram as a function of four parameters (the injection and extraction rates at the ends of the lattice, and the adsorption and desorption rates) was derived [218, 219]. They find a rich phase diagram with coexisting low and high-density phases separated by boundaries induced by the Langmuir kinetics. Langmuir kinetics have also been investigated in the

presence of bottlenecks [292]. Klumpp and Lipowsky [293] have considered asymmetric exclusion in tube-like structures such as those seen in axons or in filapodia [294, 295]. In this simplified geometry, the diffusion of motors within the tube can be explicitly modeled [293].

Since motors are used to carry cargoes across the different regions within a cell, they travel on directed filaments and microtubules. Different motors are used to carry cargo in one direction versus the other. For example, kinesins travel along microtubules in the '+' direction, while dynein travels in the '-' direction, as shown in figure 14. This scenario can be modeled using a two-species exclusion process with Langmuir kinetics overtaking. Moreover, microtubules are composed of multiple twisted filamentous tracks. Not only can motors travel in opposite directions on the same track, but filaments may be oppositely-directed within confined spaces such as axons. Motors traveling in opposite directions on the same filament or on a nearby parallel filament can be modeled using coupled chains of exclusion processes. Many groups have explored the dynamical properties of two-species and two-lane asymmetric exclusion processes (as shown in figure 7) [296, 297, 298, 299, 300]. With the proper biophysical identification of the parameters, results from these studies of interacting lattices should provide illuminating descriptions of more complex scenarios of moleculer motor-mediated transport.

4.3. mRNA translation and protein production

One very special case of interacting motors moving along a one-dimensional track arises in cell biology. In all cells, proteins are synthesized by translation of messenger RNA (mRNA) as schematised in figure 15. Complex ribosome enzymes (shown in figure 15(b)) unidirectionally scan the mRNA polymer, reading triplets of nucleotides and adding the corresponding amino acid to a growing polypeptide chain. Typically, many ribosomes are simultaneously scanning different parts of the mRNA. An electron micrograph of such a *polysome* is shown in figure 15(c).

The ribosomes are actually comprised of two subunits, each made up mostly of RNA and a few proteins. Not only do these 'ribozymes' catalyze the successive addition of the specific amino acid as they scan the mRNA, their unidirectional movement from the 5' end to the 3' end, (where the 5' denotes the end of the mRNA that has the fifth carbon of the sugar ring of the ribose as the terminus) constitutes a highly driven process. Therefore, each ribosome is also a molecular motor that rarely backtracks as it moves forward. The fuel providing the free energy necessary for codon recognition and unidirectional movement is supplied in part by the hydrolysis of GTP [301]. Quantitatively, mRNA translation is different from typical molecular motors in that ribosome processivity is very high, allowing one to reasonably neglect detachments except at the termination end. Moreover, there are no known issues with 'concerted motions' or 'facilitated exclusion'. If one ribosome prematurely pushes the one ahead of it, one would expect many polypeptides to be improperly synthesised.

Thus, at first glance, the TASEP seems to be the perfect model for this translation process, with the particles being ribosomes and a site being a codon – a triplet of nucleotides. On closer examination, it is clear that protein production is much more complicated. Many biophysical features relevant to mRNA translation are missing from the basic TASEP. The desire to have more 'realistic' models of protein production has motivated the development of various extensions to the basic TASEP. In this subsection, we will discuss only two efforts to generalize TASEP: allowing particles of
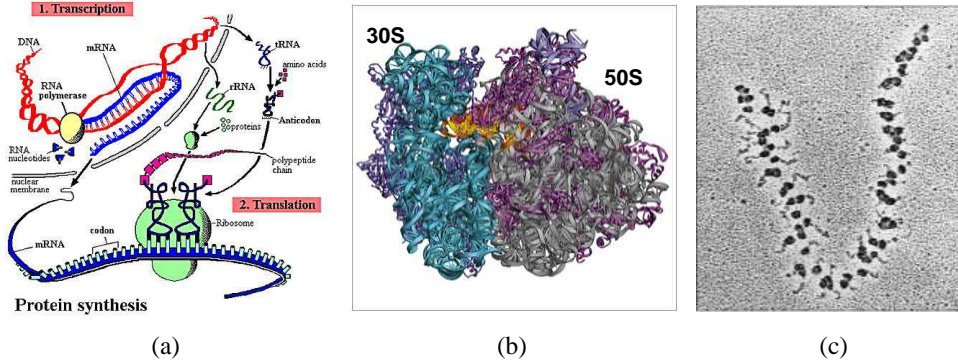
Figure 15. (a) A cartoon of the 'central dogma' in biology where mRNA is synthesized from cellular DNA and transported to the cytoplasm. The cytoplasmic mRNAs are then translated by ribosomes into polypeptides which may then finally be folded and processed into functioning proteins. (b) Crystal structure of both subunits of bacterial ribosome. (c) An electron micrograph of multiple ribosomes translating a single mRNA.

size $\ell > 1$ and incorporating inhomogeneous, site-dependent hopping rates. In each case, we will describe the cell biology which motivates the modifications.

Although the fundamental step size of ribosomes is a codon, the large size of each ribosome (20nm for prokaryotic ribosomes and 25-30nm for eukaryotic ribosomes) means that they each cover approximately 10 codons along the mRNA chain and exclude each other at this range. Therefore, TASEPs comprised of extended objects, occluding $\ell > 1$ lattice sites have therefore been developed, dating back to the late 1960's [13, 14]. Although exact results for such a generalized TASEP on a ring are available [302], the problem with open boundaries remains unsolved. Instead, various MFT's have been successful at capturing many important properties for modeling mRNA translation. Let us devote the next paragraphs to this system.

First, consider a ring of L sites filled with N particles, and note that every configuration with particles of extent ℓ can be matched with a configuration with N point particles ($\ell = 1$) on a ring of $L - N(\ell-1)$ sites. This mapping is easily understood by regarding a configuration, $\mathcal{C}$, as clusters of adjoining vacancies followed by clusters of adjoining particles (regardless of their sizes). Therefore, the stationary distribution, $P^*(\mathcal{C})$, is again flat and independent of ℓ for all p, q. Of course, the sum of the particle density ($\rho \equiv N/L$) and the hole density (ρ_{hole}) now satisfy $\ell\rho + \rho_{\text{hole}} = 1$, but with ρ lying in a limited interval $[0, 1/\ell]$. With $P^* \propto 1$, finding the probability of particle-hole pairs is straightforward, resulting in an exact expression [205] for the current density relation, $J(\rho) = \rho\rho_{\text{hole}}/(\rho + \rho_{\text{hole}} - 1/L)$, in the TASEP case. To lowest order in $1/L$, the formula

$$J = \frac{\rho\,(1 - \ell\rho)}{1 - (\ell - 1)\rho} \tag{87}$$

was known as early as 1968 [13, 14], and leads to a maximal current of $(1 + \sqrt{\ell})^{-2}$ associated with the optimal density of $\hat{\rho} = (\ell + \sqrt{\ell})^{-1}$. Note that, though $J(\rho)$ is no longer symmetric about $\hat{\rho}$, the particle-hole symmetry ($\rho \leftrightarrow \rho_{\text{hole}}$) is preserved. This invariance is expected on physical grounds, as the current arises only from exchanges of particle-hole pairs. Though the stationary measure is trivial and $G(r)$, the expectation

value of two particles separated by r sites, can be written formally as a sum of products of binomials. Of course, period-ℓ structures are to be expected in $G(r)$. Despite the conceptual simplicity of this problem, remarkably intricate patterns emerge [303], especially near complete filling, $L \cong N\ell$ [304]. Such structures are completely absent from the $\ell = 1$ case (whether in periodic or open TASEP), showing us that, even in seemingly trivial situations, statistics of extended objects can produce surprises.

Turning to the open boundary TASEP, we must first specify how a particle enters/exits the lattice. One possibility is 'complete entry, incremental exit' [305], where a particle may enter completely provided the first ℓ sites are empty, while it may exit moving one site at a time. In the NESS, exact expressions for the current like (16) can still be written. When both i and $i+\ell$ are within $[1, L]$, we have $J = \langle \sigma_i(1-\sigma_{i+\ell}) \rangle$. From the 'incremental exit' rule, we have $J = \langle \sigma_{L-\ell} \rangle = \ldots = \langle \sigma_{L-1} \rangle = \beta \langle \sigma_L \rangle$, leading to a simple profile next to the exit. The major challenge comes from the 'complete entry' condition: $J = \alpha \langle \prod_{k=1}^{\ell}(1 - \sigma_k) \rangle$. Since this problem can no longer be solved exactly, many conclusions can only be drawn from simulation studies or imposing mean field approximations. For the latter, the naïve replacement of averages of products of σ by products of $\langle \sigma \rangle$ (e.g., $\langle \sigma_i \sigma_{i+\ell} \rangle \to \langle \sigma_i \rangle \langle \sigma_{i+\ell} \rangle$) leads to extremely poor predictions. Gibbs, *et.al.* [13, 14] took into account some of the effects of exclusion at a distance and approximated $J = \langle \sigma_i(1 - \sigma_{i+\ell}) \rangle$ by

$$J = \frac{\rho_i \bar{\rho}_i}{\rho_{i+\ell} + \bar{\rho}_i} \tag{88}$$

where $\bar{\rho}_i \equiv 1 - \sum_{k=i+1}^{i+\ell} \rho_k$ is an effective hole density in the ℓ sites following i. For the ring, the profile is flat and $\rho_i = \rho$, so that (88) reduces to (87). Supplemented with the appropriate boundary equations, (88) can be regarded as a recursion relation for the profile. The successes of this approach include predicting a phase diagram that is the same as the one in figure 2(c), except that the boundaries of the maximal current phase are now at $\alpha, \beta = \left(1 + \sqrt{\ell}\right)^{-1}$. Simulations largely confirm such predictions [205, 305], suggesting that the correlations neglected by the scheme of Gibbs, *et al.* [13, 14] are indeed small. On the other hand, for more sensitive quantities like the profile, this MFT is less successful, especially for the high density phase ($\beta \ll \alpha \sim 1$). To produce better predictions, Shaw, *et al.* [103] introduced a more sophisticated MFT, taking into account some pair correlations. So far, no higher level of MFT have been attempted.

The second modification to the basic TASEP we consider here is site-dependent hopping rates. Since the translation of mRNA into polypeptides depends on the sequence of nucleotides, the hopping rates of the ribosome TASEP particles can vary dramatically as a function of its position on the lattice. The local hopping rates depend on the effective abundance of the specific amino-acid-charged tRNA that participates in each elongation step at each site. One of the first treatments of TASEPs on a nonuniform lattice considered a single defect, or slow hopping site♯, in the middle of an asymptotically long lattice. Kolomeisky derived the expected steady-state particle flux across a lattice with a single slow hopping site by ignoring particle-particle correlations across the defect [306]. He self-consistently matched the exit rate from the first half of the chain with the injection rate of the second half of the chain. This approach indicated that each long uniform region between slow sites

---

♯ If an isolated site had faster hopping than all its neighbors, the average current is hardly affected, though there are noticable changes to the profile. Thus, we focus on slow sites.

can approximately be treated as separate, but self-consistently connected, uniform exclusion processes. Later work by Chou and Lakatos developed a more refined method of connecting the current between sections separated by interior defects. Their method generalizes mean-field theory by explicitly enumerating the configurations of the sites straddling the inhomogeneity, and self-consistently matching the current across this segment with the asymptotically exact steady-state currents across the rest of the homogeneous lattice. Steady-state particle currents across localized defects can be accurately computed [307]. Using this approach, the synergistic effects of two nearby slow hopping sites were analyzed. It was shown that two defects decreased the current more when they are placed close to each other. The decrease in current approaches that of a single defect as the distance between two defects diverges since the dynamical 'interaction' from overlap of density boundary layers vanishes.
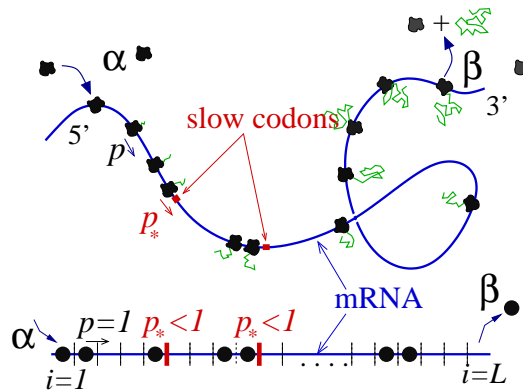
Figure 16. mRNA translation with fixed slow codons, or bottlenecks across which ribosome motion is slower ($p^* < p$) than across other codons. This local slowing down can arise from a limited supply of the appropriate amino acid-charged tRNA corresponding to the slow site.

Another method for approximately treating inhomogeneous hopping rates was developed by Shaw *et al.* [103] where the original mean-field equations of Gibbs *et al.* [13, 14] were generalized to include site-dependent elongation rates. Dong, Schmittman, and Zia [308, 309] systematically analyzed the effects of defects on the steady-state current of extended particles that occupy multiple ($w > 1$) sites. They used a combination of self-consistent mean field theory and Monte-Carlo simulations to show the importance of the location of the defect, especially if the defect is placed close entry or exit sites where they may possibly 'interact' with the end-induced density boundary layers.

As mentioned in section 3.3 hydrodynamic MFT developed for analyzing systems with slowly varying hopping rates. Continuum equations, such as (84), that incorporate spatially varying hopping rate functions $p(x)$ and $q(x)$ have been derived for the mean field ribosome density $\rho(x)$ [205, 206, 207, 124]. For single-site particles, these hydrodynamic equations can be integrated once to arrive at singular nonlinear first order differential equation where the integration constant is the steady-state particle current. Using singular perturbation theory, analytic solutions for density profiles have been found for very specific hopping rate functions $p(x)$ and $q(x)$ [124, 204].

The stochastic process underlying the models of mRNA translation described above all assume an exponentially-distributed waiting time between elongation events. Dwell time distributions would be difficult to incorporate into simple ODEs for the mean-field particle density or continuum hydrodynamic equations. Although different dwell time distributions would not qualitatively affect steady-state ribosome current and protein production rate, to model them explicitly requires incorporation of intermediate biochemical steps involved in initiation, elongation, and termination of the individual ribosomes. These steps include binding of an amino-acid charged transfer RNA (tRNA) to one of the binding sites, hydrolysis, etc. [310]. Models that include more complex elongation steps have also been developed by a number of researchers [311, 312, 313, 226, 314, 225, 315]. The main qualitative result of these studies is that the standard current phase diagram is shifted due to a varying *effective* elongation (internal hopping) rate. Since the internal hopping rate depends on the details of their models, it cannot be nondimensionalized and the standard phase diagram is roughly reproduced with $\alpha_{\text{eff}}/p_{\text{eff}}$ and $\beta_{\text{eff}}/p_{\text{eff}}$ as the tuning variable. Here α_{eff}, β_{eff}, and p_{eff} are are effective rates that might be estimated as the inverse of the mean of the associated dwell time distributions.

(a)   (b)
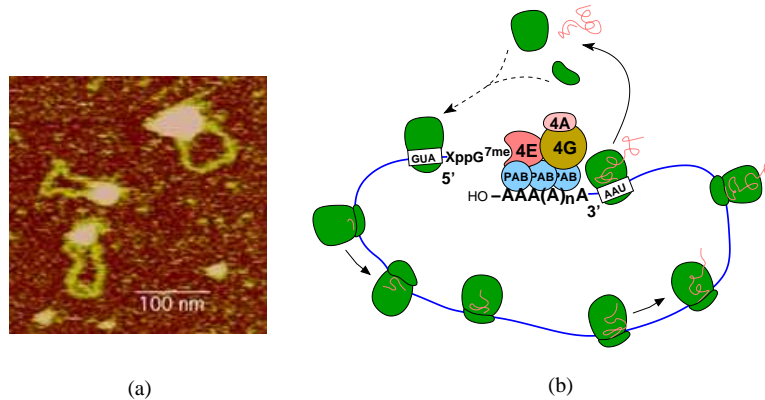
Figure 17. (a) AFM image of circularized mRNA. (b) Schematic of a model where ends of mRNA are sticky (the poly-A tails are known to bind to initiation factors [316, 317, 318]), increasing the probability of loop formation.

Finally, the mRNA translation process, much like molecular motor-facilitated intracellular transport, occurs in complex, spatially heterogeneous environments and involves many molecular players that initiate and terminate the process. For example, certain initiation factors that prime the initiation site for ribosomal entry have been shown to bind to the polyadenylated tails of mRNA, thereby forming circularized RNA. One hypothesis is that mRNA circularization facilitates the recycling of ribosomes. In circularized mRNA, ribosomes that detach from the termination site after completing translation have a shorter distance to diffuse before rebinding to the initiation site. A model for this effect was developed in [319], where an effective injection rate α_{eff} was self-consistently found by balancing the steady-state ribosome concentration at the initiation site with the diffusive ribosome flux emanating from the nearly termination site. In this model, the diffusive feedback tends to increase the protein production rate, especially when overall ribosome concentrations are low. One can also imagine a strong feedback if factors regulating translation initiation were

themselves products of translation. Newly produced cofactors can readily maintain the initiation rate α at a high value.

An even more important aspect of mRNA translation is that ribosomes and initiation factors [320], and mRNAs [321] can be actively localized to endoplasmic reticular (ER) membranes and compartments, depending on what types of proteins they code for, and where these proteins are needed. In confined cellular spaces, the supply of ribosomes and initiation factors may be limited. Moreover, there are many different mRNA copies that compete with each other for ribosomes. This global competition has been modeled by Cook *et al.* [322, 323] who defined an effective initiation rate $\alpha_{\text{eff}}(N)$ which is a monotonically increasing function of the free ribosome concentration. They considered mRNAs of different length (but of identical initiation, elongation, and termination rates) and found that steady-state protein production for different length mRNA's were comparable, but that their ribosome loading levels exhibit varying levels of sensitivity on the total ribosome mass.

4.4. Free boundary problems and filament length control

Our final example of a class of biological application of exclusion processes involves changes in the length of the underlying one-dimensional substrate. A dynamically varying lattice length arises in at least three different cellular contexts: growth of filaments such as hyphae and cellular microtubules, replication forks, and mRNA secondary structure. in each of these examples, there is a 'moving boundary' whose dynamics depends on transport within the domain bounded by the boundary.
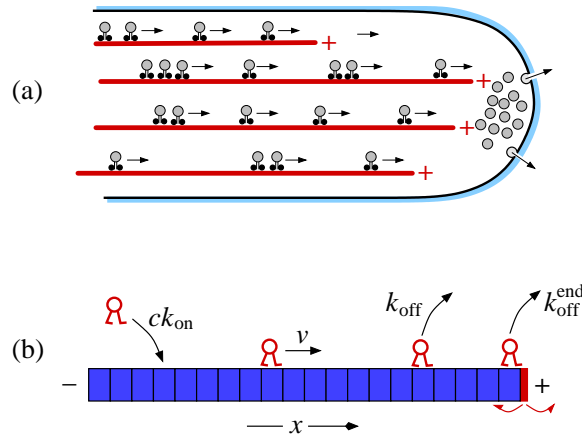
Figure 18. (a) Schematic of multiple TASEPs a dynamically growing tips. The particles are motors carrying building blocks of the underlying filaments [228]. (b) A model of microtubule length control where particles reaching the tip depolymerises the last subunit [231]. Figures are adapted from those in [228] and [231].

An analogy can be made with the classic free boundary problem arising in continuum physics. In the 'Stefan problem' a diffusive quantity mediates the growth of an interface bounding the dynamics. This diffusing quantity may be heat which melts away water-ice interface [324], or a particulate systems that deposits and makes the interface grow [233]. In systems relevant to cell biology, the dynamics

(i) occur in confined, often one-dimensional geometries, and (ii) occur on a fluctuating mesoscopic or molecular scale. In confined geometries, particle-particle exclusion become important. By contrast, this exclusion is absent when the transported field is say, heat. On small scales, statistical fluctuations of the interface, and its coupling with the fluctuating particle field can also be important.

A stochastic one-dimensional moving boundary problem can also be described within an exclusion process where the number of sites is allowed to fluctuate. Such models have been described in [232, 228, 229, 232, 230], and [231]. In [232], a fluctuating wall is coupled to an asymmetric exclusion process as shown in figure 9. The wall particle acts like a piston and defines one boundary of the lattice and has its own intrinsic forward and backward hopping rates. Particles impinge on the wall and have a certain detachment rate. Using a moving frame version of asymptotic matching [307] the expected position and fluctuations of the wall were accurately computed. The wall was found to either extend the lattice indefinitely, compress the particles and fall off the lattice at the injection site, or find an equilibrium lattice length.

In terms of specific biological applications, Evans and Sugden [228] and Sugden *et al.* [229] consider a free boundary TASEP as a model for hyphae growth in fungi (cf. figure 18(a)). The hypothesis is that kinesin motors carry cargo and move unidirectionally toward the tip. The delivered cargo can then extend the tip by incrementing the number of lattice sites of the TASEP. In this case, there is no confining wall, and the velocity tip extension is proportional to the number of arriving TASEP particles. Even though the tip is always growing with a fixed velocity, the particle density profiles can acquire different structure, including a jammed, high density phase.

Another application of dynamic-boundary TASEPs involving molecular motors was described by Hough *et al.* [231]. In their model of microtubule length control, kinesin-8 motors move along a microtubule and *depolymerize* the tip when it is reached. The tip also has an intrinsic degradation and assembly rate, the latter depending on the concentration of subunits in the bulk. Therefore, this model is similar to a TASEP with a confining wall [232] representing the end of the lattice. However, in this model, the kinesis motors also undergo Langmuir kinetics by attaching to, and detaching from the microtubule lattice. Hough *et al.* find regimes where microtubule length-dependent depolymerization rates arise, as well as how the behavior depends on bulk motor concentrations [231].

A number of potentially new models remain relatively unexplored. For example, molecular motors often encounter an obstacle. As the helicase motor separates DNA strands for transcription, it must break base pair bonds and push the replication fork forward [325, 326, 327, 328]. The fork may be represented by a confining wall that tends to reseal the single strands of DNA. Similarly, mRNA translation by ribosome 'motors' typically occur in the presence of hairpins that must be separated before the ribosomes can progress. In both of these applications the motor-wall interaction may be considered passive (ratchet-like) or active (forced separation) [328]. These limits are again related to the issue of concerted motion or faciliated exclusion mentioned earlier. The motor can actively advance the replication fork, whereby the forward motions of the leading particle and the wall occur simultaneously in a concerted fashion. Alternatively, the opening of the fork can be thermally activated, temporarily allowing the leading motor to ratchet the wall. Sometimes, due to the particular geometry, a motor may not need to move against a barrier, but may pass through it.

An interesting realisation arises in mRNA translation where ribosome may jump over hairpins, effectively making hops to an empty site far away on the lattice. This kind of 'short-cut' model has been studied using mean-field theory and simulations by Kim *et al.* [329] and have been found to exhibit coexistence of empty and jammed phases. The consequences of these rich mechanisms on cell biology remain to be explored.

5. Summary and outlook

Non-equilibrium statistical mechanics is the study of stochastic processes for a system involving many interacting degrees of freedom. As such, it concerns essentially the entire spectrum of natural phenomena, ranging over all length scales and relevant for all areas in science and engineering. While a small encyclopedia would be needed to adequately cover NESM, reviews dealing with more specialised topics are abundant in the literature. In this article, we attempt a compromise by providing (a) a bird's eye view of NESM, and (b) a 'bridge' between the two different approaches to the subject. For the former, we review some of the fundamental issues associated with NESM and why the techniques (and assumptions) of equilibrium statistical mechanics cannot be easily generalized. Using the language of stochastic processes, we base our discussions on master equations and focus on systems which violate detailed balance (or time reversal). One serious consequence is that, given a set of such rates, even the stationary distribution, P^* – a NESS analog of the Boltzmann factor $e^{-\beta\mathcal{H}}$ – is generally unknown. There is an additional challenge: the presence of persistent *probability currents* (forming closed loops, of course), K^*, much like the steady electric current loops in mangetostatics. By contrast, $K^* \equiv 0$ if the transition rates obey detailed balance, in analog to electrostatics. We emphasized that these currents play important roles in a NESS, as they lead to persistent fluxes of physically observable quantities (e.g., mass, energy, etc.) as well as constant entropy production in the surrounding medium.

Naturally, our 'bird's eye view' is both limited and colored. For example, we offer only a brief glance on fluctuation theorems and symmetry relations, a topic of NESM which has witnessed considerable progress over the past two decades. Even more generally, our focus on master equations implicitly assumes that the dynamics can be decomposed into a series of Markov processes with exponentially distributed waiting times in each configuration. Age-dependent processes described by more complex waiting time distributions of each configuration may often be better studied using theories of branching processes. Moreover, master equation approaches are not very suited for studying the statistics of individual trajectories or realisations. Understanding properties of individual trajectories in configuration space is important, for example, in problems of inference and reconstruction of the stochastic rules from data. These attributes are better analysed using techniques of, e.g., stochastic calculus or path integrals. Therefore, a comprehensive overview of the foundations of NESM and stochastic processes would include concepts and formalism from other disciplines such as probability theory, statistics, and control theory - a task far beyond our scope.

To meet the challenges posed by NESM, a wide range of approaches have been developed. On the one hand, we have model systems, sufficiently simple that rigorous mathematical analysis is feasible. At the other extreme are models which account for many ingredients deemed essential for characterizing the large variety of phenomena found in nature. Understandably, those working on either end of this spectrum are not typically familiar with the progress at the other end. A historic example appeared in

the late 1960's when Spitzer [9] and Gibbs, *et.al.* [13, 14] investigated independently the same stochastic process, but were unaware of each others' studies. In this article, we attempt to bridge this divide by providing brief reviews of a limited set of topics from both ends.

For the exclusion process, we presented many exact results, along with two complementary techniques to obtain them. The stationary distribution for a system with periodic boundary conditions (i.e., ASEP on a ring) was known to be trivial [9]. On the other hand, a rich variety of dynamic properties, even for SEP, have been discovered over the last four decades. With open boundaries, particles may enter or exit the lattice at both ends, so that the total occupation becomes a dynamic variable. As a result, this system poses much more of a challenge. Little was known until the 1990's, when the exact P^* was found [118, 120, 121] through an ingenious recognition of a matrix representation. For simplicity, we presented the details of this method only for the extreme case of TASEP, in which particles enter/exit with rate α/β (section 3.4). Once P^* is known, it is straightforward to compute the exact *particle* current, J, and the mean density profile ρ_i. A non-trivial phase diagram in the α-β plane emerged, with three distinct phases separated by both continuous and discontinuous transitions (section 3.5). In addition, algebraic singularities are always present in one of the phases. Such phenomena are novel indeed, since the conventional wisdom from EQSM predicts no phase transitions (i.e., long-range order), let alone generic algebraic singularities, for systems in one dimension, with short-ranged interactions! Beyond NESS, another powerful method – the Bethe Ansatz – have been applied successfully to obtain time-dependent properties (section 3.7). Analyzing the spectrum and the eigenvectors (Bethe wave functions) of the full Markov matrix, other physically interesting quantities in a NESS can be also computed. Examples include the fluctuations of the current (around the mean J), encoded in the large deviation function, $G(j)$. The knowledge of dynamic properties also allows us to explore, in principle, ASEPs on *infinite* lattices, for which the initial configuration must be specified and the system properties after long times are of interest. In practice, however, these problems are attacked by another technique, fascinatingly related to the theory of random matrices, representations and combinatorics (section 3.10). These powerful methods have yielded mathematically elegant and physically comprehensible results, rendering exclusion models extremely appealing for modeling real systems.

Apart from exact solutions, we also presented an important approximation scheme – the mean-field theory. Based on physically reasonable and intuitive arguments, we consider coarse-grained densities as continuum fields, obeying hydrodynamic equations, e.g., the density $\rho(x,t)$ in ASEP. Remarkably, such a MFT predicted some aspects of TASEP exactly (e.g., the current density relation $J = \rho(1-\rho)$). Though neither rigorous nor a systematic expansion (such as perturbation theory with a small parameter), MFT has provided valuable insights into behaviour which we cannot compute exactly. This is especially true when appropriate noise terms are added, so that we can access not only the (possibly inhomogeneous) stationary profiles but also the fluctuations and correlations near them. A good example is the average power spectrum associated with $N(t)$, the total mass in an open TASEP. Intimately related to the time-dependent correlation of the currents at the two ends, this quantity has eluded efforts to find an exact expression, despite our extensive knowledge about the full Markov matrix. Instead, starting with a MFT and expanding around a flat profile in the high/low density phase, many interesting properties of this power spectrum can be reasonably well understood [330, 331]. Undoubtedly, there are many other

physically interesting quantities (in ASEP and other 'exactly solvable systems') for which theoretical predictions can be obtained only from mean field approximations. Of course, as we consider modeling transport phenomena in biological systems, more realistic features must be included. Then, MFT typically offers the only route towards some quantitative understanding.

We next turned to specific generalizations of the ASEP which are motivated by problems in biological transport. While the exactly solvable ASEP consists of a single lattice of fixed length with at most one particle occupying each site and hopping along from site to site with the same rate, the variety of transport phenomena in cell biology calls for different ways to relax these constraints. Thus, in the first model for translation in protein synthesis, Gibbs, *et.al.* already introduced two features [13, 14] absent from the standard ASEP. Representing ribosomes/codons by particles/sites, and being aware that ribosomes are large molecules covering $O(10)$ codons, they considered ASEP with *extended objects*. They were also mindful that the sequence of codons in a typical mRNA consists of different codons, leading to a ribosome elongating (moving along the mRNA) with possibly different rates. The result is an ASEP with *inhomogeneous hopping rates*. Beyond these two aspects, we know that there are typically thousands of copies of many different mRNA's (synthesizing different proteins) within a single cell. Now, they compete for the same pool of ribosomes. To account for such competition, we should study multiple TASEPs, with different lengths, 'interacting' with each other through a common pool of particles. Within the cell, the ribosomes presumably diffuse around, leading to possibly more complex pathways of this 'recycling of ribosomes.'

Of course, ribosome motion along mRNA is only one specific example of molecular motors. Therefore, the TASEP is also suited for modeling cargo transport by molecular motors 'walking' along cellular microtubules. In this case, many essential biological features are also absent from the standard TASEP model. Motors are known to detach from the microtubule and reattach at other points, so that Langmuir kinetics [291] should be introduced. The cargoes they carry are typically much larger than their step size, leading us again to long-ranged particle-particle interactions. There are many lanes on a microtubule, so that we should include multiple TASEPs in parallel, with particles transfering from one lattice to another, much like vehicular traffic on a multilane highway. Molecular motors come in many varieties (dynein, kinesin, etc.) which move in opposite directions and at different speeds. Consequently, a proper model would consist of several particle species hopping in different directions. The variety of speeds is the result of complex, multi-step chemical reactions, so that the dwell times are not necessarily distributed according to simple exponentials. To account for such details, particles with internal states can be used necessary. This level of complexity is also sufficient for modeling another important biological process: transport through channels on membranes (pores). Various ions, atoms and molecules are driven in both directions, often 'squeezing by' each other. Finally, microtubules grow and shrink, a process modeled by a dynamic L, the length of our lattice. Typically, the associated rates are governed by the densities of particles at the tip, leading us to an entirely new dimension in mathematical complexity.

Finally, let us provide an outlook of NESM beyond the topics presented in the sections here. In the realm of exactly solvable models, ASEP is just one of many. Not surprisingly, all but a few are one-dimensional systems. For example, we noted in section 3.9 the zero-range process. Also introduced by Spitzer [9], it is a closely related model for mass transport. Multiple occupancy is allowed at each site, while some of the

particles hop to the next site. Thus, this process is well suited to describe passengers at bus stops, with some of them being transported to the next stop. Especially interesting is the presence of a 'condensation transition,' where a macroscopic number of particles occupy a single site as the overall particle density on a ring is increased beyond a critical value. Much progress has emerged, especially in the last two decades (see [332] for a review). Another notable example of transport is the ABC model [86, 87], mentioned at the end of section 2. In general, it also displays transitions of a non-equilibrium nature, admitting long-range order despite evolving with only short-ranged dynamics.

Apart from transport models, exact results are also known for systems with no conservation law. A good example is the kinetic Ising chain [53], coupled to two thermal reservoirs at different temperatures ($T > T'$). As a result, it settles down to a NESS, with generally unknown P^*. Depending on the details of the coupling, exact results are nevertheless available. In particular, if every other spin is updated by a heat-bath dynamics associated with T and T', then *all* multi-spin correlations are known exactly [333, 334]. Remarkably, even the full time dependence of these correlations can be obtained exactly, so that the full $P(\mathcal{C}, t)$ can be displayed explicitly as well [335] ††. As a result, it is possible to compute the energy flow *through* the system (from the hotter bath to the cooler one) in the NESS, as well as the entropy production associated with the two baths [333]. Similar exact results are available in a more common form of imposing two baths, namely, joining two semi-finite chains (coupled to T and T') at a single point. Since the energy flows from the hotter bath, across this junction, to the cooler side, we may ask for say, (a) the power injected to the latter and (b) the profile of how this injected energy is lost to the colder bath. Only the average of the latter is known [337], but the large deviation function of the total injected power can be computed exactly [338, 339]. These are just some examples of other exactly solvable systems which evolve with detailed balance violating dynamics.

In the realm of potential applications, exclusion processes extend well beyond the examples in biological transport presented here. In the general area of 'soft condensed matter,' the exclusion mechanism arises in many other systems, such as motion of confined colloids [340, 341]. Further afield, the process of surface growth in a particular two-dimensional system can be mapped to an ASEP [342, 182]. On larger scales, exclusion processes lends themselves naturally to modeling traffic flow [343, 344, 345] and service queues [346]. For each of these applications, though ASEP and its variants may not be sufficiently 'realistic', they nonetheless provide a succinct physical picture, some insights from mean-field analysis and a precise language on which sophisticated mathematical techniques can be applied. Along with the overall improvement of various technologies (in e.g., nanoscience, renewable energy), we expect that there will be many opportunities for exclusion processes to play a role, both in modeling newly discovered phenomena and in shaping directions of further research.

Broadening our outlook from exactly solvable models and potential applications to NESM in general, the vistas are expansive. It is beyond our scope to provide an exhaustive list of such systems, which would include problems in aging and branching processes, directed percolation, dynamic networks, earthquake prediction, epidemics spreading, granular materials, financial markets, persistence phenomena, population dynamics, reaction diffusion, self organized critically, etc. On the purely

††Indeed, due to the simplicity of heat-bath dynamics, some exact results are known even if the rates are *time dependent* [336].

theoretical front, many fundamental issues await further exploration. For example, the implications of probability currents, beyond the computation of physical fluxes, may be far reaching. If we pursue the analog with electromagnetism, we could ask if these currents can be linked to a form of 'magnetic fields,' if there is an underlying gauge theory, and if these concepts are constructive. Perhaps these ideas will lead us to a meaningful framework for *all* stationary states, characterized by the pair of distributions $\{P^*, K^*\}$, which encompasses the very successful Boltzmann-Gibbs picture for the equilibrium states. In particular, in attempting to describe systems which affect, and are affected by, their environment (through e.g., entropy production) NESS represents a significant increase of complexity from EQSS. Of course, the hope is that an overarching theory for NESM, from the full dynamics to predicting NESS from a given set of rates, will emerge in the near future. Such a theory should help us reach the ultimate goal for say, biology – which would be the ability to predict the form and behaviour of a living organism, based only on its intrinsic DNA sequence and the external environment it finds itself. For the latter, we have in mind both sources of input (e.g., light, air, food, stimulations) and output (e.g., waste disposal, work, reproduction). In the absence of such interactions with the environment, an isolated DNA will evolve to an equilibrium state – probably just an inert macromolecule. To fully understand the physics of life, we believe, a firm grasp of non-equilibrium statistical mechanics is absolutely vital.

6. Acknowledgments

[1] Young AP, editor. Spin Glasses and Random Fields. vol. 12 of Directions in Condensed Matter Physics. Singapore: World Scientific; 1998.

[2] de Dominicis C, Giardina I. Random Fields and Spin Glasses: A Field Theory Approach. Cambridge: Cambridge University Press; 2010.

[3] Henkel M, Pleimling M. Nonequilibrium Phase Transitions Volume 2 - Ageing and Dynamical Scaling far from Equilibrium. Heidelberg: Springer; 2010.

[4] Hill TL. Studies in irreversible thermodynamics IV. diagrammatic representation of steady state fluxes for unimolecular systems. Journal of Theoretical Biology. 1966;10:442–459.

[5] Committee on CMMP 2010 NRC Solid State Sciences Committee. Condensed-Matter and Materials Physics: The Science of the World Around Us. Washington, DC: The National Academies Press; 2007.

[6] BESAC Subcommittee on Grand Challenges for Basic Energy Sciences, *Directing Matter and Energy: Five Challenges for Science and the Imagination*. Washington, DC: U.S. Department of Energy; 2007.

[7] Zia RKP, Schmittmann B. Probability currents as principal characteristics in the statistical mechanics of non-equilibrium steady states. J Stat Mech: Theor Exp. 2007;p. P07012.

[8] Jiang DQ, Qian M, Qian MP. Mathematical Theory of Nonequilibrium Steady States: On the Frontier of Probability and Dynamical Systems. Berlin: Springer; 2004.

[9] Spitzer F. Interaction of Markov processes. Adv Math. 1970;5:246–290.

[10] Spohn H. Large Scale Dynamics of Interacting Particles. Heidelberg: Springer Verlag; 1991.

[11] Liggett TM. Stochastic Interacting Systems: Contact, Voter, and Exclusion Processes. Berlin: Springer Verlag; 1999.

[12] Schütz G. Exactly solvable models for many-body systems far from equilibrium. vol. 19 of Phase Transitions and Critical Phenomena. New York: Academic Press; 2000.

[13] MacDonald CT, Gibbs JH, Pipkin AC. Kinetics of biopolymerization on nucleic acid templates. Biopolymers. 1968;6:1–25.

[14] MacDonald CT, Gibbs JH. Concerning the kinetics of polypeptide synthesis on polyribosomes. Biopolymers. 1969;7:707–725.

[15] Chowdhury D, Santen L, Schadschneider A. Statistical physics of vehicular traffic and some related systems. Physics Reports. 2000;329:199–329.

[16] Kardar M, Parisi G, Zhang YC. Dynamic Scaling of Growing Interfaces. Phys Rev Lett. 1986;56(9):889–892.

[17] Wolf DE, Tang LH. Inhomogeneous growth processes. Phys Rev Lett. 1990;65(13):1591–1594.

[18] Wang GC, Lu TM. Physical realization of two-dimensional Ising critical phenomena: Oxygen chemisorbed on the W(112) surface. Phys Rev B. 1985;31(9):5918–5922.

[19] Lynn JW, Clinton TW, Li WH, Erwin RW, Liu JZ, Vandervoort K, et al. 2D and 3D magnetic behavior of Er in $ErBa_2Cu_3O_7$. Phys Rev Lett. 1989;63(23):2606–2609.

[20] Wolf WP. The Ising model and real magnetic materials. Braz J Phys. 2000;30(4):794–810.

[21] Wilson KG. The renormalization group and critical phenomena. Rev Mod Phys. 1983;55(3):583–600.

[22] Quinn HR. Time reversal violation. Journal of Physics: Conference Series. 2009;171(1):012001.

[23] Onsager L. Reciprocal Relations in Irreversible Processes. I. Phys Rev. 1931;37(4):405–426.

[24] Green MS. Markoff Random Processes and the Statistical Mechanics of Time-Dependent Phenomena. II. Irreversible Processes in Fluids. J Chem Phys. 1954;22(3):398–413.

[25] Kubo R. Statistical-Mechanical Theory of Irreversible Processes. I. General Theory and Simple Applications to Magnetic and Conduction Problems. Journal of the Physical Society of Japan. 1957;12(6):570–586.

[26] de Groot SR, Mazur P. Non-equilibrium thermodynamics. Amsterdam: North Holland; 1962.

[27] Jarzynski C. Nonequilibrium Equality for Free Energy Differences. Phys Rev Lett. 1997;78:2690.

[28] Crooks GE. Nonequilibrium measurements of free energy differences for microscopically reversible Markovian systems. J Stat Phys. 1998;90:1481.

[29] Crooks GE. Path-ensemble averages in systems driven far from equilibrium. Phys Rev E. 2000;61:2361.

[30] Hatano T, Sasa SI. Steady-State Thermodynamics of Langevin Systems. Phys Rev Lett. 2001;86:3463.

[31] Hummer G, Szabo A. Free energy reconstruction from nonequilibrium single-molecule pulling experiments. Proc Natl Acad Sci USA. 2001;98:3658–3661.

[32] Seifert U. Entropy Production along a Stochastic Trajectory and an Integral Fluctuation Theorem. Phys Rev Lett. 2005;95:040602.

[33] Speck T, Seifert U. Restoring a fluctuation-dissipation theorem in a nonequilibrium steady

state. EPL. 2006;74:391.

[34] Seifert U, Speck T. Fluctuation-dissipation theorem in nonequilibrium steady states. EPL. 2010;89:10007.

[35] Chetrite R, Gawedzki K. Fluctuation Relations for Diffusion Processes. Comm Math Phys. 2008;282:469–518.

[36] Katz S, Lebowitz JL, Spohn H. Non-equilibrium steady states of stochastic lattice gas models of fast ionic conductors. J Stat Phys. 1984;34:497–537.

[37] Prigogine I. Introduction to Thermodynamics of Irreversible Processes. 3rd ed. New York: Interscience; 1967.

[38] Gyarmati I. Non-equilibrium thermodynamics. Field theory and variational principles. Berlin: Springer; 1970.

[39] Jaynes ET. The Minimum Entropy Production Principle. Annual Review of Physical Chemistry. 1980;31:579–601.

[40] Gallavotti G. Entropy production and thermodynamics of nonequilibrium stationary states: A point of view. Chaos. 2004;14:680–690.

[41] Attard P. Theory for non-equilibrium statistical mechanics. Phys Chem Chem Phys. 2006;8:3585–3611.

[42] Martyushev LM, Seleznev VD. Maximum entropy production principle in physics, chemistry and biology. Physics Reports. 2006;426:1–45.

[43] Otten M, Stock G. Maximum caliber inference of nonequilibrium processes. J Chem Phys. 2010;133(3):034119.

[44] Monthus C. Non-equilibrium steady states: maximization of the Shannon entropy associated with the distribution of dynamical trajectories in the presence of constraints. J Stat Mech: Theor Exp. 2011;p. P03008.

[45] Seneta E. Non-negative matrices and Markov chains. 2nd ed. London: Springer Series in Statistics; 1981.

[46] Van Kampen NG. Stochastic Processes in Physics and Chemistry. 3rd ed. Amsterdam: Elsevier; 2007.

[47] Reichl LE. A modern course in statistical physics. 3rd ed. New York: Wiley; 2009.

[48] Risken H. The Fokker-Planck Equation: Methods of Solutions and Applications. 2nd ed. Berlin: Springer; 1989.

[49] Schadschneider A, Chowdhury D, Nishinari K. Stochastic Transport in Complex Systems: From Molecules to Vehicles. Amsterdam: Elsevier; 2011.

[50] Brown R. A brief account of microscopical observations made on the particles contained in the pollen of plants. Philosophical Magazine. 1828;4:161–173.

[51] Einstein A. Über die von der molekularkinetischen Theorie der Wärme geforderte Bewegung von in ruhenden Flüssigkeiten suspendierten Teilchen. Annalen der Physik. 1905;322:549–560.

[52] von Smoluchowski M. Zur kinetischen Theorie der Brownschen Molekularbewegung und der Suspensionen. Annalen der Physik. 1906;326:756–780.

[53] Glauber RJ. Time Dependent Statistics of the Ising Model. Journal of Mathematical Physics. 1963;4(2):294–308.

[54] Swendsen RH, Wang JS. Nonuniversal critical dynamics in Monte Carlo simulations. Phys Rev Lett. 1987;58(2):86–88.

[55] Landau DP, Binder K. A guide to Monte Carlo simulations in statistical physics. 3rd ed. Cambridge: Cambridge University Press; 2009.

[56] Metropolis N, Rosenbluth AW, Rosenbluth MN, Teller AH, Teller E. Equation of State Calculations by Fast Computing Machines. J Chem Phys. 1953;21(6):1087–1093.

[57] Ising E. Beitrag zur Theorie des Ferromagnetismus. Z Physik. 1925;31(1):253–258.

[58] Yang CN, Lee TD. Statistical Theory of Equations of State and Phase Transitions. I. Theory of Condensation. Phys Rev. 1952;87(3):404–409.

[59] Huang K. Statistical mechanics. 2nd ed. New York: Wiley; 1987.

[60] Kawasaki K. Diffusion Constants near the Critical Point for Time-Dependent Ising Models. II. Phys Rev. 1966;148(1):375–381.

[61] Kawasaki K. Kinetic equations and time correlation functions of critical fluctuations. Annals of Physics. 1970;61(1):1–56.

[62] Kolmogorov AN. Zur Theorie der Markoffschen Ketten. Math Ann. 1936;112:155–160.

[63] Schnakenberg J. Network theory of microscopic and macroscopic behavior of master equation systems. Rev Mod Phys. 1976;48(4):571–585.

[64] Haken H. Synergetics, An Introduction. 3rd ed. Berlin: Springer; 1983.

[65] Kirchhoff G. Über die Auflösung der Gleichungen, auf welche man bei der Untersuchung der

linearen Verteilung galvanischer Ströme geführt wird. Annalen der Physik und Chemie. 1847;72(12):497–508.

[66] Zia RKP, Schmittmann B. A possible classification of nonequilibrium steady states. J Phys A: Math Gen. 2006;39(24):L407–L413.

[67] Chetrite R, Gupta S. Two Refreshing Views of Fluctuation Theorems Through Kinematics Elements and Exponential Martingale. J Stat Phys. 2011;143(3).

[68] Schmittmann B, Zia RKP. Statistical Mechanics of Driven Diffusive Systems. vol. 17 of Phase Transitions and Critical Phenomena. London: Academic Press; 1995.

[69] Praestgaard EL, Schmittmann B, Zia RKP. A Lattice Gas Coupled to Two Thermal Reservoirs: Monte Carlo and Field Theoretic Studies. European Physical Journal B. 2000;18:675–695.

[70] Zia RKP, Praestgaard EL, Mouritsen OG. Getting More from Pushing Less: Negative Specific Heat and Conductivity in Non-equilibrium Steady States. American Journal of Physics. 2002;70:384–392.

[71] Evans DJ, Cohen EGD, Morriss GP. Probability of Second Law Violations in Shearing Steady states. Phys Rev Lett. 1993;71:2401.

[72] Evans DJ, Searles DJ. Equilibrium microstates which generate second law violating steady states. Phys Rev E. 1994;50:1645.

[73] Gallavotti G, Cohen EGD. Dynamical ensembles in non-equilibrium statistical mechanics. Phys Rev Lett. 1995;74:2694.

[74] Baiesi M, Maes C, Wynants B. Fluctuations and response of nonequilibrium states. Phys Rev Lett. 2009;103:010602.

[75] Kurchan J. Fluctuation theorem for stochastic dynamics. J Phys A: Math Gen. 1998;31:3719.

[76] Lebowitz JL, Spohn H. A Gallavotti-Cohen type symmetry in the large deviation functional for stochastic dynamics. J Stat Phys. 1999;95:333.

[77] Derrida B. Non-equilibrium steady states: fluctuations and large deviations of the density and of the current. J Stat Mech: Theor Exp. 2007;p. P07023.

[78] Touchette H. The large deviation approach to statistical mechanics. Phys Rep. 2009;478:1.

[79] Kubo R, Toda M, Hashitsume N. Statistical Physics II: Nonequilibrium Statistical Mechanics. 2nd ed. Berlin: Springer-Verlag; 1998.

[80] Marconi UMB, Puglisi A, Rondoni L, Vulpiani A. Fluctuation–dissipation: Response theory in statistical physics. Phys Rep. 2008;461:111–195.

[81] Gallavotti G. Fluctuation theorem and chaos. Eur Phys J B. 2008;64:315–320.

[82] Jarzynski C. Nonequilibrium work relations: foundations and applications. Eur Phys J B. 2008;64:331.

[83] Bertini L, De Sole A, Gabrielli D, Jona-Lasinio G, Landim C. Macroscopic Fluctuation Theory for stationary non-equilibrium states. J Stat Phys. 2002;107:635.

[84] Grinstein G. Generic scale invariance in classical nonequilibrium systems. Journal of Applied Physics. 1991;69:5441–5446.

[85] Dorfman JR, Kirkpatrick TR, Sengers JV. Generic Long range Correlations in Molecular Fluids. Annual Review of Physical Chemistry. 1994;45:213–239.

[86] Evans MR, Kafri Y, Koduvely HM, Mukamel D. Phase separation and coarsening in one-dimensional driven diffusive systems: Local dynamics leading to long-range Hamiltonians. Phys Rev E. 1998;58(3):2764–2778.

[87] Clincy M, Derrida B, Evans MR. Phase transition in the ABC model. Phys Rev E. 2003;67(6):066115.

[88] Baxter RJ. Exactly solved models in statistical mechanics. 1st ed. New-York: Dover Publications; 2008.

[89] Sutherland B. Beautiful Models: 70 Years of Exactly Solved Quantum Many-Body Problem. 1st ed. Singapore: World Scient. Pub. Comp.; 2004.

[90] Krug J. Boundary-induced phase transitions in driven diffusive systems. Phys Rev Lett. 1991;67:1882.

[91] Harris TE. Diffusion with 'collisions' between particles. J Appl Prob. 1965;2:323.

[92] Liggett TM. Interacting Particle Systems. 1st ed. New-York: Springer-Verlag; 1985.

[93] Evans MR, Blythe RA. Non-equilibrium dynamics in low dimensional systems. Physica A. 2002;313:110.

[94] Karzig T, von Oppen F. Signatures of critical full counting statistics in a quantum-dot chain. Phys Rev B. 2010;81:045317.

[95] Evans MR. Bose-Einstein condensation in disordered exclusion models and relation to traffic flow. Europhys Lett. 1996;36:13.

[96] Derrida B. An exactly soluble non-equilibrium system: the asymmetric simple exclusion process. Phys Rep. 1998;301:65.

[97] Krapivsky PL, Redner S, Ben-Naim E. A Kinetic View of Statistical Physics. 1st ed. Cambridge: Cambridge University Press; 2010.

[98] Barma M. Dynamics of field-driven interfaces in the two-dimensional Ising. J Phys A: Math Gen. 1992;25:L693.

[99] Barma M. Driven diffusive systems with disorder. Physica A. 2006;372:22.

[100] Chatterjee S, Barma M. Dynamics of fluctuation-dominated phase ordering: Hard-core passive sliders on a fluctuating surface. Phys Rev E. 2006;73:011107.

[101] Chatterjee S, Barma M. Shock probes in a one-dimensional Katz-Lebowitz-Spohn model. Phys Rev E. 2008;77:061124.

[102] Harris RJ, Stinchcombe RB. Disordered asymmetric simple exclusion process: Mean-field treatment. Phys Rev E. 2004;70:016108.

[103] Shaw LB, Sethna JP, Lee KH. Mean-field approaches to the totally asymmetric exclusion process with quenched disorder and large particles. Phys Rev E. 2004;70(2):021901.

[104] Shaw LB, Kolomeisky AB, Lee KH. Local Inhomogeneity in Asymmetric Simple Exclusion Processes with Extended Objects. J Phys A: Math Gen. 2004;37:2105–2113.

[105] Zia RKP, Dong JJ, Schmittmann B. Modeling Translation in Protein Synthesis with TASEP: A Tutorial and Recent Developments. J Stat Phys. 2011;144:405–428.

[106] Derrida B, Janowski SA, Lebowitz JL, Speer ER. Exact solution of the totally asymmetric exclusion process: shock profiles. J Stat Phys. 1993;73:813.

[107] Mallick K. Shocks in the asymmetric exclusion model with an impurity. J Phys A: Math Gen. 1996;29:5375.

[108] Speer ER. The two species totally asymmetric exclusion process in Micro, Meso and Macroscopic approaches in Physics. C. maes and a. verbeure ed. ed. Leuven: NATO Workshop 'On three levels'; 1993.

[109] Mallick K, Mallick S, Rajewsky N. Exact solution of an exclusion process with three classes of particles and vacancies. J Phys A: Math Gen. 1999;32:8399.

[110] Ferrari PA, Martin JB. Stationary distributions of multi-type totally asymmetric exclusion processes. Ann Prob. 2007;35:807.

[111] Evans MR, Ferrari PA, Mallick K. Matrix Representation of the Stationary Measure for the Multispecies TASEP. J Stat Phys. 2009;135:217.

[112] Mallick K. Some exact results for the exclusion process. J Stat Mech: Theor Exp. 2011;p. P01024.

[113] Gantmacher FR. Matrix theory. 1st ed. New-York: Chelsea; 1964.

[114] Jain K, Marathe R, Chaudhuri A, Dhar A. Driving particle current through narrow channels using classical pump. Phys Rev Lett. 2007;99:190601.

[115] Born M, Green HS. A General Kinetic Theory of Liquids. I. The Molecular Distribution Functions. Royal Society of London Proceedings Series A. 1946;188:10–18.

[116] Kirkwood JG. The Statistical Mechanical Theory of Transport Processes I. General Theory. J Chem Phys. 1946;14:180–201.

[117] Kirkwood JG. The Statistical Mechanical Theory of Transport Processes II. Transport in Gases. J Chem Phys. 1947;15:72–76.

[118] Derrida B, Domany E, Mukamel D. An exact solution of a one dimensional asymmetric exclusion model with open boundaries. J Stat Phys. 1992;69:667.

[119] Janowski SA, Lebowitz JL. Finite size effects and Shock fluctuations in the asymmetric exclusion process. Phys Rev A. 1992;45:618.

[120] Derrida B, Evans MR, Hakim V, Pasquier V. Exact solution of a 1D asymmetric exclusion model using a matrix formulation. J Phys A: Math Gen. 1993;26:1493.

[121] Schütz GM, Domany E. Phase Transitions in an exactly soluble one-dimensional exclusion process. J Stat Phys. 1993;72:277.

[122] Schütz GM. Exactly Solvable Models for Many-Body Systems Far from Equilibrium, Phase Transitions and Critical Phenomena vol 19. C. domb and j. l. lebowitz ed. ed. San Diego: Academic Press; 2001.

[123] Blythe RA, Evans MR. Nonequilibrium steady states of matrix-product form: a solver's guide. J Phys A: Math Theor. 2007;40:R333.

[124] Lakatos G, O'Brien J, Chou T. Hydrodynamic mean-field solutions of 1D exclusion processes with spatially varying hopping rates. Journal of Physics A: Mathematical and General. 2006;39(10):2253.

[125] Alcaraz FC, Rittenberg V. Different facets of the raise and peel model. J Stat Mech: Theor Exp. 2007;p. P07009.

[126] Sasamoto T. One-dimensional partially asymmetric exclusion process with open boundaries: orthogonal polynomial approach. J Phys A: Math Gen. 1999;32:7109.

[127] Sasamoto T. Density profile of the one-dimensional partially asymmetric simple exclusion process with open boundaries. J Phys Soc Japan. 2000;69:1055.

[128] Ferrari PA. Shock fluctuations in the asymmetric simple exclusion. Prob Theor Rel Fields. 1992;91:81.

[129] Ferrari PA, Fontes LRG. Current fluctuations for the asymmetric exclusion process. Ann Prob. 1994;22:1.

[130] Ferrari PA, Fontes LRG, Kohayakawa Y. Invariant measures for a two-species asymmetric process. J Stat Phys. 1994;76:1153.

[131] Derrida B. Microscopic versus macroscopic approaches to non-equilibrium systems. J Stat Mech: Theor Exp. 2011;p. P01030.

[132] Dhar D. An exactly solved model for interfacial growth. Phase Transitions. 1987;9:51.

[133] Kandel D, Domany E, Nienhuis B. A six-vertex model as a diffusion problem: derivation of correlation functions. J Phys A: Math Gen. 1990;23:L755.

[134] Rajesh R, Dhar D. An exactly solvable anisotropic directed percolation model in three dimensions. Phys Rev Lett. 1998;81:1646.

[135] Gwa LH, Spohn H. Bethe solution for the dynamical-scaling exponent of the noisy Burgers equation. Phys Rev A. 1992;46:844.

[136] Kim D. Bethe Ansatz solution for crossover scaling functions of the asymmetric XXZ chain and the Kardar-Parisi-Zhang-type growth model. Phys Rev E. 1995;52:3512.

[137] Kim D. Asymmetric XXZ chain at the antiferromagnetic transition: spectra and partition functions. J Phys A: Math Gen. 1997;30:3817.

[138] Golinelli O, Mallick K. Spectral gap of the totally asymmetric exclusion process at arbitrary filling. J Phys A: Math Gen. 2005;38:1419.

[139] Golinelli O, Mallick K. The asymmetric simple exclusion process: an integrable model for non-equilibrium statistical mechanics. J Phys A: Math Gen. 2006;39:12679.

[140] Derrida B, Lebowitz JL. Exact large deviation function in the asymmetric exclusion process. Phys Rev Lett. 1998;80:209.

[141] Derrida B, Evans MR. Bethe Ansatz solution for a defect particle in the asymmetric exclusion process. J Phys A: Math Gen. 1999;32:4833.

[142] Bethe H. Zur Theory der Metalle. I Eigenwerte und Eigenfunctionen Atomkette. Zeits für Physik. 1931;71:205–226,.

[143] Gaudin M. La fonction d'onde de Bethe. 1st ed. Paris: Masson; 1983.

[144] Langlands RP, Saint-Aubin Y. Algebro-geometric aspects of the Bethe equations. in 'strings and symmetries' ed. Berlin: Springer Lecture Notes in Physics Vol. 447; 1995.

[145] Golinelli O, Mallick K. Spectral Degeneracies in the Totally Asymmetric Exclusion Process. J Stat Phys. 2005;120:779.

[146] Bogoliubov NM. Determinantal representation of correlation functions in the totally asymmetric exclusion model. SIGMA. 2009;5:052 (arXiv:0904.3680).

[147] Schütz GM. Exact solution of the master equation of the asymmetric exclusion process. J Stat Phys. 1997;88:427.

[148] Priezzhev VB. Exact Nonstationary Probabilities in the Asymmetric Exclusion Process on a Ring. Phys Rev Lett. 2003;91:050601.

[149] Priezzhev VB. Non-stationary Probabilities for the asymmetric exclusion process on a ring. Pramana J Phys. 2005;64:915.

[150] van Beijeren H, Kutner R, Spohn H. Excess noise for driven diffusive systems. Phys Rev Lett. 1985;54:2026.

[151] Halpin-Healy T, Zhang YC. Kinetic roughening phenomena, stochastic growth, directed polymers and all that. Phys Rep. 1995;254:215.

[152] Majumdar SN, Barma M. Tag diffusion in driven systems, growing interfaces and anomalous fluctuations. Phys Rev B. 1991;44:5306.

[153] de Gier J, Essler FHL. Exact spectral gaps of the asymmetric exclusion process with open boundaries. J Stat Mech: Theor Exp. 2006;p. P12011.

[154] de Masi A, Ferrari PA. Self-Diffusion in one-dimensional lattice gases in the presence of an external field. J Stat Phys. 1984;38:603.

[155] Proeme A, Blythe RA, Evans MR. Dynamical transition in the open-boundary totally asymmetric exclusion process. Journal of Physics A: Mathematical and Theoretical. 2011;44(3):035003.

[156] Gorissen M, Vanderzande C. Finite size scaling of current fluctuations in the totally asymmetric exclusion process. Journal of Physics A: Mathematical and Theoretical. 2011;44(11):115005.

[157] Mitsudo T, Takesue S. The numerical estimation of the current large deviation function in the asymmetric exclusion process with open boundary conditions. arXiv. 2011;p.

arXiv:1012.1387v2.

[158] Flindt C, Novotný Tcv, Jauho AP. Current noise in a vibrating quantum dot array. Phys Rev B. 2004 Nov;70(20):205334.

[159] Jiang DQ, Qian M, Qian MP. Mathematical Theory of Nonequilibrium Steady-States. Lecture Notes in Mathematics. Berlin: Springer-Verlag; 2004.

[160] Shargel BH. The measure-theoretic identity underlying transient fluctuation theorems. J Phys A. 2009;42:135002.

[161] Prolhac S, Mallick K. Current fluctuations in the exclusion process and Bethe Ansatz. J Phys A: Math Theor. 2008;41:175002.

[162] Prolhac S. Fluctuations and skewness of the current in the partially asymmetric exclusion process. J Phys A: Math Theor. 2008;41:365003.

[163] Derrida B, Mallick K. Exact diffusion constant for the one-dimensional partially asymmetric exclusion process. J Phys A: Math Gen. 1997;30:1031.

[164] Prolhac S. Tree structures for the current fluctuations in the exclusion process. J Phys A: Math Theor. 2010;43:105002.

[165] Prolhac S, Mallick K. Cumulants of the current in a weakly asymmetric exclusion process. J Phys A: Math Theor. 2009;42:175001.

[166] Appert-Rolland C, Derrida B, Lecomte V, Van Wijland F. Universal cumulants of the current in diffusive systems on a ring. Phys Rev E. 2008;78:021122.

[167] Bodineau T, Derrida B. Current fluctuations in nonequilibrium diffusive systems: An additivity principle. Phys Rev Lett. 2004;92:180601.

[168] Bodineau T, Derrida B. Distribution of currents in non-equilibrium diffusive systems and phase transitions. Phys Rev E. 2005;72:066110.

[169] Bodineau T, Derrida B. Cumulants and large deviations of the current through non-equilibrium steady states. C R Physique. 2007;8:540.

[170] de Gier J, Essler FHL. Bethe Ansatz solution of the Asymmetric Exclusion Process with Open Boundaries. Phys Rev Lett. 2005;95:240601.

[171] de Gier J, Essler FHL. Slowest relaxation mode of the partially asymmetric exclusion process with open boundaries. J Phys A: Math Theor. 2008;41:485002.

[172] Alcaraz FC, Lazo MJ. The Bethe ansatz as a matrix product ansatz. J Phys A: Math Gen. 2004;37:L1.

[173] Cantini L. Algebraic Bethe Ansatz for the two-species ASEP with different hopping rates. J Phys A: Math Theor. 2008;41:095001.

[174] Arita C, Kuniba A, Sakai K, Sawabe T. Spectrum of a multi-species asymmetric simple exclusion process on a ring. J Phys A: Math Theor. 2009;42(34):345002.

[175] Povolotsky AM. Bethe Ansatz solution of zero-range process with non-uniform stationary state. Phys Rev E. 2004;69:061109.

[176] Dorlas T, Povolotsky A, Priezzhev V. From Vicious Walkers to TASEP. J Stat Phys. 2009;135:483–517.

[177] Majumdar SN, Mallick K, Nechaev S. Bethe Ansatz in the Bernoulli Matching Model of Random Sequence Alignment. Phys Rev E. 2008;77:011110.

[178] Priezzhev VB, Schütz GM. Exact solution of the Bernoulli matching model of sequence alignment. J Stat Mech: Theor Exp. 2008;p. P09007.

[179] Tracy CA, Widom H. Integral Formulas for the Asymmetric Simple Exclusion Process. Comm Math Phys. 2008;279:815.

[180] Rakos A, Schütz GM. Current distribution and random matrix ensembles for an integrable asymmetric fragmentation process. J Stat Phys. 2005;118:511.

[181] Tracy CA, Widom H. Level-Spacing distributions and Airy kernel. Comm Math Phys. 1994;159:151.

[182] Kriecherbauer T, Krug J. A pedestrian's view on interacting particle systems, KPZ universality and random matrices. J Phys A: Math Theor. 2010;43:403001.

[183] Johansson K. Shape fluctuation and random matrices. Comm Math Phys. 2000;209:437.

[184] Spohn H. KPZ equation in one dimension and line ensembles. Pramana J Phys. 2005;64:1.

[185] Spohn H. Exact solutions for KPZ-type growth processes, random matrices, and equilibrium shapes of crystals. Physica A. 2006;369:71–99.

[186] Ferrari PL. From Interacting Particle Systems to Random Matrices. J Stat Mech: Theor Exp. 2011;p. P10016.

[187] Baik J, Deift P, Johansson K. On the distribution of the length of the longest increasing subsequence of random permutations. J Am Math Soc. 1999;12:1119–1178.

[188] Tracy CA, Widom H. A Fredholm determinant representation in ASEP. J Stat Phys. 2008;132:291.

[189] Tracy CA, Widom H. Asymptotics in ASEP with step initial condition. Comm Math Phys. 2009;290:129.

[190] Tracy CA, Widom H. Total current fluctuation in ASEP. J Math Phys. 2009;50:095204.

[191] Tracy CA, Widom H. Formulas for Joint Probabilities for the Asymmetric Simple Exclusion Process. J Math Phys. 2010;51:063302.

[192] Sasamoto T, Spohn H. The 1+1 dimensional Kardar-Parisi-Zhang equation and its universality class. J Stat Mech: Theor Exp. 2010;2010:P11013.

[193] Sasamoto T, Spohn H. One-dimensional KPZ equation: an exact solution and its universality. Phys Rev Lett. 2010;104:230602.

[194] Amir G, Corwin I, Quastel J. Probability Distribution of the Free Energy of the Continuum Directed Random Polymer in $1 + 1$ dimensions. Comm Pure Appl Math. 2011;64:466537.

[195] Calabrese P, LeDoussal P, Rosso A. Free-energy distribution of the directed polymer at high temperature. EPL. 2010;90:20002.

[196] Dotsenko V. Bethe ansatz derivation of the Tracy-Widom distribution for one-dimensional directed polymers. EPL. 2010;90:20003.

[197] Prolhac S, Spohn H. The height distribution of the KPZ equation with sharp wedge initial condition: numerical evaluations. Phys Rev E. 2011;84:011119.

[198] Calabrese P, LeDoussal P. An exact solution for the KPZ equation with flat initial conditions. Phys Rev Lett. 2011;106:250603.

[199] Imamura T, Sasamoto T. Exact analysis of the KPZ equation with half Brownian motion initial condition. e-print. 2011;p. arXiv:1105.4659.

[200] Prolhac S, Spohn H. Two-point generating function of the free energy for a directed polymer in a random medium. J Stat Mech: Theor Exp. 2011;2011:P01031.

[201] Prolhac S, Spohn H. The one-dimensional KPZ equation and the Airy Process. J Stat Mech: Theor Exp. 2011;2011:P03020.

[202] Aldous D, Diaconis P. Longest increasing subsequences: from patience sorting to the Baik-Deft-Johansson theorem. Bull Am Math Soc. 1999;36:413–432.

[203] Corwin I. The Kardar-Parisi-Zhang equation and universality class. e-print. 2011;p. arXiv:1106.1596.

[204] Stinchcombe RB, de Queiroz SLA. Smoothly-varying hopping rates in driven flow with exclusion. Phys Rev E. 2011;83:061113.

[205] Shaw LB, Zia RKP, Lee KH. Modeling, Simulations, and Analyses of Protein Synthesis: Driven Lattice Gas with Extended Objects. Physical Review E. 2003;68:021910.

[206] Schnherr G, Schtz GM. Exclusion process for particles of arbitrary extension: hydrodynamic limit and algebraic properties. Journal of Physics A: Mathematical and General. 2004;37(34):8215.

[207] Schoenherr G. Hard rod gas with long-range interactions: Exact predictions for hydrodynamic properties of continuum systems from discrete models. Physical Review E. 2005;71:026122.

[208] de Dominicis C, Brézin E, Zinn-Justin J. Field-theoretic techniques and critical dynamics. I. Ginzburg-Landau stochastic models without energy conservation. Phys Rev B. 1975;12:4945–4953.

[209] Halperin BI, Hohenberg PC, Ma Sk. Renormalization-group methods for critical dynamics: I. Recursion relations and effects of energy conservation. Phys Rev B. 1974 Jul;10:139–153.

[210] Halperin BI, Hohenberg PC, Ma Sk. Renormalization-group methods for critical dynamics: II. Detailed analysis of the relaxational models. Phys Rev B. 1976;13:4119–4131.

[211] Bausch R, Janssen HK, Wagner H. Renormalized field theory of critical dynamics. Zeitschrift für Physik B Condensed Matter. 1976;24:113–127.

[212] Janssen HK, Schmittmann B. Field theory of long-time behaviour in driven diffusive systems. Zeitschrift fr Physik B Condensed Matter. 1986;63:517–520.

[213] Janssen HK, Schmittmann B. Field theory of critical behaviour in driven diffusive systems. Zeitschrift fr Physik B Condensed Matter. 1986;64:503–514.

[214] Leung Kt, Cardy JL. Field theory of critical behaviour in a driven diffusive system. J Stat Phys. 1986;44:567–588.

[215] Janssen HK, Oerding K. Renormalized field theory and particle density profile in driven diffusive systems with open boundaries. Phys Rev E. 1996;53(5):4544–4554.

[216] Oerding K, Janssen HK. Surface critical behavior of driven diffusive systems with open boundaries. Phys Rev E. 1998;58(2):1446–1454.

[217] Becker V, Janssen HK. Field Theory of Critical Behavior in Driven Diffusive Systems with Quenched Disorder. J Stat Phys. 1999;96:817–859.

[218] Parmeggiani A, Franosch T, Frey E. Phase Coexistence in Driven One-Dimensional Transport. Phys Rev Lett. 2003;90(8):086601.

[219] Parmeggiani A, Franosch T, Frey E. Totally asymmetric simple exclusion process with Langmuir kinetics. Phys Rev E. 2004;70(4):046101.

[220] Pierobon P, Frey E, Franosch T. Driven lattice gas of dimers coupled to a bulk reservoir. Phys Rev E. 2006;74(3):031920.

[221] Frey E, Parmeggiani A, Franosch T. Collective Phenomena in Intracellular Processes. Genome Informatics. 2004;15(1):46–55.

[222] Wood AJ. A totally asymmetric exclusion process with stochastically mediated entrance and exit. Journal of Physics A: Mathematical and Theoretical. 2009;42(44):445002.

[223] Muhuri S, Pagonabarraga I. Collective vesicle transport on biofilaments carried by competing molecular motors. EPL. 2008;84:58009.

[224] Pronina E, Kolomeisky AB. Asymmetric Coupling in Two-Channel Simple Exclusion Processes. Physica A. 2006;372:12–21.

[225] Reichenbach T, Franosch T, Frey E. Exclusion Processes with Internal States. Phys Rev Lett. 2006;97(5):050603.

[226] Garai A, Chowdhury D, Chowdhury D, Ramakrishnan TV. Stochastic kinetics of ribosomes: Single motor properties and collective behavior. Phys Rev E. 2009;80(1):011908.

[227] Papoulis A. Probability, Random Variables, and Stochastic Processes. New York, NY: McGraw-Hill; 1984.

[228] Evans MR, Sugden KEP. An exclusion process for modelling fungal hyphal growth. Physica A: Statistical Mechanics and its Applications. 2007;384:53–58.

[229] Sugden KEP, Evans MR, Poon WCK, Read ND. Model of hyphal tip growth involving microtubule-based transport. Phys Rev E. 2007;75(3):031909.

[230] Sugden KEP, Evans MR. A dynamically extending exclusion process. J Stat Mech: Theor Exp. 2007;p. P11013.

[231] Hough LE, Schwabe A, Glaser MA, McIntosh JR, Betterton MD. Microtubule depolymerization by the kinesin-8 motor Kip3p: a mathematical model. Biophysical Journal. 2009;96:3050–3064.

[232] Nowak SA, Fok PW, Chou T. Dynamic boundaries in asymmetric exclusion processes. Physical Review E. 2007;76:031135.

[233] Fok PW, Chou T. Interface Growth Driven by Surface Kinetics and Convection. SIAM J Appl Math. 2009;70:24–39.

[234] Levitt DG. Dynamics of a Single-File Pore: Non-Fickian Behavior. Phys Rev A. 1973;8:3050–3054.

[235] Alexander S, Pincus P. Diffusion of labeled particles on one-dimensional chains. Phys Rev B. 1978;18(4):2011–2012.

[236] Karger J. Straightforward Derivation of the Long-Time Limit of the Mean-Square Displacement in One-Dimensional Diffusion. Phys Rev A. 1992;45:4173–4174.

[237] Barkai E, Silbey R. Diffusion of tagged particle in an exclusion process. Phys Rev E. 2010;81(4):041129.

[238] Sholl DS, Fichthorn KA. Concerted Diffusion of Molecular Clusters in a Molecular Sieve. Phys Rev Lett. 1997;79(19):3569–3572.

[239] Sholl DS, Lee CK. Influences of concerted cluster diffusion on single-file diffusion of CF_4 in $AlPO_4$-5 and Xe in $AlPO_4$-31. J Chem Phys. 2000;112(2):817–824.

[240] Khantha M, Cordero NA, Alonso JA, Cawkwell M, Girifalco LA. Interaction and concerted diffusion of lithium in a (5,5) carbon nanotube. Phys Rev B. 2008;78(11):115430.

[241] Gabel A, Krapivsky PL, Redner S. Facilitated Asymmetric Exclusion. Phys Rev Lett. 2010;105(21):210603.

[242] Chou T. How Fast Do Fluids Squeeze through Microscopic Single-File Pores? Phys Rev Lett. 1998;80(1):85–88.

[243] Kolomeisky AB. Channel-Facilitated Molecular Transport Across Membranes: Attraction, Repulsion and Asymmetry. Phys Rev Lett. 2007;98:048105.

[244] Derrida B, Douot B, Roche PE. Current fluctuations in the one dimensional Symmetric Exclusion Process with open boundaries. J Stat Phys. 2004;115:717–748.

[245] Santos JE, M G, Schütz GM. Exact time-dependent correlation functions for the symmetric exclusion process with open boundary. Phys Rev E. 2001;64(3):036107.

[246] Jovanovic-Talisman T, Tetenbaum-Novatt J, McKenney AS, Zilman A, Peters R, Rout MP, et al. Artificial nanopores that mimic the selectivity of the nuclear pore complex. Nature. 2009;457:1023–1027.

[247] Zilman A, Talia SD, Chait B, Rout M, Magnasco M. Efficiency, selectivity and robustness of the transport through the nuclear pore complex. PLoS Computational Biology. 2007;p. e127.

[248] Chou T. Kinetics and thermodynamics across single-file pores: Solute permeability and rectified osmosis. J Chem Phys. 1999;110(1):606–615.

[249] Doyle DA, Cabral JM, Pfuetzner RA, Kuo A, Gulbis JcM, Cohen SL, et al. The Structure of the Potassium Channel: Molecular Basis of K+ Conduction and Selectivity. Science. 1998;280(5360):69–77.

[250] Zilman A. Effects of Multiple Occupancy and Interparticle Interactions on Selective Transport through Narrow Channels: Theory versus Experiment. Biophysical Journal. 2009;96(4):1235 – 1248.

[251] Gwan JF, Baumgaertner A. Cooperative transport in a potassium ion channel. J Chem Phys. 2007;127(4):045103.

[252] Hodgkin L, Keynes RD. The potassium permeability of a giant nerve fibre. J Physiol. 1955;128:6188.

[253] Bernéche S, Roux B. Energetics of ion conduction through the K+ channel. Nature. 2001;414:73–77.

[254] Khalili-Araghi F, Tajkhorshid E, Schulten K. Dynamics of K+ ion conduction through Kv1.2. Biophysical Journal. 2006;91:L72–L74.

[255] Yesylevskyy SO, Kharkyanen VN. Barrier-less knock-on conduction in ion channels: peculiarity or general mechanism? Chemical Physics. 2005;312(1-3):127 – 133.

[256] Zilman A, Talia SD, Jovanovic-Talisman T, Chait BT, Roux MP, Magnasco MO. Enhancement of Transport Selectivity through Nano-Channels by Non-Specific Competition. PLoS Comput Biol. 2010 06;6:e1000804.

[257] Chou T, Lohse D. Entropy-Driven Pumping in Zeolites and Biological Channels. Phys Rev Lett. 1999;82(17):3552–3555.

[258] Ilan B, Tajkhorshid E, Schulten K, Voth GA. The mechanism of proton exclusion in aquaporin channels. Proteins: Structure, Function, and Bioinformatics. 2004;55:223–228.

[259] de Grotthuss CJT. Sur la décomposition de l'eau et des corps qu'elle tient en dissolution l'aide de l'lectricité galvanique. Ann Chim. 1806;58:5473.

[260] Agmon N. The Grotthuss mechanism. Chemical Physics Letters. 1995;244(5-6):456 – 462.

[261] Pomes R, Roux B. Structure and dynamics of a proton wire: a theoretical study of H+ translocation along the single-file water chain in the gramicidin A channel. Biophysical Journal. 1996;71:19–39.

[262] Voth GA. Computer Simulation of Proton Solvation and Transport in Aqueous and Biomolecular Systems. Accounts of Chemical Research. 2006;39(2):143–150.

[263] Cui Q, Karplus M. Is "proton wire" concerted or step-wise? A model study of proton transfers in carbonic anhydrase. J Phys Chem. 2003;107:1071–1078.

[264] Ramsey IS, Mokrab Y, Carvacho I, Sands ZA, Samson MP, Clapham DE. An aqueous H^+ permeation pathway in the voltage-gated proton channel Hv1. Nature Structural & Molecular Biology. 2010;17:869875.

[265] de Grioot BL, Frigato T, Helms V, Grubmuller H. The Mechanism of proton exclusion in the Aquaporin-1 water channel. Journal of Molecular Biology. 2003;333:279–293.

[266] Jensen M, Rthlisberger U, Rovira C. Hydroxide and Proton Migration in Aquaporins. Biophysical Journal. 2005;89(3):1744 – 1759.

[267] Dellago C, Naor MM, Hummer G. Proton Transport through Water-Filled Carbon Nanotubes. Phys Rev Lett. 2003;90(10):105902.

[268] Chou T. An interacting spinflip model for one-dimensional proton conduction. Journal of Physics A: Mathematical and General. 2002;35(21):4515.

[269] Chou T. Water Alignment, Dipolar Interactions, and Multiple Proton Occupancy during Water-Wire Proton Transport. Biophsyical Journal. 2004;86:28272836.

[270] Schumaker MF. Numerical Framework Models of Single Proton Conduction Through Gramicidin. Frontiers in Bioscience. 2003;8:s982991.

[271] Markovitch O, Agmon N. Structure and Energetics of the Hydronium Hydration Shells. The Journal of Physical Chemistry A. 2007;111(12):2253–2256.

[272] Chowdhury D, Schadschneider A, Nishinari K. Physics of transport and traffic phenomena in biology: from molecular motors and cells to organisms. Physics of Life Reviews. 2005;2(4):318 – 352.

[273] Chowdhury D, Basu A, Garai A, Greulich P, Nishinari K, Schadschneider A, et al. Intracellular traffic: bio-molecular motors on filamentary tracks. The European Physical Journal B - Condensed Matter and Complex Systems. 2008;64:593–600.

[274] Lau AWC, Lacoste D, Mallick K. Nonequilibrium Fluctuations and Mechanochemical Couplings of a Molecular Motor. Phys Rev Lett. 2007;99:158102.

[275] Lacoste D, Lau AW, Mallick K. Fluctuation theorem and large deviation function for a solvable

model of a molecular motor. Phys Rev E. 2008;78:011915.

[276] Lacoste D, Mallick K. Fluctuation theorem for the flashing ratchet model of molecular motors. Phys Rev E. 2009;80:021923.

[277] Wang H, Oster G. Ratchets, power strokes, and molecular motors. Applied Physics A. 2002;75:315–323.

[278] Astumian RD. Thermodynamics and Kinetics of Molecular motors. Biophys J. 2010;98:2401–2409.

[279] Cooper GM, Hausman RE. The Cell: A molecular approach. Sunderland, MA: Sinauer Associates; 2007.

[280] Jülicher F, Prost J. Cooperative Molecular Motors. Phys Rev Lett. 1995;75(13):2618–2621.

[281] Jülicher F, Ajdari A, Prost J. Modeling molecular motors. Rev Mod Phys. 1997;69(4):1269–1282.

[282] Vilfan A, Frey E, Schwabl F. Elastically coupled molecular motors. The European Physical Journal B - Condensed Matter and Complex Systems. 1998;3:535–546.

[283] Badoual M, Jülicher F, Prost J. Bidirectional cooperative motion of molecular motors. Proc Natl Acad USA. 2002;99:6696–6701.

[284] Stukalin EB, III HP, Kolomeisky AB. Coupling of Two Motor Proteins: a New Motor Can Move Faster. Phys Rev Lett. 2005;94:238101.

[285] Kolomeisky AB, Fisher ME. Molecular Motors: A theorist's perspective. Annual Reviews of Physical Chemistry. 2007;58:675–695.

[286] Brugués J, Casademunt J. Self-Organization and Cooperativity of Weakly Coupled Molecular Motors under Unequal Loading. Phys Rev Lett. 2009;102(11):118104.

[287] Evans MR, Juhász R, Santen L. Shock formation in an exclusion process with creation and annihilation. Phys Rev E. 2003;68(2):026117.

[288] Juhász R, Santen L. Dynamics of an exclusion process with creation and annihilation. Journal of Physics A: Mathematical and General. 2004;37(13):3933–3944.

[289] Mirin N, Kolomeisky AB. The Effect of detachments in asymmetric simple exclusion processes. J Stat Phys. 2003;110:811–823.

[290] Greulich P, Schadschneider A. Disordered driven lattice gases with boundary reservoirs and Langmuir kinetics. Phys Rev E. 2009;79(3):031107.

[291] Adamson AW, Gast AP. Physical Chemistry of Surfaces. New York, NY: John Wiley & Sons, Inc.; 1997.

[292] Pierobon P, Mobilia M, Kouyos R, Frey E. Bottleneck-induced transitions in a minimal model for intracellular transport. Phys Rev E. 2006;74(3):031906.

[293] Klumpp S, Lipowsky R. Traffic of Molecular Motors Through Tube-Like Compartments. J Stat Phys. 2003;113:233–268.

[294] Alberts B, Bray D, lewis J, Raff M, Raff K, Roberts K, et al. Molecular Biology of the Cell. New York, New York: Garland Science; 1994.

[295] Lipowsky R, Chai Y, Klumpp S, Liepelt S, Müller MJI. Molecular motor traffic: From biological nanomachines to macroscopic transport. Physica A: Statistical Mechanics and its Applications. 2006;372(1):34 – 51.

[296] Kolomeisky AB. Exact Solutions for a Partially Asymmetric Exclusion Model with Two Species. Physica A. 1997;245:523–533.

[297] Pronina E, Kolomeisky AB. Spontaneous Symmetry Breaking in Two-Channel Asymmetric Exclusion Processes with Narrow Entrances. J Phys A: Math Theor. 2007;40:2275–2286.

[298] Tsekouras K, Kolomeisky AB. Inhomogeneous Coupling in Two-Channel Asymmetric Exclusion Processes. J Phys A: Math Theor. 2008;41:465001.

[299] Du HF, Yuan YM, Hu MB, Wang R, Jiang R, Wu QS. Totally asymmetric exclusion processes on two intersected lattices with open and periodic boundaries. J Stat Mech: Theor Exp. 2010;p. P03014.

[300] Kim KH, den Nijs M. Dynamic screening in a two-species asymmetric exclusion process. Phys Rev E. 2007;76(2):021107.

[301] Nilsson J, Nissen P. Elongation factors on the ribosome. Current Opinion in Structural Biology. 2005;15(3):349 – 354.

[302] Alcaraz FC, Bariev RZ. Exact solution of the asymmetric exclusion model with particles of arbitrary size. Phys Rev E. 1999;60(1):79–88.

[303] Gupta S, Barma M, Basu U, Mohant PK. Driven k-mers: Correlations in space and time. e-print. 2011;p. arXiv:1106.3910.

[304] Zia RKP, Dong JJ, Schmittmann B. Unpublished;.

[305] Lakatos G, Chou T. Totally asymmetric exclusion processes with particles of arbitrary size. Journal of Physics A: Mathematical and General. 2003;36(8):2027.

[306] Kolomeisky AB. Asymmetric Simple Exclusion Model with Local Inhomogeneity. J Phys A: Math Gen. 1998;31:1153–1164.

[307] Chou T, Lakatos G. Clustered Bottlenecks in mRNA Translation and Protein Synthesis. Phys Rev Lett. 2004;93(19):198101.

[308] Dong JJ, Schmittmann B, Zia RKP. Inhomogeneous exclusion processes with extended objects: The effects of defect locations. Physical Review E. 2007;76:051113.

[309] Dong JJ, Schmittmann B, Zia RKP. Towards a Model for Protein Production Rates. J Stat Phys. 2007;128:21–34.

[310] Chen C, Stevens B, Kaur J, Cabral D, Liu H, Wang Y, et al. Single-Molecule Fluorescence Measurements of Ribosomal Translocation Dynamics. Molecular Cell. 2011;42(3):367 – 377.

[311] Basu A, Chowdhury D. Traffic of interacting ribosomes: Effects of single-machine mechanochemistry on protein synthesis. Physical Review E. 2007;75:021902.

[312] Garai A, Chowdhury D, Ramakrishnan TV. Fluctuations in protein synthesis from a single RNA template: Stochastic kinetics of ribosomes. Physical Review E. 2009;79:011916.

[313] Garai A, Chowdhury D, Chowdhury D, Ramakrishnan TV. Stochastic kinetics of ribosomes: Single motor properties and collective behavior. Physical Review E. 2009;80:011908.

[314] Pierobon P. Traffic of Molecular Motors: From Theory to Experiments. Springer Berlin Heidelberg; 2009.

[315] Ciandrini L, Stansfield I, Romano MC. Role of the particle's stepping cycle in an asymmetric exclusion process: A model of mRNA translation. Phys Rev E. 2010;81(5):051904.

[316] Sachs AB. The role of poly(A) in the translation and stability of mRNA. Curr Opin Cell Biol. 1990;2:1092–1098.

[317] Wells SE, Hillner PE, Vale RD, Sachs AB. Circularization of mRNA by Eukaryotic Translation Initiation Factors. Molecular Cell. 1998;2(1):135 – 140.

[318] Kahvejian A, Svitkin YV, Sukarieh R, M'Boutchou MN, Sonenberg N. Mammalian poly(A)-binding protein is a eukaryotic translation initiation factor, which acts via multiple mechanisms. Genes and Dev. 2005;19:104–113.

[319] Chou T. Ribosome Recycling, Diffusion, and mRNA Loop Formation in Translational Regulation. Biophysical Journal. 2003;85:755–773.

[320] Willett M, Pollard HJ, Vlasak M, Morley SJ. Localization of ribosomes and translation initiation factors to talin/β3-integrin-enriched adhesion complexes in spreading and migrating mammalian cells. Biol Cell. 2010;102:265–276.

[321] Lerner RS, Nicchitta CV. mRNA translation is compartmentalized to the endoplasmic reticulum following physiological inhibition of cap-dependent translation. RNA. 2006;12:775–789.

[322] Cook LJ, Zia RKP, Schmittmann B. Competition between many Totally Asymmetric Simple Exclusion Processes for a Finite Pool of Resources. Physical Review E. 2009;80:031142.

[323] Cook LJ, Zia RKP. Feedback and Fluctuations in a Totally Asymmetric Simple Exclusion Process with Finite Resources. J Stat Mech: Theor Exp. 2009;p. P02012.

[324] Carslaw HS, Jaeger JC. Conduction of heat in solids. Oxford university Press; 2004.

[325] Betterton MD, F, Jülicher. Opening of nucleic-acid double strands by helicases: Active versus passive opening. Phys Rev E. 2005;71(1):011904.

[326] Betterton MD, Jülicher F. Velocity and processivity of helicase unwinding of double-stranded nucleic acids. Journal of Physics: Condensed Matter. 2005;17(47):S3851.

[327] Garai A, Chowdhury D, Betterton MD. Two-state model for helicase translocation and unwinding of nucleic acids. Phys Rev E. 2008;77(6):061910.

[328] Manosas M, Xi XG, Bensimon D, Croquette V. Active and passive mechanisms of helicases. Nucleic Acids Res. 2010;38(16):55185526.

[329] Kim M, Santen L, Noh JD. Asymmetric simple exclusion process in one-dimensional chains with long-range links. J Stat Mech: Theor Exp. 2011;2011:P04003.

[330] Adams DA, Zia RKP, Schmittmann B. Power Spectra of the Total Occupancy in the Totally Asymmetric Simple Exclusion Process. Phys Rev Lett. 2007;99(2):020601.

[331] Cook LJ, Zia RKP. Power spectra of a constrained totally asymmetric simple exclusion process. J Stat Mech: Theor Exp. 2010;2010:P07014.

[332] Evans MR, Hanney T. Nonequilibrium statistical mechanics of the zero-range process and related models. Journal of Physics A: Mathematical and General. 2005;38(19):R195.

[333] Rácz Z, Zia RKP. Two-temperature kinetic Ising model in one dimension: Steady-state correlations in terms of energy and energy flux. Phys Rev E. 1994;49(1):139–144.

[334] Schmittmann B, Schmüser F. Stationary correlations for a far-from-equilibrium spin chain. Phys Rev E. 2002;66(4):046130.

[335] Mobilia M, Schmittmann B, Zia RKP. Exact dynamics of a reaction-diffusion model with

spatially alternating rates. Phys Rev E. 2005;71(5):056129.

[336] Aliev MA. Generating function of spin correlation functions for kinetic Glauber-Ising model with time-dependent transition rates. Journal of Mathematical Physics. 2009;50:083302.

[337] Lavrentovich MO, Zia RKP. Energy flux near the junction of two Ising chains at different temperatures. Europhysics Letters. 2010;91(5):50003.

[338] Farago J, Pitard E. Injected Power Fluctuations in 1D Dissipative Systems. J Stat Phys. 2007;128:1365–1382.

[339] Farago J, Pitard E. Injected power fluctuations in one-dimensional dissipative systems: Role of ballistic transport. Phys Rev E. 2008;78(5):051114.

[340] Wei QH, Bechinger C, Leiderer P. Single-File Diffusion of Colloids in One-Dimensional Channels. Science. 2000;287(5453):625–627.

[341] Champagne N, Vasseur R, Montourcy A, Bartolo D. Traffic Jams and Intermittent Flows in Microfluidic Networks. Phys Rev Lett. 2010;105(4):044502.

[342] Rost H. Non-equilibrium behaviour of a many particle process: Density profile and local equilibria. Probability Theory and Related Fields. 1981;58:41–53.

[343] Sopasakis A, Katsoulakis MA. Stochastic Modeling and Simulation of Traffic Flow: Asymmetric Single Exclusion Process with Arrhenius look-ahead dynamics. SIAM Journal on Applied Mathematics. 2006;66(3):921–944.

[344] Schreckenberg M, Schadschneider A, Nagel K, Ito N. Discrete stochastic models for traffic flow. Phys Rev E. 1995;51(4):2939–2949.

[345] Karimipour V. Multispecies asymmetric simple exclusion process and its relation to traffic flow. Phys Rev E. 1999;59(1):205–212.

[346] Srinivasan R. Queues in Series via Interacting Particle Systems. Mathematics of Operations Research. 1993;18:39–50.